TECHNISCHE UNIVERSITÄT WIEN

VIENNA UNIVERSITY OF TECHNOLOGY

DIPLOMARBEIT

Evaluation of thermoluminescence glow curve kinetic parameters for selected phosphors

Ausgeführt am

Atominstitut der österreichischen Universitäten

der Technischen Universität Wien

unter der Anleitung von
Univ.Prof. Dipl.-Ing. Dr.techn. Norbert Vana und
Univ.Ass. Dipl.-Ing. Dr.techn. Michael Hajek

durch

Elmar Idl

Allerheiligenplatz 11/30 1200 Wien

Wien 29.11.2008

_____
Elmar Idl

Danksagung

Der größte Dank gilt meinen Eltern, ohne deren steten Beistand dieses Studium nicht möglich gewesen wäre.

Ich möchte auch meinem Bruder danken, der immer wusste mich mit Wort und Film auf andere Gedanken zu bringen um mich mal abschalten zu lassen.

Dank gebührt auch all meinen Freunden die mich durch alle Hochs und Tiefs begleitet haben und immer helfend zur Seite standen.

Für die akademische Betreuung dieser Diplomarbeit bedanke ich mich bei Herrn Univ.-Prof. Dipl.-Ing. Dr.techn. Norbert Vana und Univ.-Ass. Dipl.-Ing. Dr.techn. Michael Hajek.

Außerdem möchte ich mich bei Herrn ADir.Ing. Manfred Fugger bedanken, der für einen reibungslosen Ablauf im Labor sorgte.

Kurzfassung

Im Rahmen der vorliegenden Arbeit wurden verschiedene Typen von Thermolumineszenzdosimetern auf ihre Glowkurven-Struktur untersucht. Dabei wurde das T_m-T_{stop} Verfahren [1], ein spezielles Analyseverfahren, das von McKeever (1985) vorgeschlagen wurde, verwendet.

Die von dieser Methode erhaltenen Daten wurden anschließend auf drei verschiedene Arten (lokales Maximum; annealed peak; Entfaltung mit GLOW FIT [2])ausgewertet und deren Ergebnisse verglichen.

Abstract

In the course of this diploma thesis different types of thermoluminescence dosimeters were analyzed with respect to their glow curve structure. A dedicated procedure (T_m-T_{stop} [1]), which was suggested by McKeever (1985) was used for that purpose.

The obtained data was then evaluated with three different methods (local maximum, annealed peak, deconvolution with GLOW FIT [2]). Finally, the results were compared with each other.

Contents

I. Introduction

In order to understand the complex procedures giving rise to thermoluminescence it is necessary to field-test existing models.

One way to decide whether a glow peak can be described by a first- or second-order kinetics model is given by the T_m-T_{stop} technique [1]. The pretensions the measuring conditions have to fulfill for this method are very high, since hundreds of measurements have to be performed under the same experimental protocol and within a certain timeframe. It therefore was a central issue to analyze how well this method could be applied within the given conditions.

Seven TLD (Thermoluminescent Dosimeter) classes were chosen and subjected to different doses of gamma radiation. For each class, the temperature interval to be investigated was defined in order to cover the distinctive glow curve structure. Three different methods were used to evaluate the obtained data.

This work is divided into three main parts.

In the beginning, an introduction to the phenomenon of thermoluminescence and the concept of absorbed dose is given. The first- and second-order kinetics model is explained and, in addition, the T_m-T_{stop} method [1] is described along with the three methods used for evaluation.

Part two specifies the used laboratory equipment and software. It describes in detail the experimental protocols of preparation, readout and analysis of TLD phosphors.

The results are presented in the last part, where the results of each method are shown individually at first and then comparatively at the end of each chapter.

II. Chapter

II.1 Introduction to Thermoluminescence

II.1.1 Luminescence:

Luminescence is a general term which describes the emission of light from a substance following the absorption of energy. The wavelength of the emitted light can range from the near infrared to the near ultraviolet spectrum, but is, as described by Stoke´s law, always at equal or longer wavelength as the stimulation was.

Luminescence itself can be divided into two main categories using the time (τ) until emission is perceived [3]. However, this is a purely phenomenological classification (figure II-1).

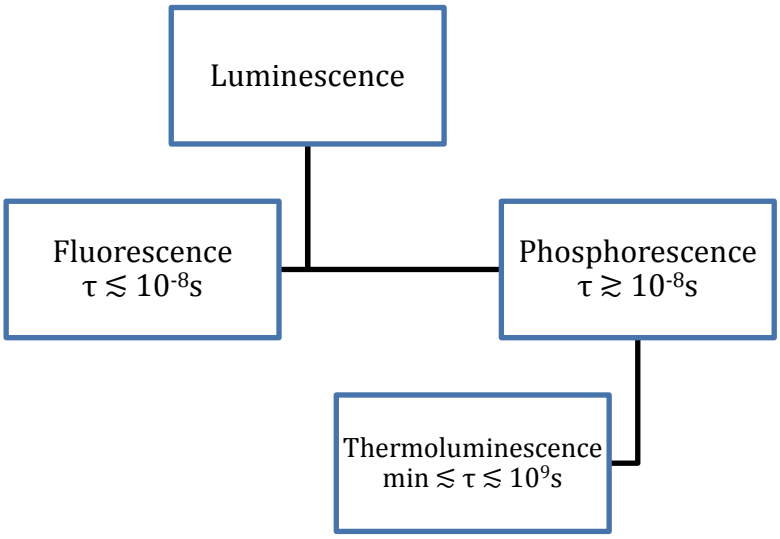

Figure II-1: Phenomenological classification of Luminescence utilizing the time τ until emission is perceived.

The emission during or shortly after stimulation is called fluorescence, which in effect corresponds to the time distribution of excitation (e.g. radiation). The time of 10^{-8}s equals the typical lifetime of an atomic energy state for an electrical dipole-transition within the visible spectrum [4]. The decay of the excited luminescent centers, after the excitation has ceased, is essentially similar to an exponential decay.

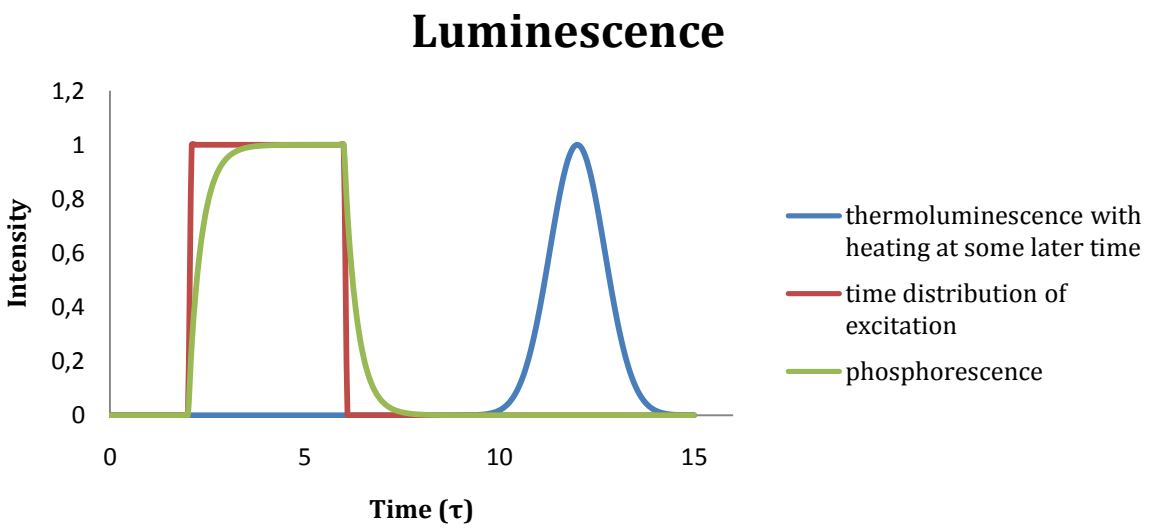

Figure II-2: Emission characteristics of luminescence effects. The excitation curve equals the emission distribution of the phosphorescence effect.

Figure II-2 depicts the process for τ longer than 10^{-8}s, which is called phosphorescence. The possible range for τ is considerable. It can range from a few µs (television screens) to several hours (clock faces). A change in temperature will affect τ, which is another distinction between phosphorescence and fluorescence (fluorescence shows almost no temperature dependence). Increasing the temperature during observation will reduce τ and vice versa. Within certain boundaries the total amount of light emitted will stay the same nonetheless. A mathematical explanation for the luminescence effect will be given in chapter II-3.

II.1.2 Thermoluminescence

"Thermoluminescence is the emission of light from an insulator or semiconductor when it is thermally stimulated. This is not to be confused with the light spontaneously emitted from a substance when it is heated to incandescence. Thermoluminescence is the thermally stimulated emission of light following the previous absorption of energy from radiation." [3]

In the definition given above three main conditions any substance must fulfill in order to be termed thermoluminescent, are given.

- A specific band gap structure is needed, which only semiconductors or insulators can provide. This is the main reason why electrically conducting materials will never show thermoluminescence.
- The substance has absorbed energy from previous exposure to ionizing radiation.
- The thermoluminescence can only be stimulated if the material is heated. This is also a onetime effect, once heated up and cooled down no second heating will produce thermoluminescence again if the substance has not been exposed to ionizing radiation once more.

The most common way to display thermoluminescence data is to plot the measured light intensity as a function of the applied heating temperature – this is known as a *glow curve* (figure II-3).

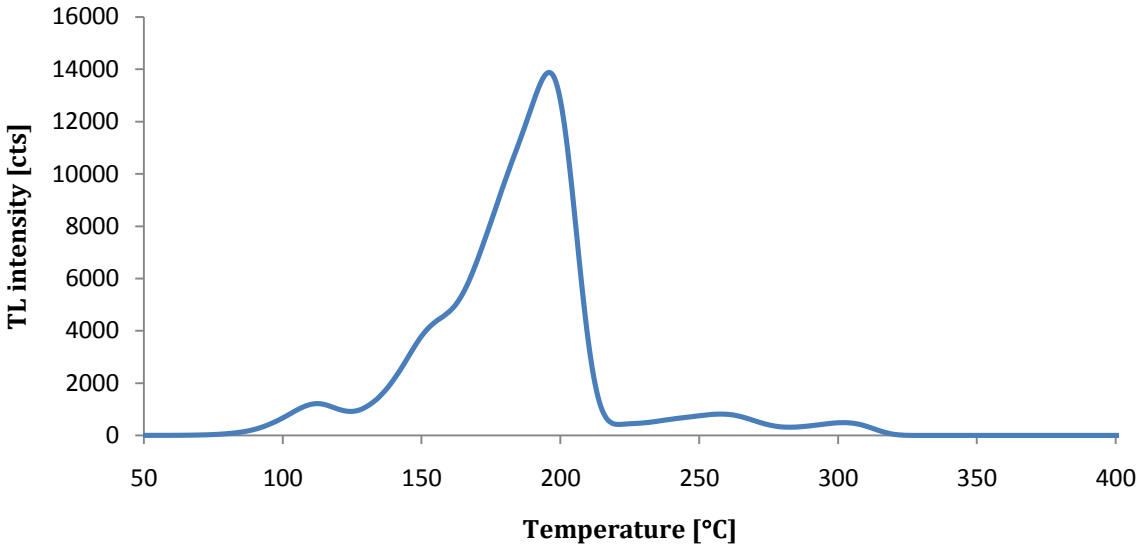

Figure II-3: glow curve of a ^{7}LiF:Mg,Ti (with ~300 ppm Mg, ~11 ppm Ti extruded chip irradiated to 2,06 mGy and measured with a heating rate of 1°C/s

The shown glow curve was measured from a ^{7}LiF:Mg,Ti (with ~300 ppm Mg, ~11 ppm Ti) extruded chip. The temperatures at which

the maxima emerge on average correspond to the activation energies of the respective centers. This means that, if a certain thermoluminescence active material is thermally stimulated within a certain temperature range, only those peaks whose trap depth corresponds to the applied temperature will occur.

The area under a peak corresponds to the number of trapped electrons which in turn is directly related to the amount of energy which has been absorbed by the sample. This fact makes thermoluminescent phosphors valuable dosimeters.

II.2 Absorbed Dose

A short introduction how to quantify the energy of ionizing radiation, which is transferred to and finally absorbed in matter, is given in this chapter.

Macroscopic Aspects:

As ionizing radiation enters a volume of matter (figure II-4 [5]) it loses an amount of energy dE by either creating electromagnetic radiation (E'_γ) and/or a secondary particle (T'). But only a part of these energies ($E'_{\gamma i}$ and T'_i) remains in the considered volume, since the secondary radiation may exit, thus taking a fraction of the energy out of the volume.

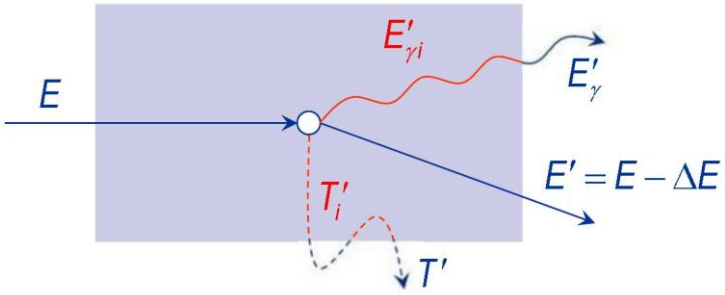

Figure II-4: Energy deposition in small mass elements

$$\left.\begin{array}{ll} \textit{Transferred energy} & dE = E_B + E'_i + T' \\ \textit{Absorbed energy} & dE_{abs} = E_B + E'_{\gamma i} + T'_i \end{array}\right\} \quad dE \geq dE_{abs} \qquad (1)$$

E_B … *Binding energy of the electron*

Transferred and absorbed energy are equal only, if the secondary radiation is absorbed entirely inside the considered volume.

The absorbed dose D is defined as the expectation value of the absorbed energy (dE_{abs}) divided by the mass (dm) of the volume.

Absorbed Dose $$D = \frac{\overline{dE_{abs}}}{dm} \quad (2)$$

$\overline{dE_{abs}}$ … *mean energy imparted by ionizing radiation to the matter in a volume element*

dm … *mass of the matter in the considered volume element*

The expectation value is necessary because of the stochastic nature of the energy deposition.

The unit of the absorbed dose is given by

$$1Gray\ (Gy) = \frac{1Joule\ (J)}{1kilogramm\ (kg)} \quad (3)$$

Microdosimetry

The definition used in microdosimetry for the energy imparted (here ε), which takes the energy equivalent of any change in rest mass into account, is:

$$\varepsilon = \sum \varepsilon_{in} - \sum \varepsilon_{ex} + \sum Q \quad (4)$$

Here ε is a stochastic quantity which is the difference between the sum of the kinetic energies of all the directly and indirectly ionizing particles, which have entered a volume ($\sum \varepsilon_{in}$) and the sum of the kinetic energies of all those which have left it ($\sum \varepsilon_{ex}$) plus the energy equivalent of any change in rest mass (decrease: positive sign; increase: negative sign), $\sum Q$, that took place in nuclear or elementary particle reactions within the volume.

Absorbed Dose $$D = \frac{d\bar{\varepsilon}}{dm} \quad (5)$$

$d\bar{\varepsilon}$ … *mean energy imparted by ionizing radiation to the matter in a volume element*

dm … *mass of the matter in the considered volume element*

II.3 One Trap - One Recombination Center Model

II.3.1 Introduction

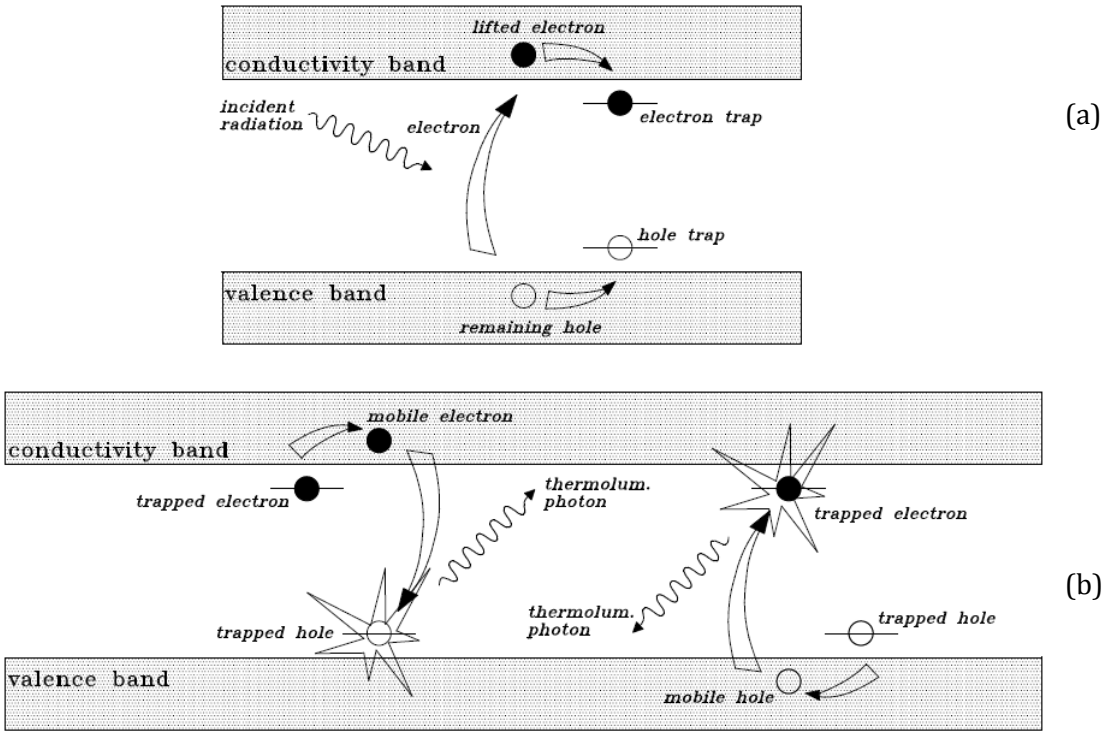

Figure II-5: (a) Energy levels in a thermoluminescence detector; (b) the process of thermoluminescence.

During equilibrium most of the charge carriers reside within the valence band, in a semiconductor/insulator. In a perfect crystalline structure, the only other possible place, within the semiconductor/insulator, for the charge carriers to occupy is the conduction band. However, this band is separated from the valence band by an energy gap E_g. Within this energy range no charge carrier may reside for any period of time.

If a more real crystal lattice is taken into account, then there are a number of impurities and deviations from the perfect crystalline structure. These cause local variations in the band structure, resulting in new energy states charge carriers may occupy, some of which are within the former "forbidden" energy range.

The model described here uses two such energy levels. One (R) is situated below the Fermi energy near the valence band, with the function of a recombination centre. The other (T) above the Fermi energy, below the conduction band with the function of an electron trap (figure II-5 [6]).

If, in this model, energy $h\nu > E_g$ is absorbed by an electron, it will be excited into the conduction band, leaving a positive charge surplus (hole) behind. This excited electron remains in the conduction band for a very short period of time (~10^{-8}s) only, then it can either become trapped at T or recombine with a hole in the valence band.

The probability (p) for the release of an electron from an occupied trap into the conduction band is given by the Boltzmann equation.

$$p = s * e^{\left(-\frac{E}{k_B T}\right)} \tag{6}$$

Here, s is the frequency factor or attempt-to-escape frequency. In this simple model it is considered a constant which is not temperature dependent, with values in the order of the lattice vibration frequency (10^{12} – $10^{14}s^{-1}$). E is the energy difference separating the trap from the conduction band, k_B is Boltzmann´s constant (8,617 * 10^{-5}eV/K) and T the absolute Temperature.

Since the lifetime of the trap is given by

$$\tau = \frac{1}{p} \tag{7}$$

it follows that if $E \gg k_B T_0$, with T_0 being the temperature the sample was kept at since the radiation exposure, the trapped electron will remain there for a long period of time. This means that, depending on the trap depth, several traps will be populated. Since a free electron is created along with its

corresponding hole, the same applies to the hole and its respective trap R.

This situation represents a non-equilibrium state, since T is situated above the Fermi energy E_f and R below it. Reverting to equilibrium is depending on E/T_0 and thus can take a very long time ($\leq 10^9$ years).

It is obvious that the return to equilibrium can be speeded up if the temperature is raised above T_0. As a result the probability of releasing a trapped electron into the conduction band increases. Such an electron has again two paths to follow. This means it can get retrapped at a similar electron trap it was previously released from, or it can recombine with a recombination centre at R. However, in first-order kinetics the possibility of retrapping is considered insignificant compared to the probability of recombination at R. A finite retrapping possibility is taken into account in the second-order kinetics model.

If the electron recombines at R, the released energy is emitted as a photon. This is the light which is observed as thermoluminescence.

The intensity I(t) of the observed light per unit time equals the number of recombining holes and electrons at R. It can be written as

$$I(t) = -\frac{dm}{dt} \quad , \tag{8}$$

where m ($1/m^3$) equals the density of holes which are trapped at R. The negative sign is needed to describe the decrease of m as the recombination process is in progress.

This model assumes that every recombination produces a photon and that all such photons can be detected.

The recombination rate will also be proportional to the number of free electrons (n_c) in the conduction band and the corresponding density of holes (m). This means

$$I(t) = -\frac{dm}{dt} = n_c m A_m \tag{9}$$

with the constant A_m as being recombination probability expressed in $m^3 s^{-1}$.

The rate of change of concentration of trapped electrons n is equal to the rate of thermal release minus the rate of retrapping:

$$-\frac{dn}{dt} = np - n_c (N-n) A_n \tag{10}$$

Here, N is the density of electron traps and A_n the probability of retrapping ($m^3 s^{-1}$) for electrons. In the same way as above, the concentration of free electrons is equal to the rate of thermal release minus the rate of retrapping and the rate of recombination:

$$\frac{dn_c}{dt} = np - n_c(N-n)A_n - n_c m A_m \tag{11}$$

These three equations form the basis of many thermoluminescence analyses. Important to note is that the processes described herein only apply to a single electron trap and a single recombination center.

However, even under these strong simplifications there is no analytical solution yet. Hence, some additional simplifying assumptions must be made, to develop analytical expressions.

The quasi-equilibrium [7] assumption is named so, because it requires that the concentration of electrons in the conduction band is quasi stationary.

$$\left|\frac{dn_c}{dt}\right| \ll \left|\frac{dn}{dt}\right|; \qquad \left|\frac{dn_c}{dt}\right| \ll \left|\frac{dm}{dt}\right|. \tag{12}$$

Since charge neutrality is required, it follows that

$$n_c + n = m, \tag{13}$$

which means with $n_c \approx 0$ that $n \approx m$ and

$$I(t) = -\frac{dm}{dt} \approx -\frac{dn}{dt}. \tag{14}$$

Because of $\frac{dn_c}{dt} \approx 0$, n_c can be expressed as

$$n_c = \frac{np}{A_n(N-n)+mA_m} \tag{15}$$

so that I(t) can be written as

$$I(t) = \frac{mA_m np}{A_n(N-n)+mA_m} = \frac{mA_m ns*e^{(-\frac{E}{k_B T})}}{A_n(N-n)+mA_m}. \tag{16}$$

II.3.2 First-order kinetics:

With the current set of assumptions this equation still cannot be solved analytically. As mentioned before, one way to solve it is to assume a negligible retrapping probability p, as Randall and Wilkins [8] did. This can be expressed as

$$mA_m \gg (N-n)A_n. \tag{17}$$

Under this assumption, the fraction in the above equation for I(t) reduces to

$$I(t) = -\frac{dn}{dt} = ns*e^{(-\frac{E}{k_B T})}. \tag{18}$$

This is called a first-order process, named after the power of n. If the temperature is kept constant,

$$p = s*e^{(-\frac{E}{k_B T})} \tag{19}$$

becomes a constant and I(t) will become an exponential decay function of time $I(t)=I_0 e^{-tp}$. This corresponds to the phosphorescence effect shown in figure II-2.

However, if the temperature is not constant, but varies in time, p is no longer constant and solving the differential equation for I(t) yields:

$$I(t) = -\frac{dn}{dt} = n_0 s * e^{\left(-\frac{E}{k_B T(t)}\right)} e^{-s\int_0^t e^{\left(-\frac{E}{k_B T(t')}\right)} dt'}, \qquad (20)$$

with n_0 being the total number of trapped electrons at time t = 0. If a continuous increase in temperature is observed, the intensity increases initially, will then reach a maximum and finally decrease as the number of trapped electrons becomes small compared to the situation prior to the temperature increase. This intensity function is called a first-order peak.

If a specific temperature function is used, namely a linear heating rate, as is used in most thermoluminescence experiments:

$$T(t) = T_0 + \beta t, \qquad (21)$$

the above function for the intensity is modified to

$$I(T) = -\frac{1}{\beta}\frac{dn}{dt} = n_0 \frac{s}{\beta} * e^{\left(-\frac{E}{k_B T}\right)} e^{-\frac{s}{\beta}\int_{T_0}^{T} e^{\left(-\frac{E}{k_B T'}\right)} dT'}. \qquad (22)$$

This is the Randall-Wilkins first-order expression for a single peak. Important to note is the stability of the peak position with varying n_0 values (figure II-6). This property will be utilized in the T_m-T_{stop} method.

Another characteristic of a first-order peak is its asymmetry. The peak is broader on its low-temperature side and narrower on the high-temperature side. Halperin and Bramer [9] defined a geometric factor

$$\mu_g = \frac{\delta}{\omega} \qquad (23)$$

which is the relation of the full-width-at-half-maximum of both sides, where δ stands for the high-temperature side, ω

for the low-temperature side. A typical value for a first-order peak would be 0,42. The reason for this asymmetry is the dominance of the first exponential factor

$$e^{\left(-\frac{E}{k_B T}\right)} \qquad (24)$$

for the low-temperature side.

This circumstance can be employed in the initial rise method to acquire the trap depth (E) of the said peak. TL intensity is plotted over $\frac{1}{T}$ to obtain the slope of the now linear lower-temperature side of the peak, given by $\frac{E}{k_B}$ so that E can be obtained.

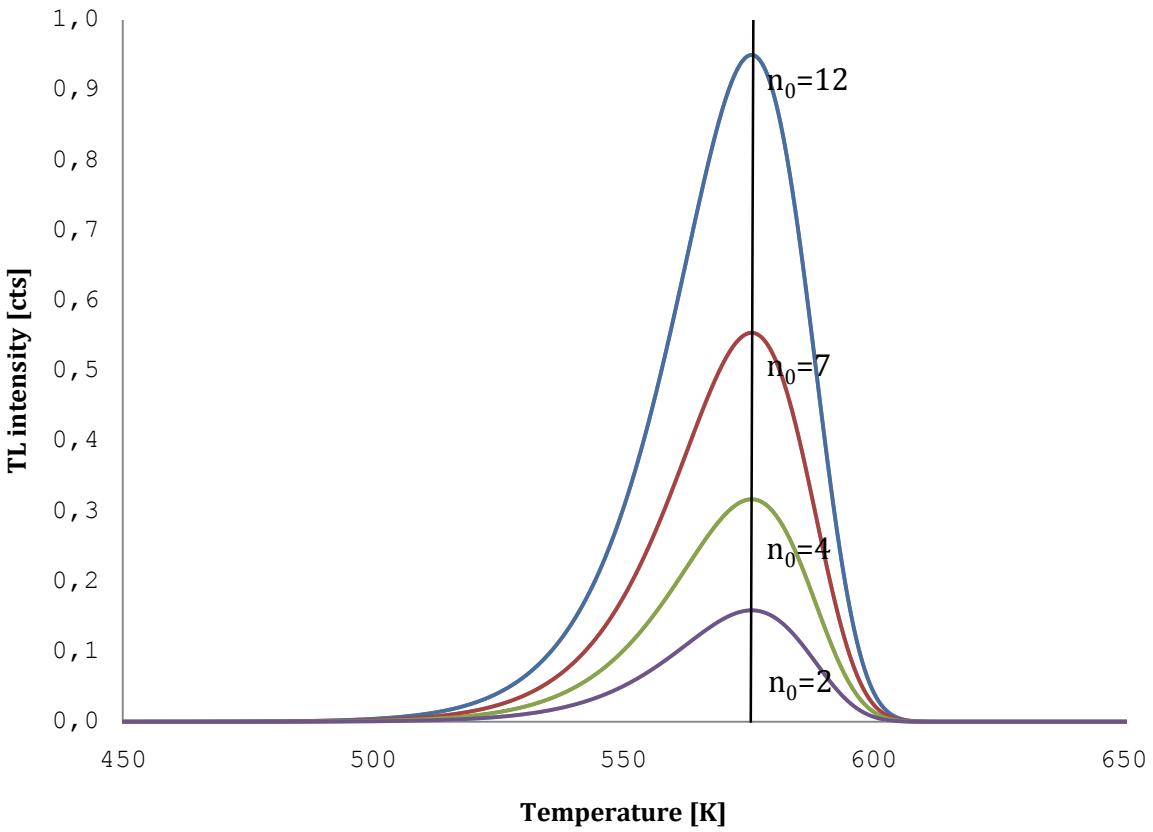

Figure II-6: Randall-Wilkins first-order peaks for different concentration (n_0) of charge carriers after irradiation.

The Randall-Wilkins first-order expression for a single peak is also the equation which was used to deconvolve all of the measured glow curves to obtain the temperature of peak maxima, as will be explained later in more detail.

II.3.3 Second-order kinetics:

Contrary to the first-order assumption (retrapping is negligible), Garlick and Gibson [10] considered the dominance of the retrapping process and the trap niveau being far from saturation.

$$I(T)=\frac{n_0^2}{N}\frac{s}{\beta}e^{-\frac{E}{kT}}\left[1+\frac{n_0 s}{N\beta}\int_{T_0}^{T}e^{-\frac{E}{kT'}}dT'\right]^{-2} \qquad (25)$$

This curve features near symmetry, with the high-temperature side slightly broader. Since $I(T) \propto n_0^2$, equation (23) is termed a second order peak.

The main difference to a first-order peak concerning this work is, since the initial concentration n_0 is not a linear multiplicative constant anymore, it influences the whole shape of the glow curve. One consequence is the shifting of the peak position with varying n_0 values, which results in a different behavior of the peak when the T_m-T_{stop} method is applied to such a peak.

II.4 T_m-T_{stop}:

II.4.1 Basics:

This method was suggested by McKeever [1] to resolve glow curves into their individual peaks.

In the previous chapter the development of a single-trap model was explained. The glow curve of such a sample would be represented by a single peak at a temperature which approximately corresponds to its activation energy.

However, if a real sample is measured it becomes apparent, that the number of peaks, as well as their intensity is not known a priori.

This is the problem the T_m-T_{stop} method tries to solve, as each point of a measured glow curve can be thought of as the summation of an unknown number of peaks with an unknown intensity, if the background signal from spurious luminescence and electronic noise is not taken into account.

In order to reduce the complex situation to a more manageable size, McKeever's method uses a set of manipulated glow curves. To obtain these, two heating cycles, for each sample, are needed, but only the second is recorded. These cycles are equivalent in using the same heating rate, but differ in the highest temperature that is reached.

In the first heating cycle which is called the "pre-heating process", the sample is heated up to a certain temperature T_{stop}, using a standard heating rate of 1 to 5°Cs^{-1}. Important to note is that, once defined, this heating rate must be retained in all the other measurements needed to generate the T_m-T_{stop} diagram. Once T_{stop} is reached, the sample is cooled down to room temperature in the measuring chamber.

At this point the second heating cycle starts. Again at the same linear heating rate, only this time the thermal stimulation of the sample continues to its highest point, usually in the range between 400 and 500°C in order to record the residual glow curve.

From the recorded glow curve only the position (temperature T_m) of the peak at the lowest temperature is noted.

The whole process is then repeated, ideally on the freshly irradiated same sample, for a different temperature T_{stop}, with temperature increments in the order of 2 to 5°C. In this way, the whole temperature region in which the chip is usually read out is covered. For practical reasons, it is obvious that the measuring cycle would take much too long if only one sample is read out and irradiated over and over again. Usually several samples from within the same batch are selected which display similar glow curves.

A plot of all T_m values against the T_{stop} values finally yields the T_m–T_{stop} diagram (Figure II-7).

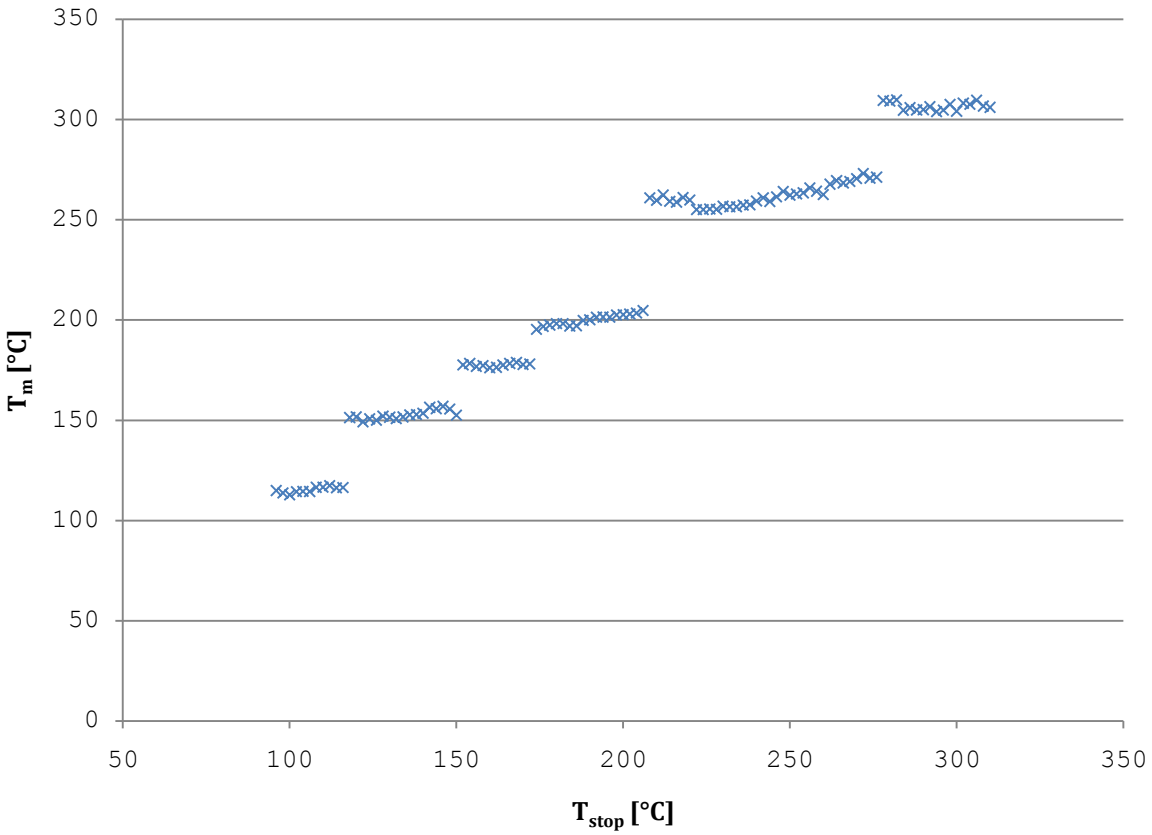

Figure II-7: T_m-T_{stop} diagram obtained from a TLD-700, irradiated to 8,07mGy

The plot is a straight line, for a single-peak glow curve, ending at a temperature T_{stop} at which the peak would be completely annealed. For a glow curve containing several first-order peaks, the T_m-T_{stop} diagram resembles a staircase function. Each of the flat regions identifies an individual peak.

When peaks are very close, corresponding to a quasi-continuous distribution of trapping centers, the T_m-T_{stop} plot gets a more continuous form (Figure II-7: Temperature range 250 to 270°C). This also sets a limit to this technique, since individual peaks can no longer be identified. This resolution is usually in the order of 5 to 8°C.

Important to note is that the standard application of this method has difficulties resolving smaller peaks in the vicinity of more prominent peaks, even if they are separated

by more than 20°C. To counteract this effect, special measures can be taken, as will be explained later.

II.4.2 Visualizing T_m-T_{stop}:

This chapter will try to give a better insight into the procedures during a T_m-T_{stop} experiment.

But first, an approximation for the heating process must be made, since the form of the heating shoulder has significant influence on the way each peak gets annealed, resulting in a different resolution the T_m-T_{stop} method can achieve. It can be thought of as the probe for this measurement, and the broadness of the shoulder defines how fine it is.

The temperature function is highly dependent on the heating rate as well as the actual way the temperature is applied to the sample, which in turn means that each heating device will be characterized by its own function. Of course, this function is modified for each sample in turn, depending on its size, form and type (i.e. a single crystal, a sintered chip or a powder).

For this visualization model a Gauss function was chosen, whose negative gradient is higher than that of the high-temperature shoulder of the peaks, ensuring that the "probe" does not interfere with the structure of the peaks.

The following graphs will use first-order peaks, as were derived in the previous chapter, in order to simulate the glow curves.

II.4.3 Single Peak

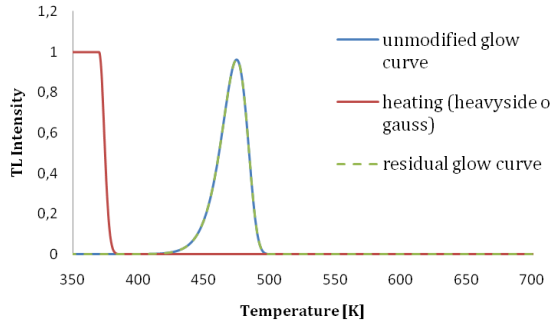

Figure II-8: Residual and unmodified glow curve are equal. The pre-heating temperature is too low (370 K).

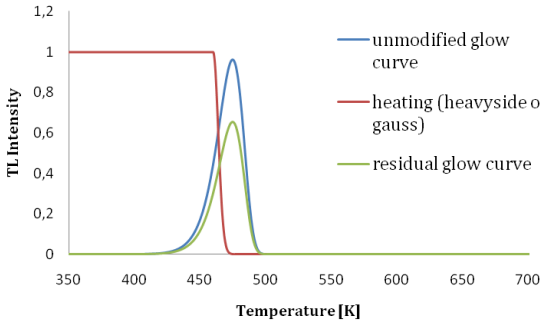

Figure II-9: The preheating (460 K) anneals part of the glow curve. The residual signal equals unmodified minus heating.

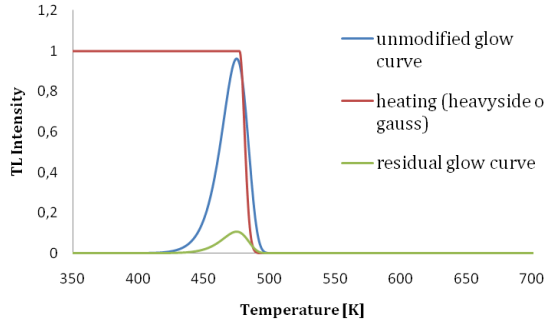

Figure II-10: Even if the preheating (477 K) is higher than the peak maximum, a residual signal remains.

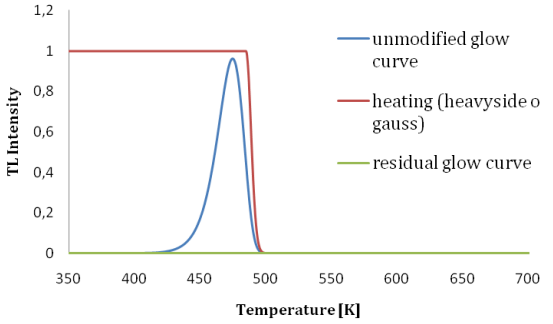

Figure II-11: The residual glow curve is fully annealed if the pre-heating temperature is beyond the upper shoulder of the glow curve.

The figures II-8 to II-11 show the effect of pre-heating on a single-peak glow curve. As can be deducted from the Wilkins formula (22) (also see Figure II-6), the peak position itself will not change if part of the peak is annealed, but it will simply decrease in intensity, until nothing remains if the heating reaches beyond the upper shoulder of the peak. This is also one of the main characteristics of a first-order peak as was mentioned earlier.

It also defines one inherent problem as well. The peak will not vanish immediately once the temperature of the pre-heating surpasses the temperature (T_m) of peak maximum intensity, but will steadily decrease in intensity until such a point where the heating is well beyond the upper shoulder of the peak. The

problems arising from this fact will be clear if two peaks are considered.

II.4.4 Two Peaks

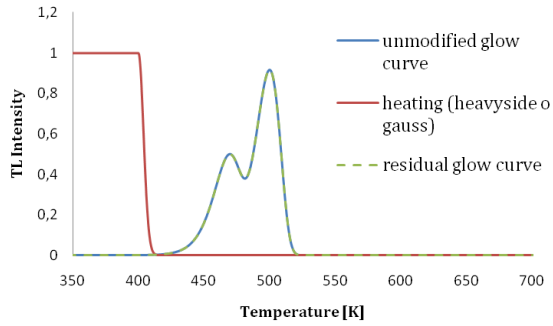

Figure II-12: The pre-heating stops at 400 K and does not have any influence.

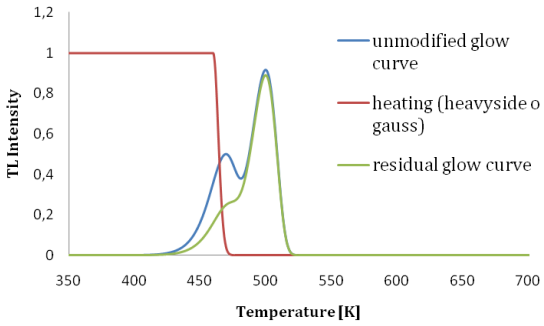

Figure II-13: Pre-heating stops at 460 K. Only the first peak is partially annealed.

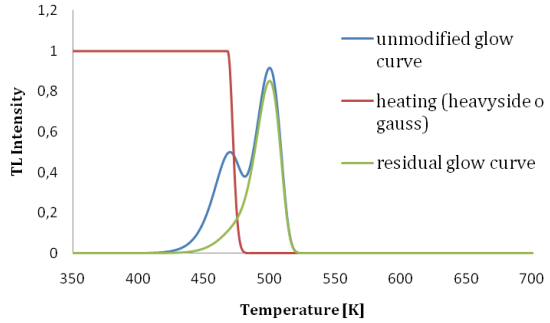

Figure II-14: Same situation as in II-10. However, here the residual signal of peak 1 cannot form a maximum.

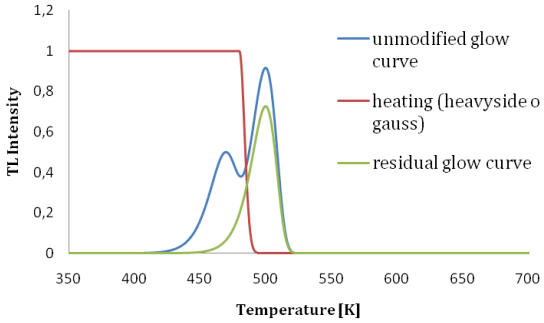

Figure II-15: The pre-heating (480 K) now starts to noticeably anneal the second peak.

In this example a glow curve consisting of two peaks is considered. Peak 1 resembles a smaller, broader peak followed by a more prominent and sharper peak 2. As can be seen from figure II-13, a problem with the T_{stop} values arises even before the temperature of maximum intensity of the composite peak is reached. Because the following peak is much more prominent, the resulting glow curve will not show any local extremum in the region of peak 1, thus reducing the number of measurement points to identify this peak. This situation gets worse if T_{stop} is increased. There are still traces of peak 1 to be found in the glow curve in figure II-14, but there is no way to read out a peak position without additional help.

For the T_m-T_{stop} plot of these two hypothetical peaks it is not a problem, however, since at some point there is a definite local maximum for peak 1. So if the local maximum vanishes into a saddle point, the next local maximum is noted, and so on. As long as local maxima exist, this method works fine and produces a T_m-T_{stop} diagram.

II.4.5 Annealed Peak Method

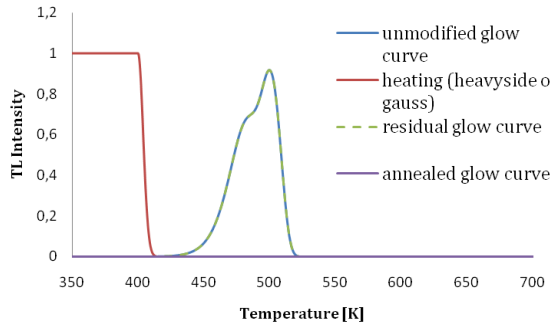

Figure II-16: Two peaks (477 K and 500 K). No local maximum of the first peak is discernible.

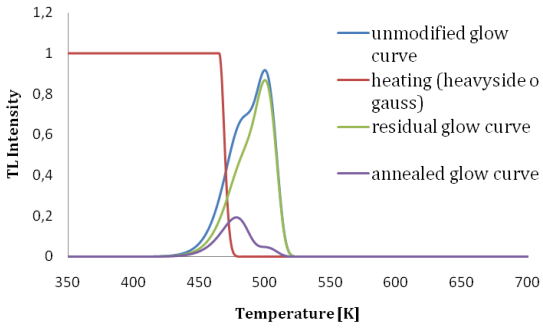

Figure II-17: The annealed peak glow curve equals unmodified glow curve minus residual glow curve.

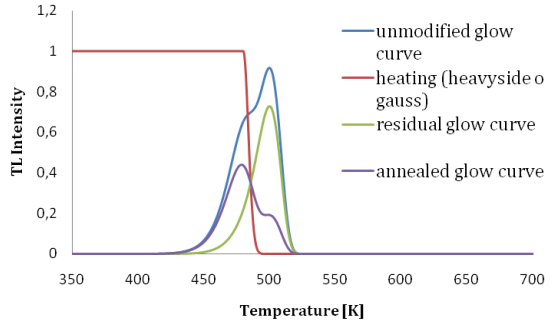

Figure II-18: Preheating starts to anneal the second peak..

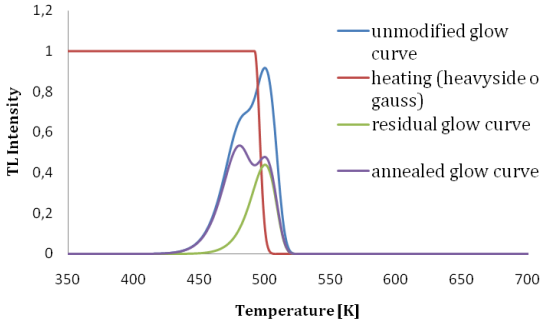

Figure II-19: The second peak is partly annealed and can also be seen in the curvature of the annealed peak curve.

If the situation in figure II-16 is taken into account, it would not be possible to note either of the peaks. The two peaks are separated by 23 K, so this is by far above the resolution given earlier.

The figures II-17 to II-19 show one way to solve this situation. The blue curve depicts the "annealed" peak which was "removed" from the original glow curve during the pre-

heating cycle. This curve features switched prominence of the glow peaks, so peak 1 is the dominant one and peak 2 is almost nonexistent for low temperatures T_{stop} (figures II-17 and II-18). The situation is best explained by considering that the annealing now seems to extend from high to low temperatures, thus reversing the real situation.

With increasing T_{stop} (figure II-19) the usability of this curve decreases since peak 1 is fully established. The increase in intensity suffers a switch from the shoulder of peak 1 to peak 2, which means that the increase rate stalls. How abrupt this change manifests, depends on the temperature separation and of the different parameters of peak 1 and 2.

To obtain the "annealed peak curve" it is necessary to first record a reference glow curve for the measured chip, for the same experimental protocol (irradiation dose and heating rate). Even if the curve has a slight offset in temperature, due to statistical variations, this can be corrected by aligning the reference at the prominent peak of the measured glow curve. As can be seen in figure II-17, even for closely neighboring peaks T_{stop} is still far away from the position of the prominent peak, thus ensuring a minimum of influence. But even at this point the smaller peak develops a well established extremum. This is due to the asymmetry of a first-order peak.

II.4.6 Deconvolution

Currently, the best method to obtain a T_m-T_{stop} diagram is to use a glow curve deconvolution software to unfold the peak positions in the remaining glow curve. Here the residual glow curve is considered as a "standard" glow curve and the remaining known peak positions are set as constraints so as to

calculate the first peak in this glow curve with the highest accuracy. The corresponding T_m will then be noted in the T_m-T_{stop} diagram.

This works well for low temperatures and high doses. If T_{stop} increases, one restraint after the other is lost due to annealing, this leads to decreased accuracy. Low photon count rates can impose additional difficulties on the deconvolution software as the black-body background dominates and the signal-to-noise ratio decreases rapidly.

For this work, all three methods mentioned above were used to allow for comparison of the results. A detailed description of each method is presented in chapter III.2

III. Chapter

III.1 Experimental Realization

III.1.1 Process:

The measurements within this work were performed from 6 Jun 2007 to 19 November 2007. Within this time period a weekly schedule was chosen for the experiment. This means that, for example, one type of phosphor was read out on Wednesday, annealed on Thursday and irradiated anew on Monday. The specific experimental protocols are listed in chapter IV for each chip type below each individual heading.

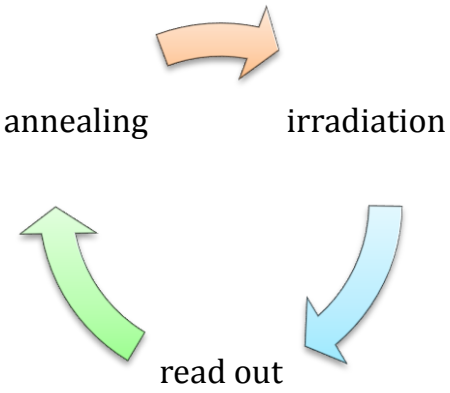

It was essential to verify the reliability of the measuring cycle so that each chip showed no variation in its glow curve during hundreds of measurements. This was partly achieved by keeping the time between irradiation and readout a constant, in order to control low-temperature fading. Another important factor in providing the same shape of the glow curves was the uniformity of the annealing process. The type of the annealing procedure had been carefully selected for reproducibility and was done in two different ovens, which are described below.

III.1.2 Used devices:

III.1.2.1 TL-Reader:

In this experiment the TL-DAT.II [11] was used, which features contact heating on a Nikrothal 80 austenitic alloy planchet. Nikrothal 80 is a composition of 20% chrome and 80% nickel, for use up to operating temperatures of 1200°C. Its chemical composition gives good oxidation resistance, especially under conditions of frequent switching or wide temperature fluctuations.

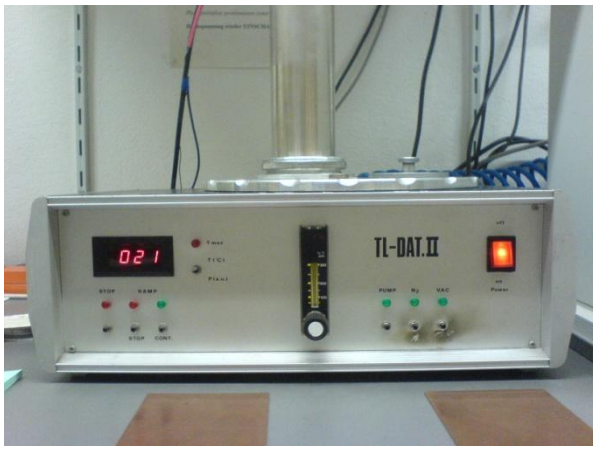

Figure III-1: TL-DAT.II in standby mode.

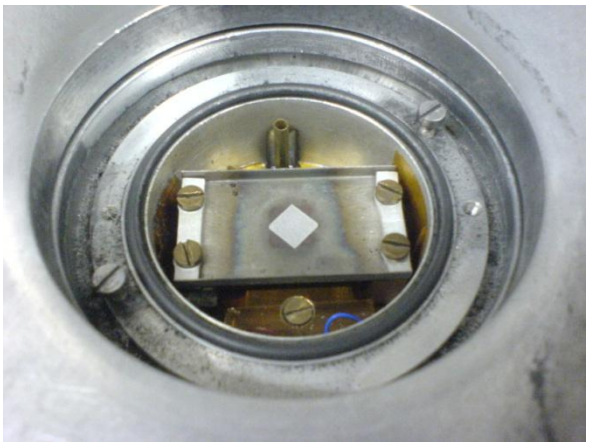

Figure III-2: View into the sample chamber. A TLD-700 has been placed on the Nikrothal 80 planchet.

Positioning a TLD on the plate (figure III-2) turned out to be crucial. As there was no possibility to fix the TLD in place, there were always slight variations of the TLD´s position on the heating plate with respect to the underlying heating coil. Since the plate showed a natural temperature gradient to its outlying regions, a chip positioned off center was heated up always a step behind the pre-programmed temperature, hence the observed temperature shifts of the measured glow curves. The usual practice to correct the above mentioned temperature shifts would have been to align the glow curves with their main peak. However, temperature aligning was not possible with two of the methods used in this work (local maximum and deconvolution), which means that this systematical problem had to be minimized in another way. This was one of the reasons

why a heating rate of $1°Cs^{-1}$ was chosen, to be as close to the temperature equilibrium of the TLD-plate-system as possible.

In addition, the sample chamber was always evacuated prior to the measurement (to minimize spurious luminescence) and was flooded with inert gas (5.0-grade high-purity N_2) during the measurement (to minimize chemiluminescence). However, the amount of N_2 flooding the chamber and with it the sample was another major factor influencing the sample temperature. Several measurements had to be discarded and repeated due to sudden variations in the gas flow.

III.1.2.2 Photomultiplier:

The used photomultiplier tube was a Thorn EMI 9635 QB with a bialkali photocathode (Thorn EMI Gencom, Inc., Fairfield, NJ, USA), which was usually shielded by a Corning 7-59 (blue) infrared filter, except for CaF_2 phosphors (see IV.1.1 TLD-300).

III.1.2.3 Annealing Ovens:

Two annealing ovens were used for this work.

- Heraeus KM 170 (Heraeus Instruments GmbH, Hanau, Germany). This oven uses controlled slow cooling (~24 h) with a strictly exponential cooling rate which is controlled by the heating capacity of the oven (see figure III-3 [12]). This oven was used for the PF, PG, TLD-300, TLD-700 and TLD-600 types of TLDs.

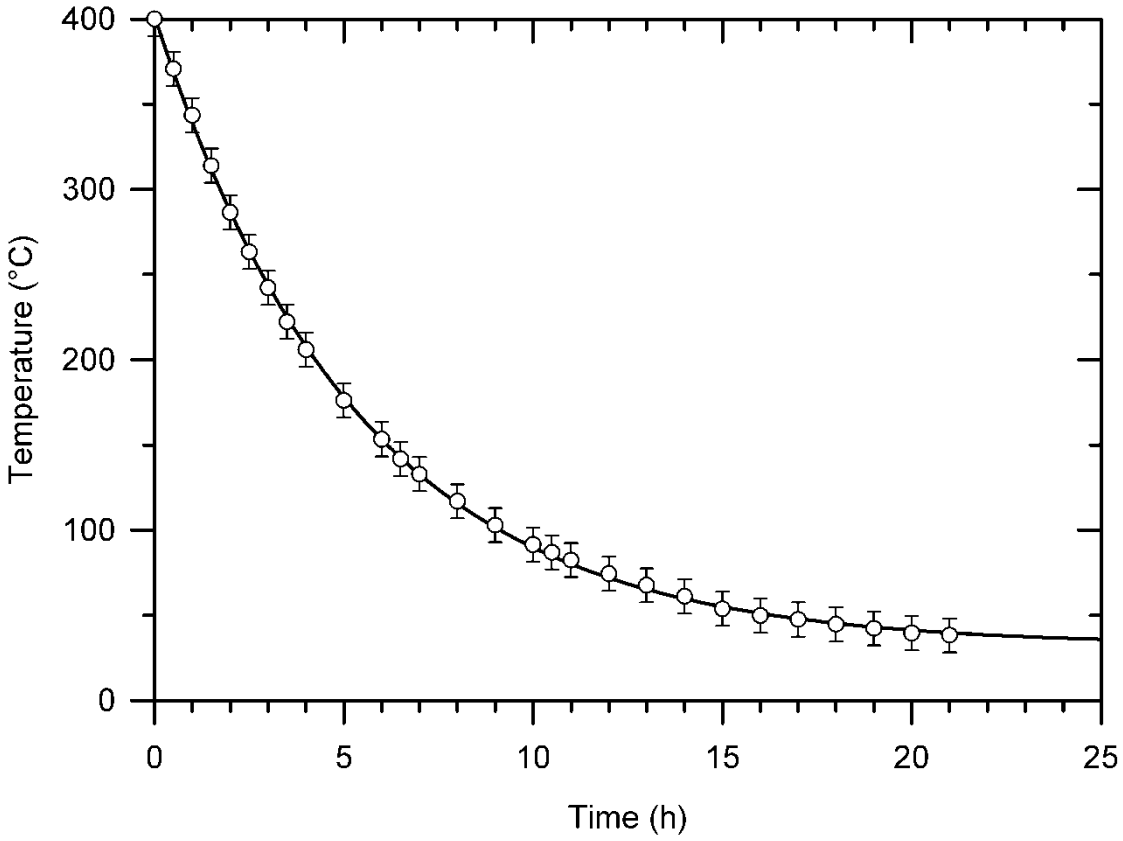

Figure III-3: Cooling rate of the Heraeus KM 170

- The second oven was a TLD-oven-LAB 01/400 (Könn GmbH, 9.2003). It was used for the MTT-7 type of phosphors. The chosen annealing cycle can be seen from figure III-4.

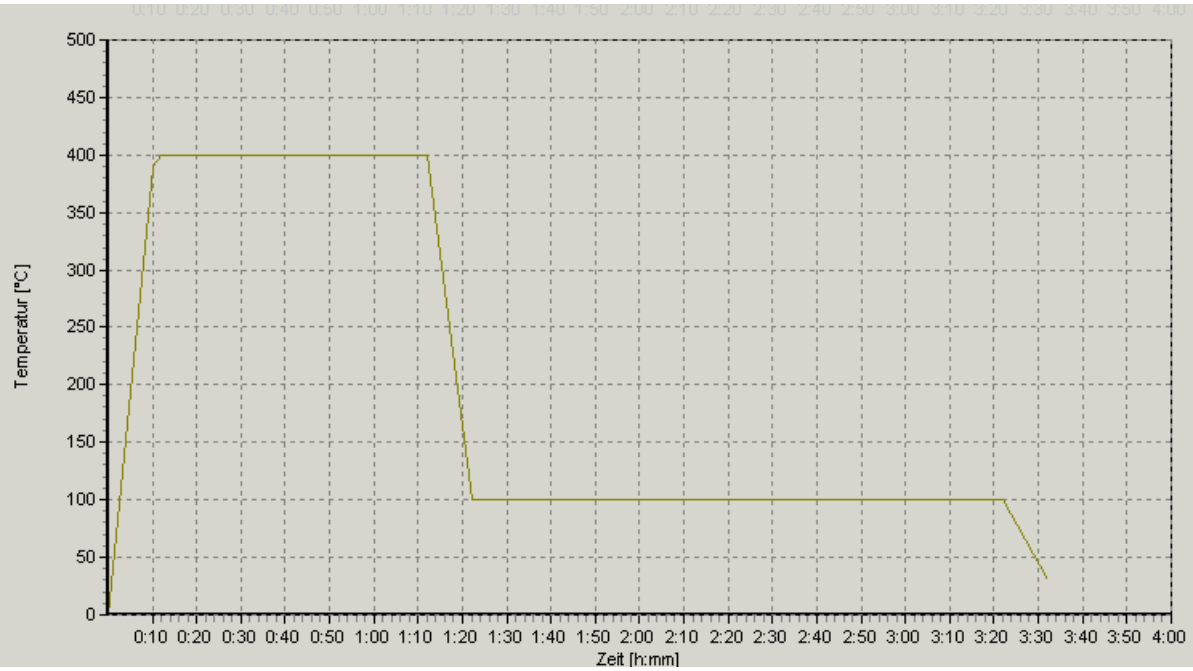

Figure III-4: Annealing cycle used for the MTT-7 type of TLDs in the LAB 01/400 oven.

This oven was also used for the tempering of half of the MTT-7 phosphors for 30 minutes at 120°C. The used heating cycle for this process is shown in figure IV-54.

III.1.2.4 Irradiation Source:

Exposure was performed using the gamma rays of a Cs^{137} source with an activity of 20,64 GBq at the 25.10.2000 (halve life of 30,17 years).

For specific irradiation durations and applied doses see each individual TLD experimental protocol.

III.2 Data Processing

The files from the software of the TL-DAT.II where loaded into an in-house developed analysis software and into GLOW FIT to deconvolve them, respectively.

Within the glow curve analysis software the background was subtracted and a 21-point smoothing was applied. Difficulties arose from certain background signals.

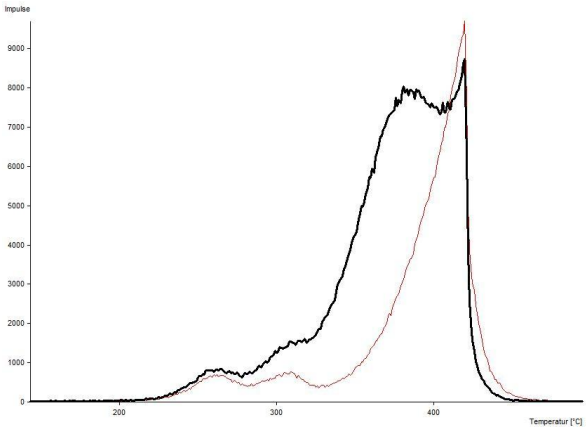

Figure III-5: The same TLD-700 was measured at the same T_{stop} temperature (246°C) two times. The red curve shows the black body background.

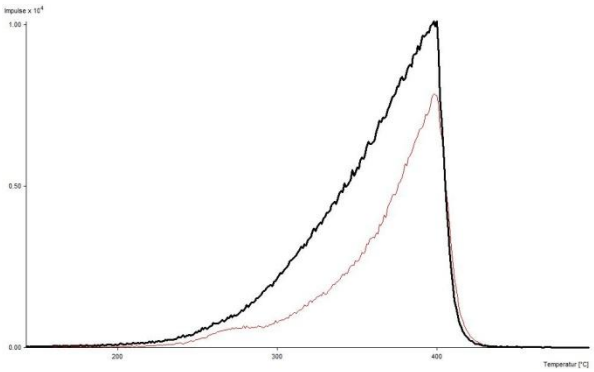

Figure III-6: Two measurements of the same MTT-7 phosphor (T_{stop} 260°C) show different background signals. The red curve shows the black body background.

As shown in figure III-5 and III-6 it was impossible to get a clean background fit from these curves. Figure III-5 shows a TLD-700 chip pre-heated to 246°C. Figure III-6 shows a MTT-7 chip pre-heated to 260°C. In both cases, the red glow curve represents the repeated measurement with the same TLD and the black body background.

Figure III-5 shows a very prominent "peak" at high temperatures. This behavior was observed mainly with sintered chips. It was not possible to verify a systematical structure for this effect. Therefore these measurements were discarded and then repeated.

The effect in figure III-6 was a systematical effect that appeared, whenever the flow rate of the inert gas (5.0-grade high-purity N_2) was far below the optimum level. Besides the

non-existent exponential increase which did not allow for a background subtraction at all, the signal-to-noise ratio was worsened considerably and in the shown case did not allow the expected peak to be resolved at all.

The results for the first two methods (local maximum, annealed peak method) could both be obtained directly within the glow curve analysis software.

For the deconvolution method, the final steps were made in the GLOW FIT program. As explained earlier, the pre-heating reduces the intensity of those peaks which are near or below the pre-heating temperature. Higher peaks are affected too, but only if -due to their broadness- some significant part of their low-temperature shoulder extends into this temperature range.

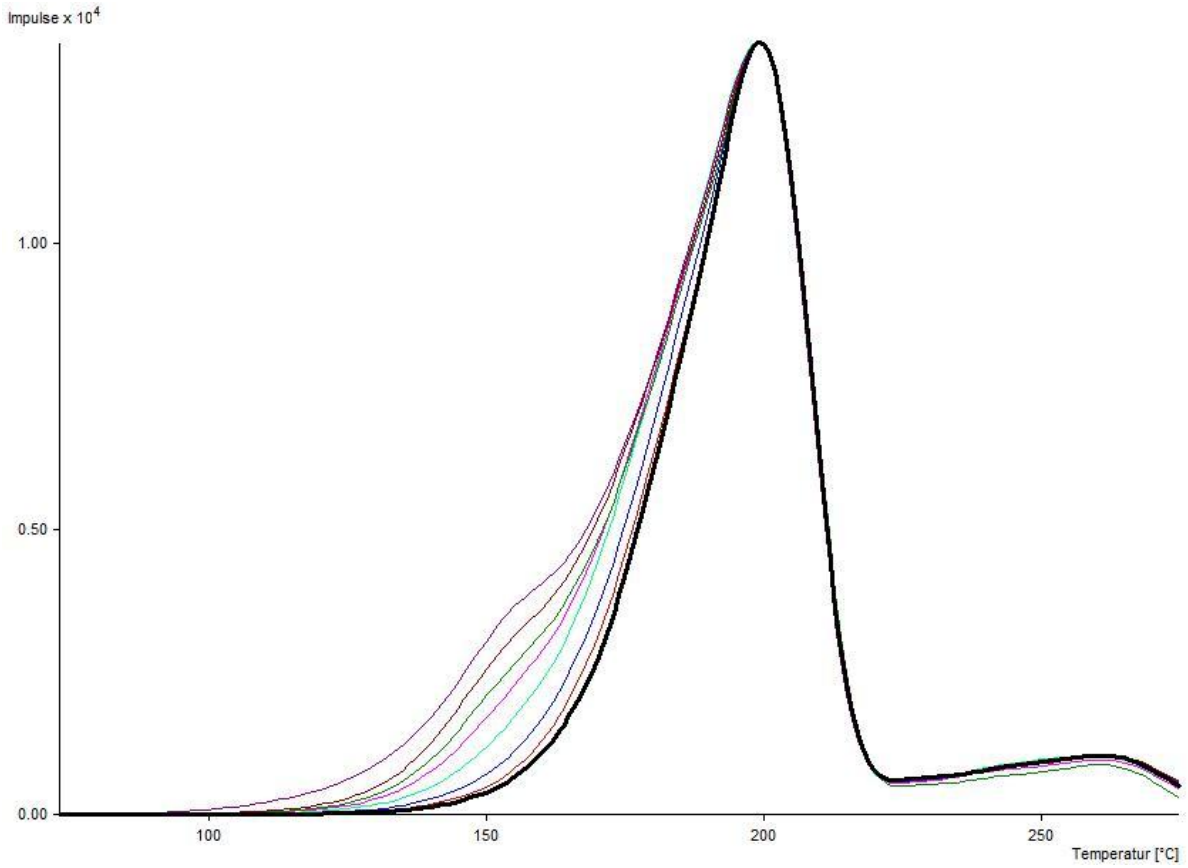

Figure III-7: TLD-700 (selection of glow curves for temperatures T_{stop} from 114 to 166°C, aligned at 199°C)

It can be shown with a series of preheated glow curves, with steadily increasing pre-heating temperatures, as in figure III-7 that the lowest peak diminishes over a certain temperature region. It gets increasingly difficult to judge if a peak really exists in a given glow curve. One definite sign is the changing curvature as shown in figure III-8. However, this is by no means a way to measure an accurate position for a given peak. With increasing number of peaks this can get very complicated and without additional help cannot be solved reproducibly. This was the main reason for choosing the program GLOW FIT to deconvolve glow curves in order to identify the individual peaks.

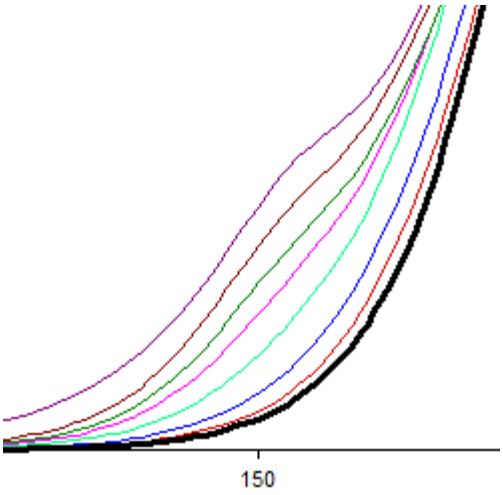

Figure III-8: Change in curvature for increasing T_{stop} values.

III.2.1 GLOW FIT

GLOW FIT [2] is a program written in C++ for use in the MS Windows environment. It is in its<current version solely based on the first-order kinetics model of Randall and Wilkins (see chapter II.3.2). Up to ten peaks may be deconvolved at the same time using an iterative procedure (least square Levenberg-Marquardt method) which starts from trial values (freely definable). The notable difference to other deconvolution software is the use of pattern files in which the trial values for specific phosphor types can be stored. Another feature is the possibility to set constrained peak parameters for deconvolutions.

It is a usual and necessary practice to define some a priori information such as known maxima or other well known aspects

to “guide” the deconvolution algorithm. However, this was not always possible for glow curves used in this work. Contrary to the usual practice of aligning different measurements of the same TLD type at a certain peak maximum (thereby eradicating the effect of different chip positions on the heating plate as mentioned before), it could not be done here, because of a simple, though unforgiving reason. Since it would be necessary to align all measurements to the same maximum, this could hardly be done with those measurements which were pre-heated to a higher temperature than this maximum, effectively annealing this peak. So the only possible ways was indicating expected peaks in the GLOW FIT program as best as possible and not fix anything. However, as explained in chapter II.4.5 with the use of the annealed peak method it is possible to obtain a restraint for GLOW FIT in especially difficult situations.

From the deconvolution, the temperature of the first peak was recorded if his intensity was higher than ~150 counts. If the complete intensity of the residual signal was no higher than ~400 counts, this rule did not apply. This situation especially arose in the high-temperature region above 230°C where the residual glow curve intensity generally was very small, because of the relatively small dose of ~8 to 20 mGy.

With increasing pre-heating temperature the intensity of the observed peak decreased, until it was of the order mentioned above, which defined the point of switching to the next peak and thus creating a step in the T_m-T_{stop} diagram. This peak was then removed from the deconvolution process as it was no longer needed. Every deconvolution was saved and the peak position and intensity of the first peak noted. These provided the necessary information for the finally resulting T_m-T_{stop} diagram.

III.2.2 Nomenclature

It is important to note that the identified peaks were numbered consecutively as they were found with each method. Hence peak 2 identified with the local maximum method does not necessarily correlate to peak 2 found with the deconvolution technique. Also, this nomenclature is sometimes not in accordance with the established denotation.

IV. Chapter

IV.1 TLD-300 (CaF_2:Tm; single crystals)

IV.1.1 Experimental Protocol

Irradiation Parameters:

distance from source	1 m
duration	2 h
source	Cs-137
absorbed dose	2,06 mGy
number of dosimeters	9

Three days passed between irradiation and readout. As TLD-300 emits partly in the infrared, the IR filter (Corning 7-59 (blue), see chapter 2 experimental realization) in front of the photomultiplier was removed before the measurements. The annealing commenced three days after the measurement together with the TLD-600, TLD-700, PF and PG dosimeters in the Heraeus KM 170 (see chapter III.1.2.3).

Measurement Parameters:

heating rate	$1°Cs^{-1}$
heating interval	~25°C – 400°C
T_{stop} increment	2°C
T_{stop} interval	90°C – 266°C

IV.1.2 Reference Curve

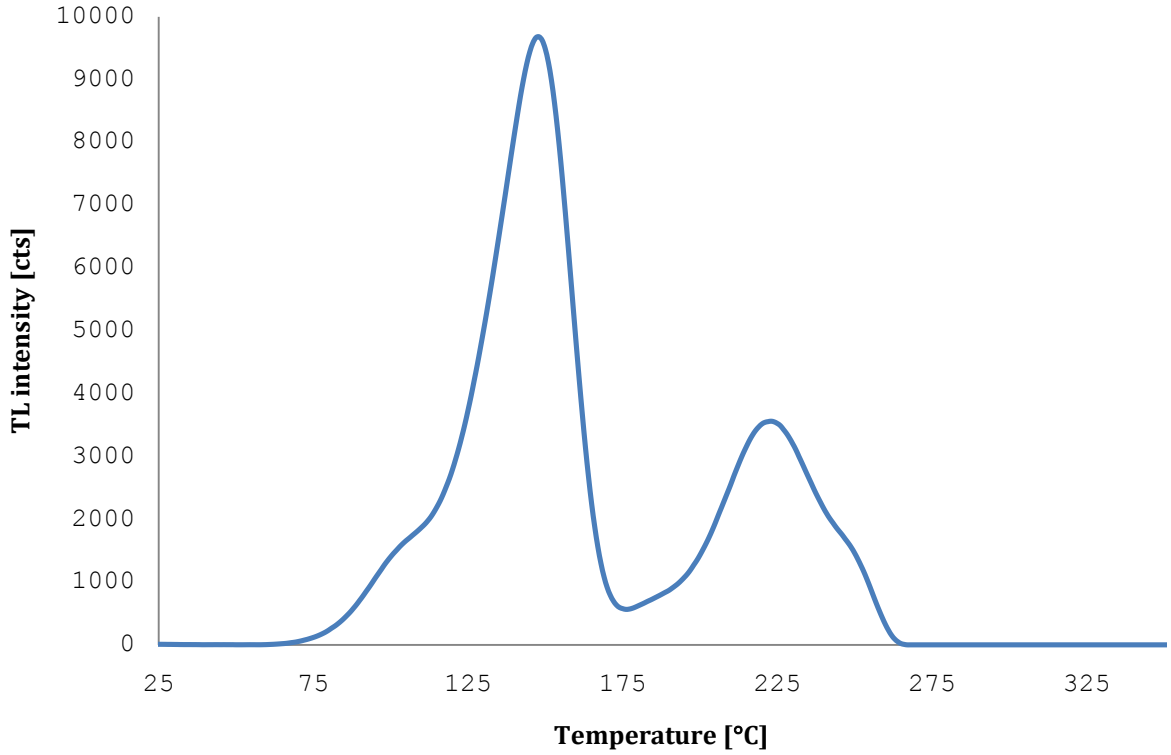

Figure IV-1: Reference curve for the TLD-300 phosphor

Using the above irradiation and readout parameters the glow curve of a TLD-300 phosphor will look like in figure IV-1. This curve was obtained from 27 measurements. Each of the nine TLD-300 chips was measured three times, and then the arithmetic mean for the position of the highest peak intensity was calculated. All curves were then aligned at this temperature, in this case 148°C. The maximum shift was ±4°C. The final step was obtaining the normalized mean of all the curves which is the curve shown in figure IV-1. This curve will be used in the annealed peak method and is shown here as a reference.

IV.1.3 Local Maximum Method

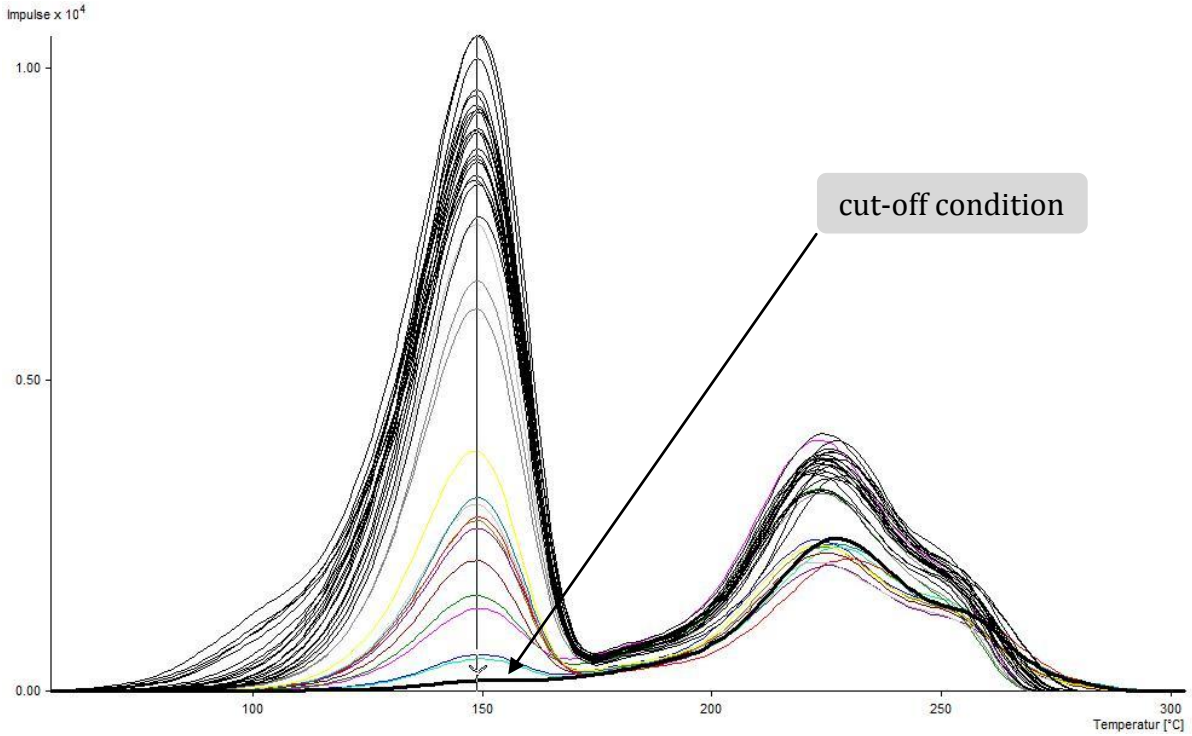

Figure IV-2: TLD-300; T_{stop} values from 90 to 158°C

The T_{stop} range for the residual glow curves shown in figure IV-2 is from 90 to 158°C. For better visibility the peaks were aligned at 148°C. The bold black curve which is shown almost at the bottom of the figure, represents the cut-off condition for this peak. With this method the barely visible peak at ~100°C could not be resolved, since it develops no local maximum.

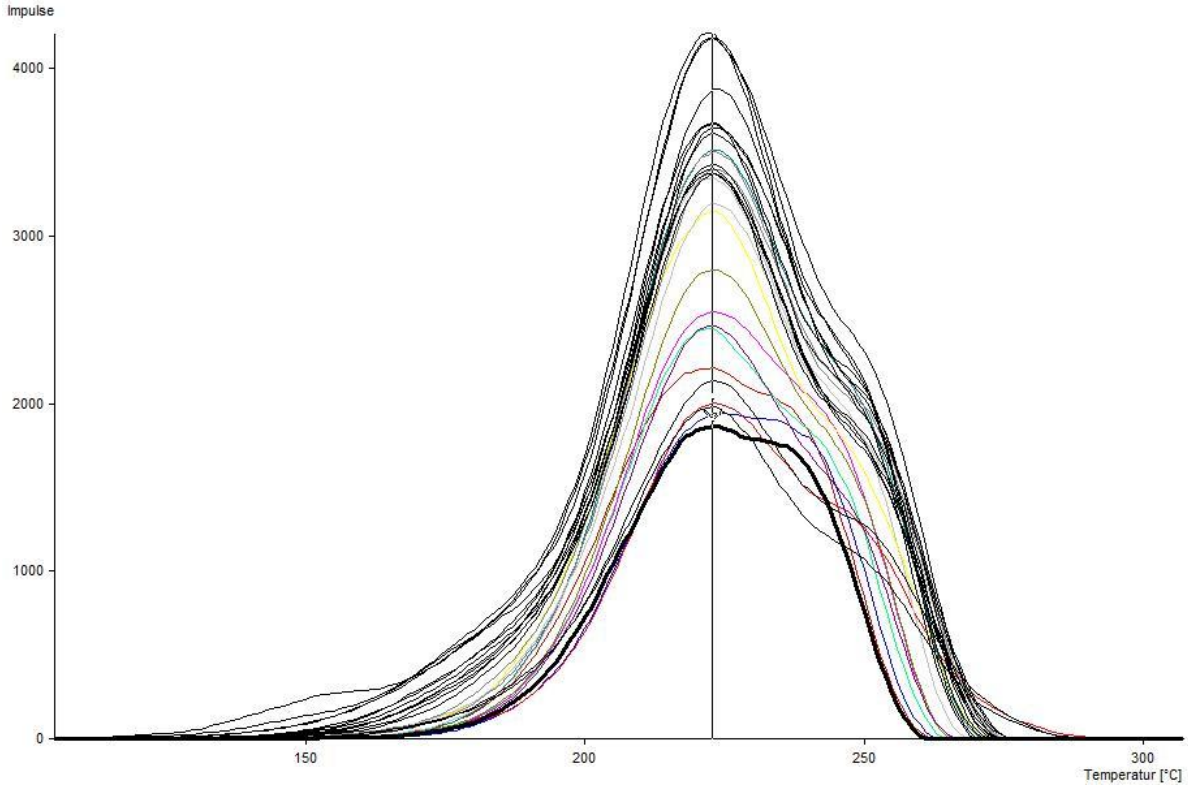

Figure IV-3: TLD-300; T_{stop} values from 160 to 222°C

In figure IV-3 the residual glow curves for T_{stop} ranging from 160 to 222°C are shown. Like before the black curve depicts the cut-off condition. The curves were also aligned, this time at the dominant peak at 223°C. At ~180°C seems to be another peak. Nevertheless, since it does not develop a local maximum it has to be ignored here.

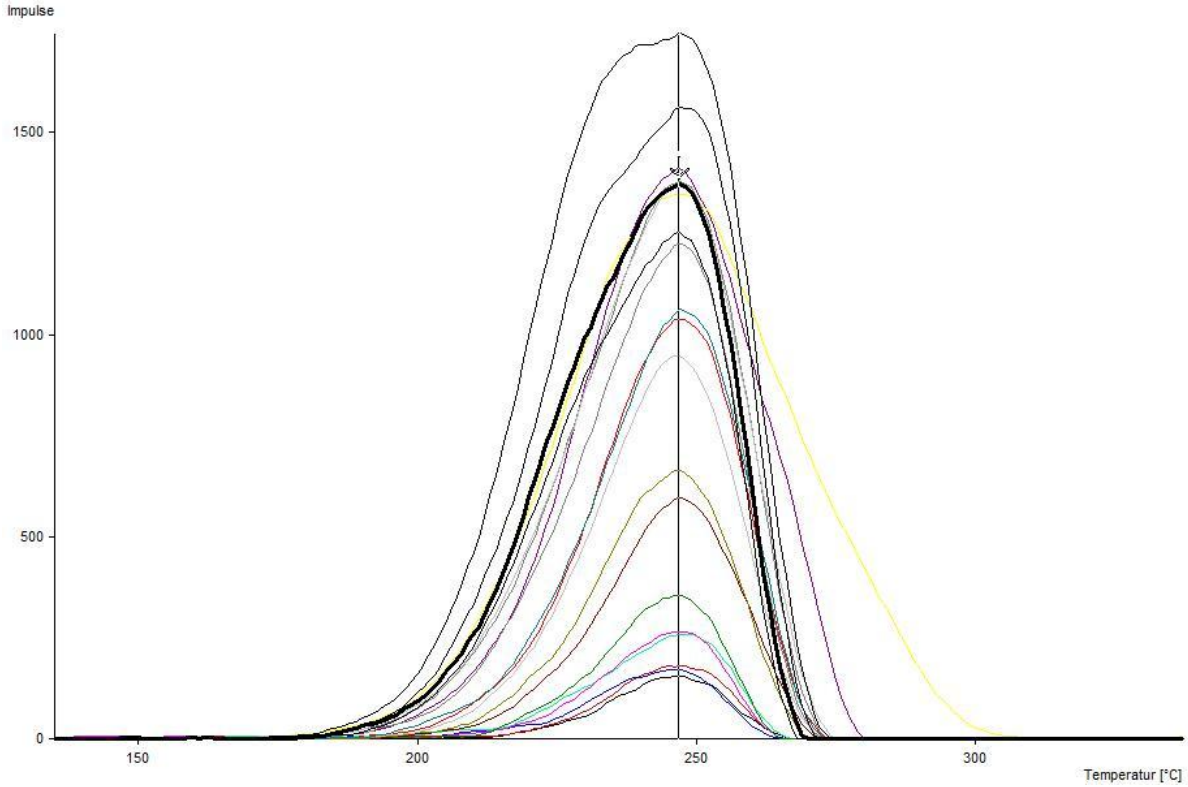

Figure IV-4: TLD-300; T_{stop} values from 224 to 260°C

The residual glow curves shown in figure IV-4 show the highest pre-heating temperature for the TLD-300 phosphors. The range for T_{stop} is 224 to 260°C. Again, the curves have been aligned for better viewing purposes. However, the temperature shift associated with the aligning was rather high (+3°C to -15°C). It seems that this last "peak" actually consists of two peaks, and the temperature shifts represent the transition from one to the other. Or, as with the highest T_m value peak of the PG-TLDs, it might as well be a second-order peak.

IV.1.3.1 Local Maximum Method T_m–T_{stop} Diagram

Using all the curves shown before the following graph can be drawn. However, due to the poor resolution of the local maximum method only three peaks could be identified.

Identified peaks for TLD-300 using the local maximum method

Peak 1	150,5°C ± 2,38°C
Peak 2	228,5°C ± 3,05°C
Peak 3	254°C ± 5,05°C

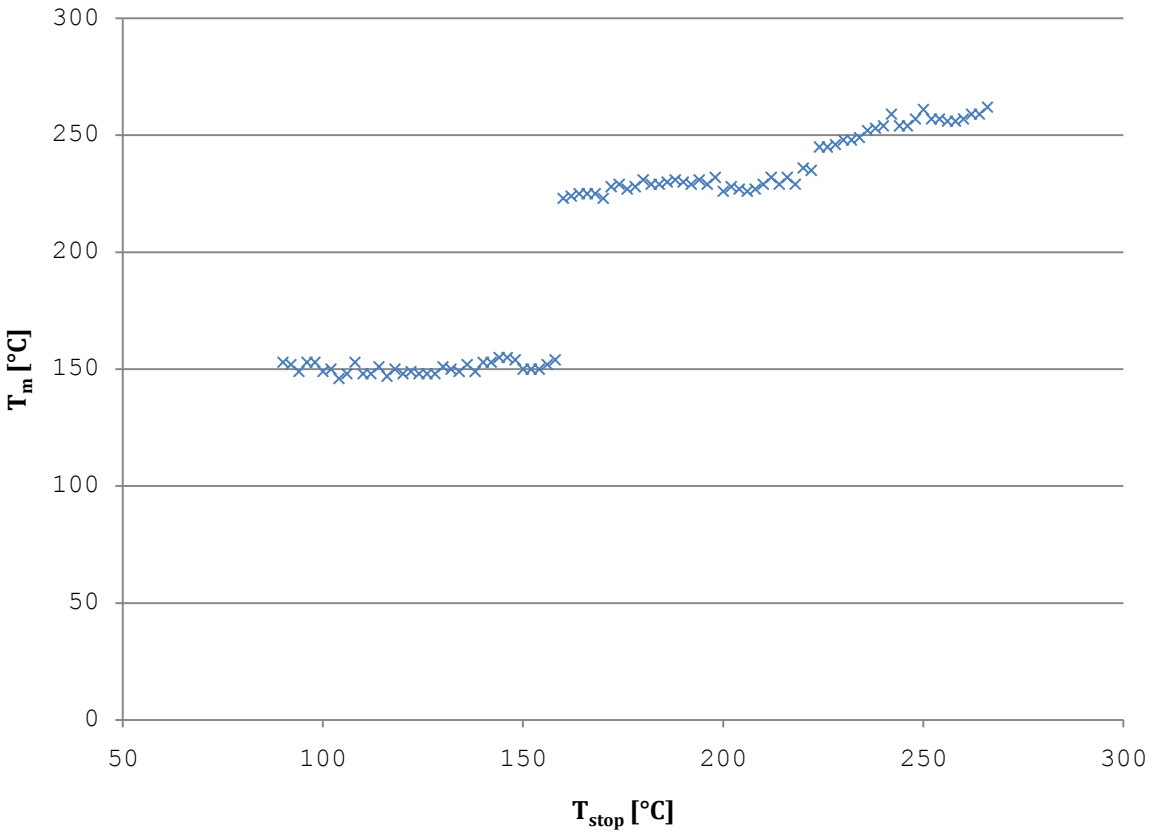

Figure IV-5: T_m-T_{stop} (90-266°C) diagram for the TLD-300 phosphor using the local maximum method

IV.1.4 Annealed Peak Method

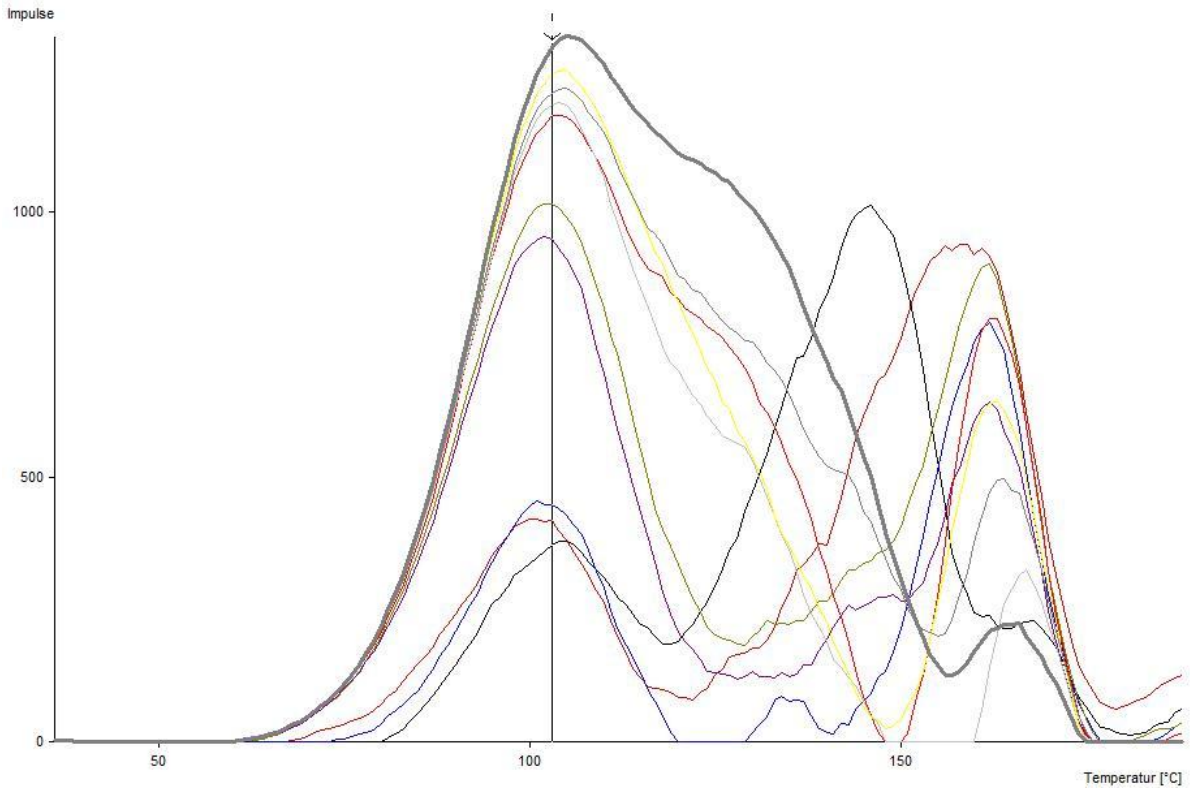

Figure IV-6: TLD-300; annealed peak method; T_{stop} values from 90 to 120°C

The curves shown in figure IV-6 have been obtained through the use of the annealed peak method. The T_{stop} range shown here is from 90°C to 120°C. As explained in chapter II.4.5 the T_m-T_{stop} measurements have been aligned at the most prominent peak of the glow curve (here 148°C). Then they were subtracted from the reference curve shown in figure IV-1. The vertical cursor shows the first identified maximum using local maximum rules to identify a peak. Contrary to the curves shown above in figure IV-2 to IV-4, where lower intensity equaled higher T_{stop} values, these curves show reversed significance. This results in a better developed maximum at higher T_{stop} values. Following this, the cut-off condition for this maximum is the curve with the highest intensity (T_{stop} = 120°C) shown in the above figure. It is also possible to discern the increase in intensity of the next maximum, which has not formed a local maximum yet (~125°C). The rather large peaks at ~148°C in the above curve

are artifacts stemming from the subtraction from the reference curve, and will be disregarded at this point.

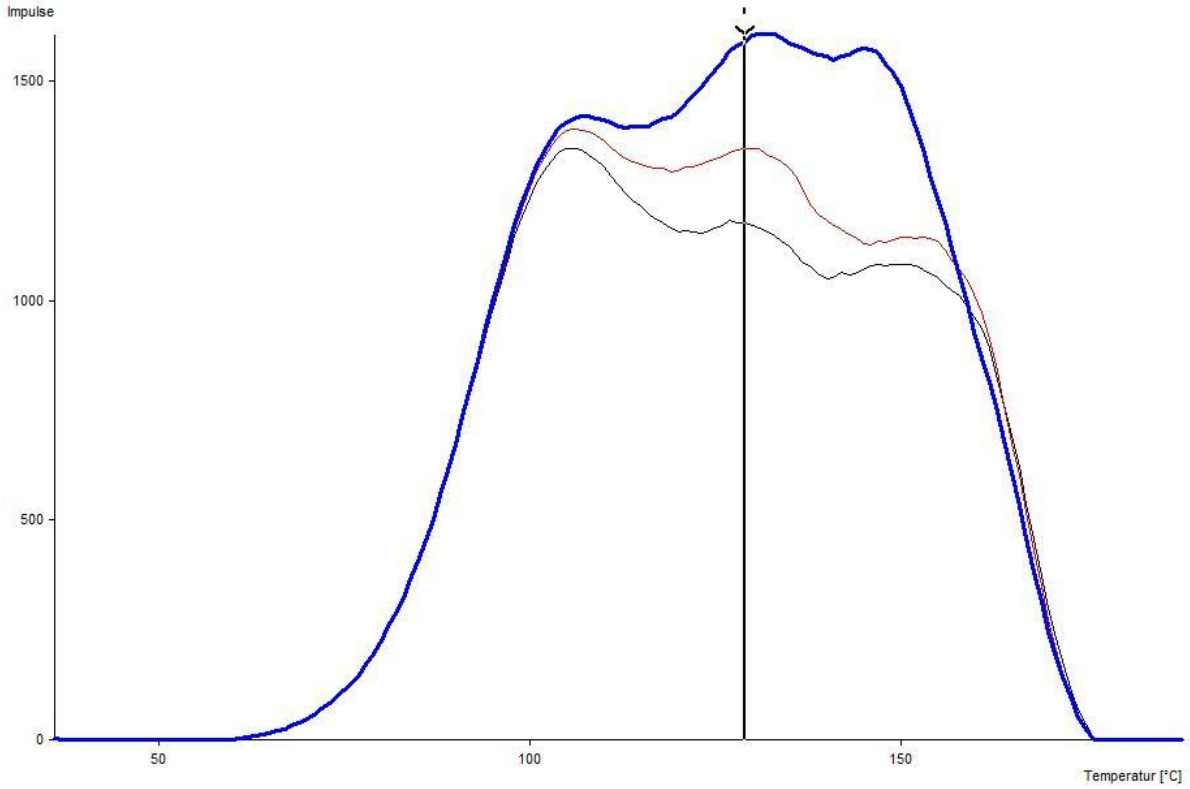

Figure IV-7: TLD-300; annealed peak method; T_{stop} values: 122,124,126°C

The three curves displayed in figure IV-7 (T_{stop} = 122,124,126°C) show the next maximum, which can be identified. The blue curve (126°C) shows the cut-off condition for this maximum, as the most prominent peak which is already visible at ~150°C is increasing in intensity very fast. This increase limits the possibility to see the peak at 128°C to a small temperature window of 6°C within this method.

Another feature of the annealed peak method can be seen at the first maximum shown. The increase of a maximum stagnates and its slight increase is only fed through the lower temperature shoulders of the following peaks, once the T_{stop} temperature has passed its high-temperature shoulder.

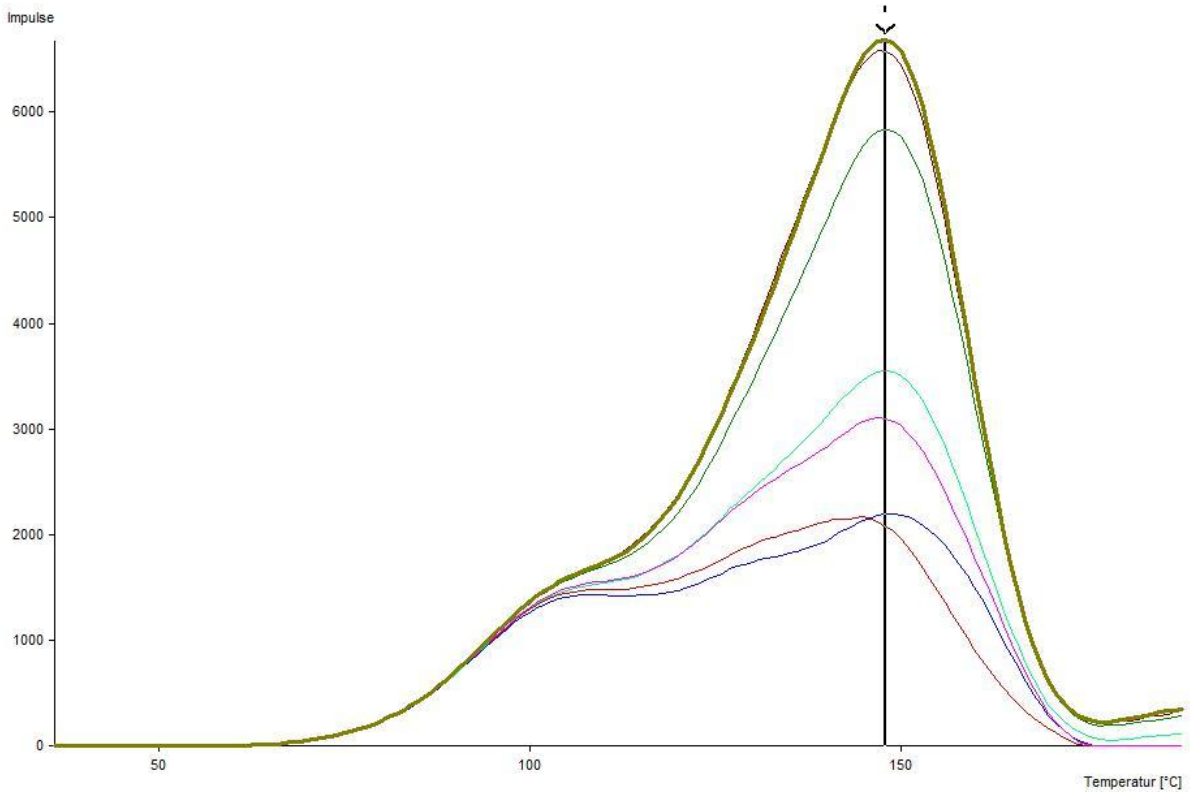

Figure IV-8: TLD-300; annealed peak method; T_{stop} values from 128 to 140°C

Finally, the last and most prominent peak of the TLD-300 dosimeter resolved by this method is shown in figure IV-8. These curves represent T_{stop} values from 128 to 140°C.

It is, not possible to further increase the T_{stop} values with this method since the curves have to be aligned at the same peak. Since the peak at 148°C diminishes with higher T_{stop} values it cannot be used for alignment purposes anymore.

IV.1.4.1 Annealed Peak Method T_m–T_{stop} Diagram

Using all the data from the annealed peak curves, three peaks can be identified in the following T_m-T_{stop} diagram. The larger statistical uncertainty can be explained due to the subtraction and shifting processes.

Identified peaks for TLD-300 using the annealed peak method

Peak 1	102,9°C ± 4,47°C
Peak 2	128,7°C ± 1,82°C
Peak 3	147,4°C ± 3,88°C

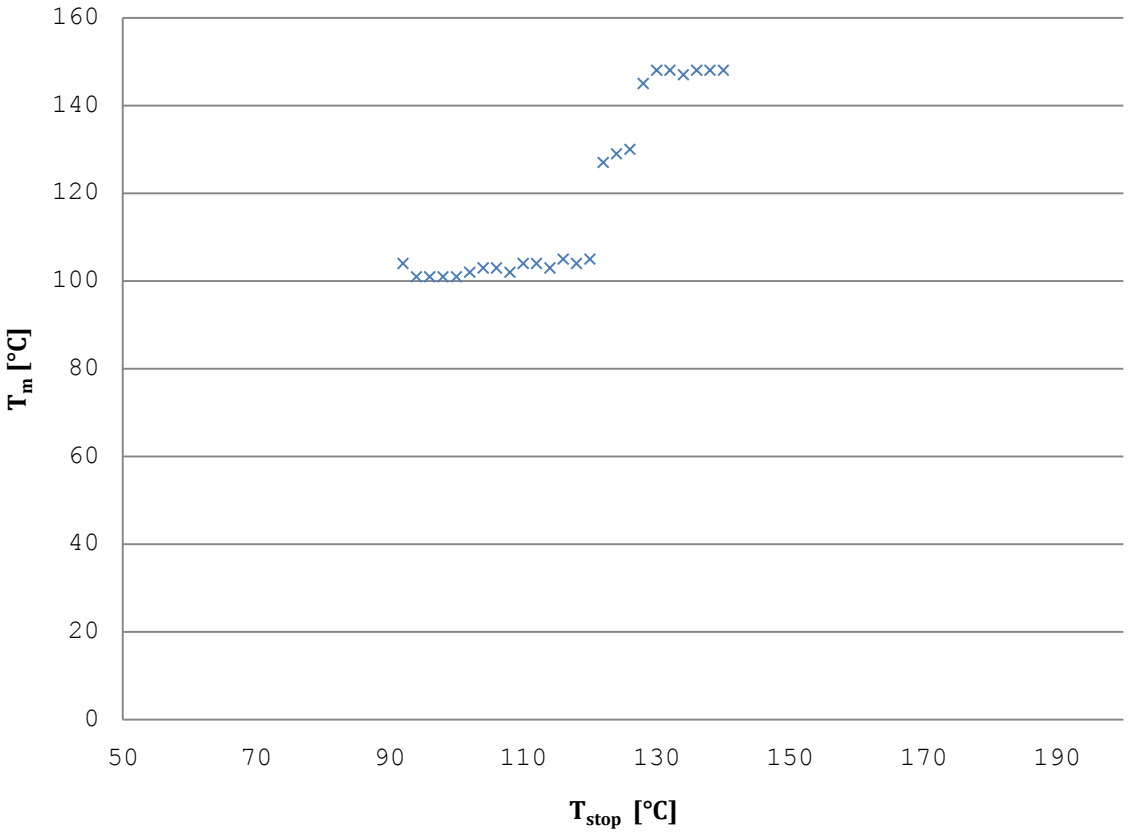

Figure IV-9: T_m-T_{stop} (90-140°C) diagram for the TLD-300 phosphor using the annealed peak method

Comparing figure IV-9 with the initial T_m-T_{stop} diagram (see IV-5) the advantages of this method are apparent. Using no other way to identify maxima, this method resolves not only the obvious peak at 102°C but another one at 128°C which will also be found with the deconvolution software.

IV.1.5 Deconvolution Method

Using the deconvolution software GLOW FIT on the 88 measurements, six peaks can consistently be identified. Due to poor signal strength at high temperatures the statistical uncertainty is higher than anywhere else. Because of this, it was not possible to decide if at T_{stop} temperatures 232 and 234°C another peak is resolved or not.

Identified peaks for TLD-300 using GLOW FIT

Peak 1	105,6°C ± 1,31°C
Peak 2	127,6°C ± 1,88°C
Peak 3	150,7°C ± 2,2°C
Peak 4	181,6°C ± 4,03°C
Peak 5	226,4°C ± 2,22°C
Peak 6	255,5°C ± 5,81°C

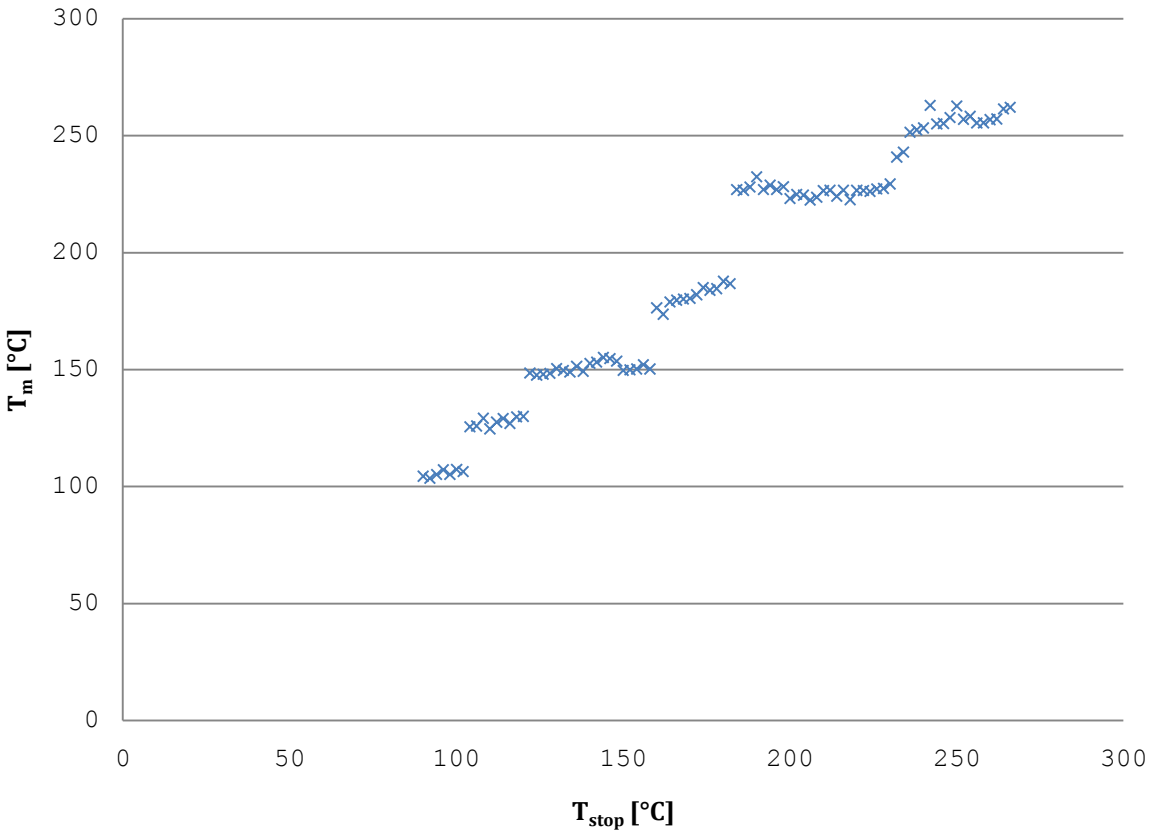

Figure IV-10: T_m-T_{stop} (90-266°C) diagram for the TLD-300 phosphor using the deconvolution software GLOW FIT

IV.1.6 TLD-300: Results

Identified peaks for TLD-300

Local Maximum	Annealed Peak	Deconvolution
	102,9°C ± 4,47°C	105,6°C ± 1,31°C
	128,7°C ± 1,82°C	127,6°C ± 1,88°C
150,5°C ± 2,38°C	147,4°C ± 3,88°C	150,7°C ± 2,2°C
		181,6°C ± 4,03°C
228,5°C ± 3,05°C		226,4°C ± 2,22°C
254°C ± 5,05°C		255,5°C ± 5,81°C

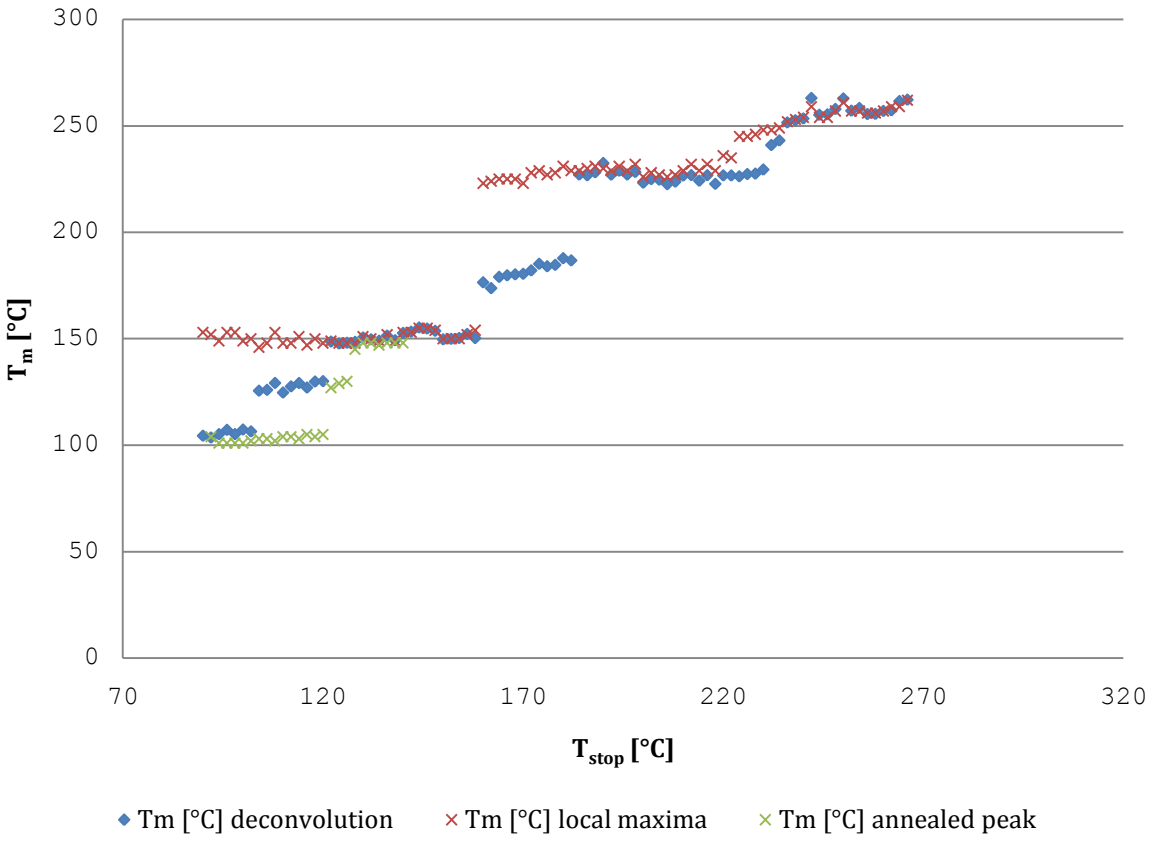

Figure IV-11: Results for the TLD-300 phosphor

Figure IV-11 shows the results obtained from all three methods in one graph for comparison. Here, the accuracy of the different methods becomes apparent. Also another distinction for the annealed peak method can be seen, which will be even more significant with other phosphor types. All the detected peaks will be found at a higher T_{stop} value than with the other

methods – however, the T_m values agree within the statistical uncertainties.

IV.2 TLD-600 (^{6}LiF:Mg,Ti with ~300 ppm Mg, ~11 ppm Ti; extruded chips)

IV.2.1 Experimental Protocol

Irradiation Parameters:

distance from source	1,43 m
duration	16 h
source	Cs-137
absorbed dose	8,07 mGy
number of dosimeters	12

One day passed between irradiation and measurement. The annealing process followed the day after the measurement, and was the same as with the TLD-300, TLD-700, PF and PG dosimeters, which took 24 hours (see chapter III.1.2.3).

Measurement Parameters:

heating rate	1°Cs^{-1}
heating interval	~25°C – 420°C
T_{stop} increment	2°C
T_{stop} interval	80°C – 290°C

IV.2.2 Reference Curve

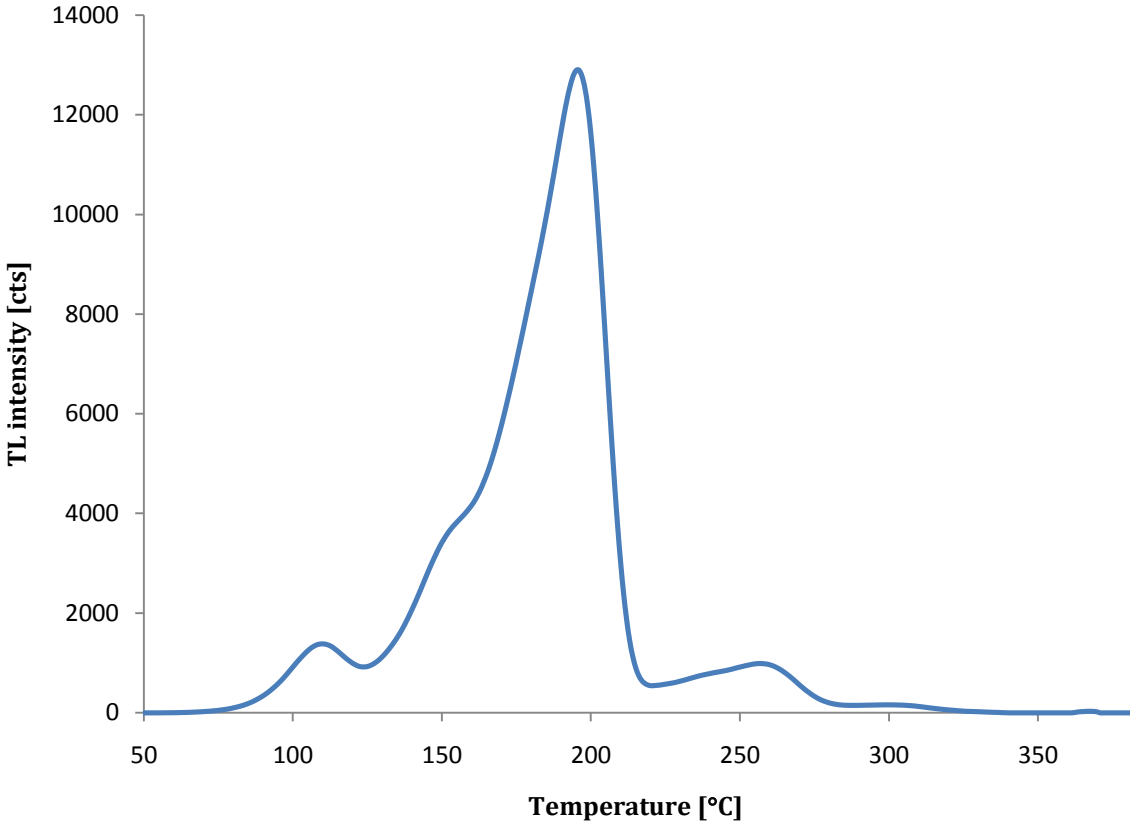

Figure IV-12: Reference curve for the TLD-600 phosphor

The curve was obtained from 48 measurements. Each of the twelve TLD-600 chips was measured four times, then the arithmetic mean for the position of the highest peak intensity was calculated. All curves were then aligned at this temperature, in this case 195°C. The maximum shift was ±2°C. The final step was obtaining the normalized mean of all the curves which is the curve shown in figure IV-12. This curve will be used in the annealed peak method and is shown here as a reference.

IV.2.3 Local Maximum Method

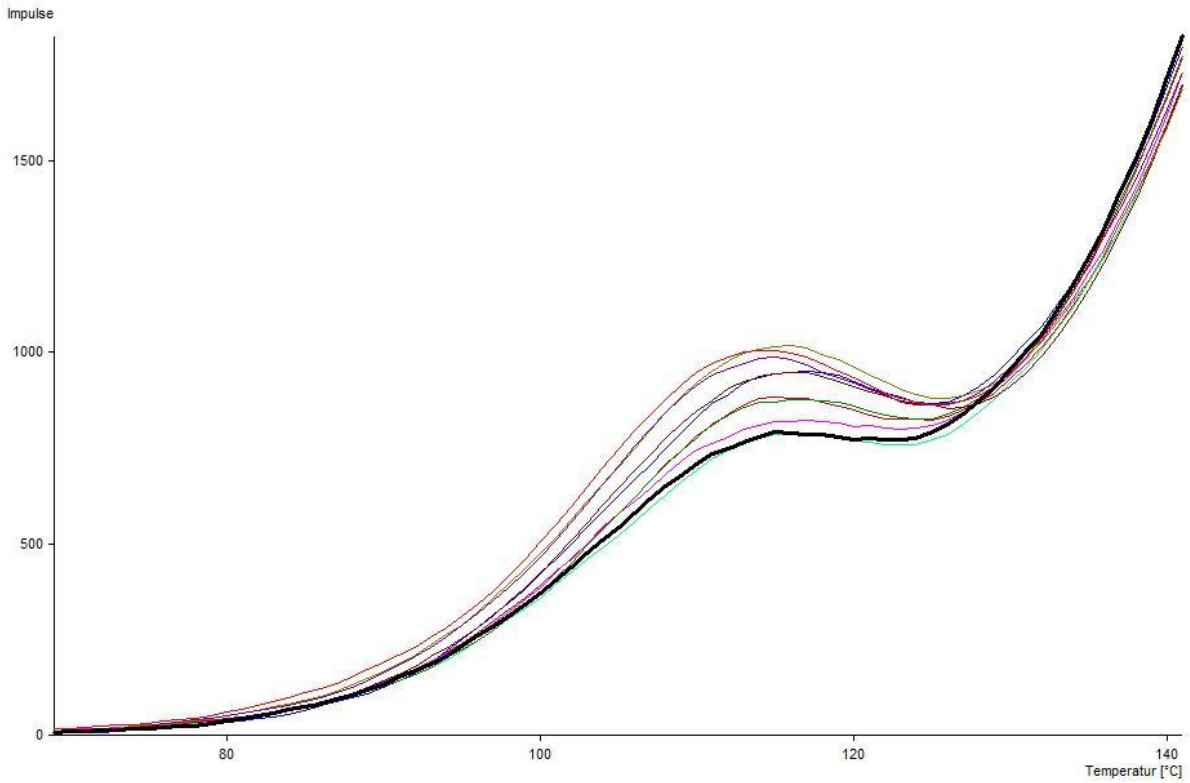

Figure IV-13: TLD-600; T_{stop} values from 80 to 98°C

Figure IV-13 shows the first local maximum. Like in the previous chapter the curves (T_{stop} values from 80 to 98°C) have been aligned for better visibility of the decrease of the maximum with increasing T_{stop} values. The black curve represents the cut-off condition.

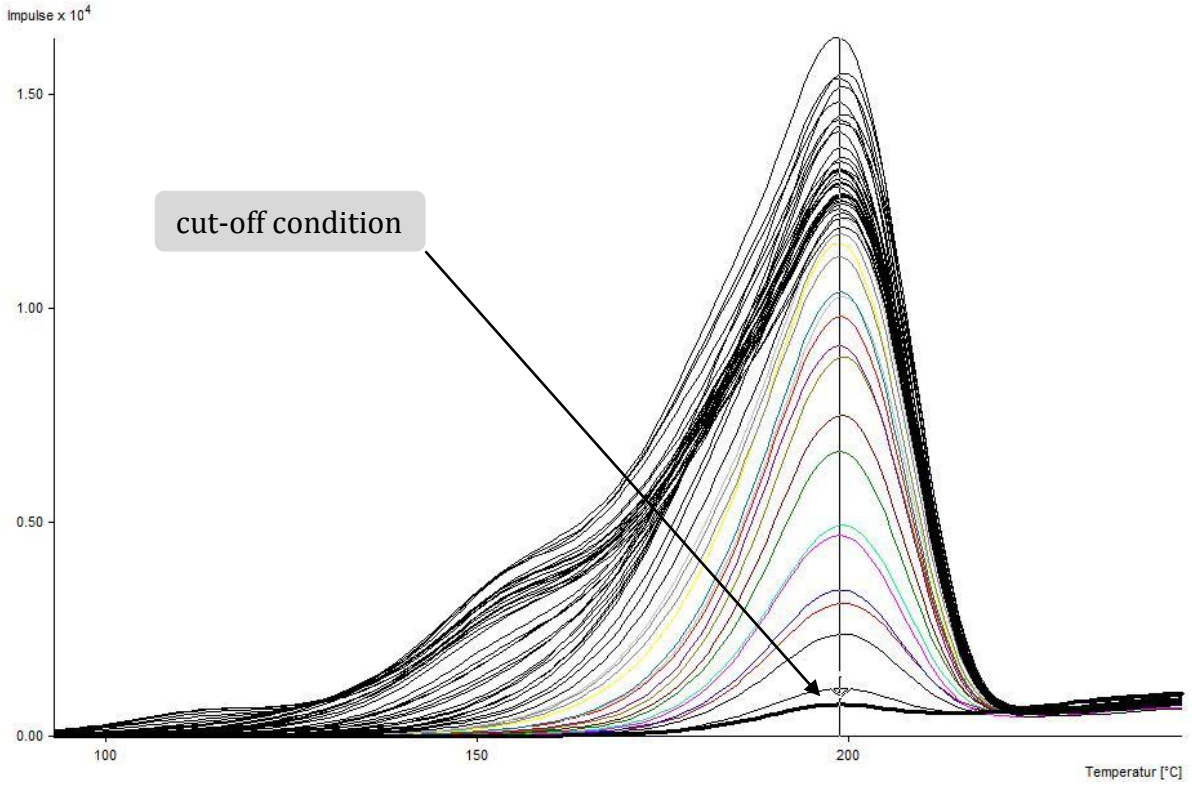

Figure IV-14: TLD-600; T_{stop} values from 100 to 204°C

Figure IV-14 shows the resulting curves for T_{stop} values between 100 and 204°C. Again all the curves have been aligned, this time at 199°C. The peak at ~150°C does not form a local maximum and cannot be resolved with this method, so the next peak at 199°C is noted with this method. The bold black curve at the bottom of all the other curves is the last one where this peak can be identified, and represents the cut-off condition. The above figure shows the poor resolution of this method like no other in this work. But although no definite temperature for a peak within this region (100 to 204°C) could be deducted (except for the main peak), it is possible to gain knowledge about peak positions for other methods.

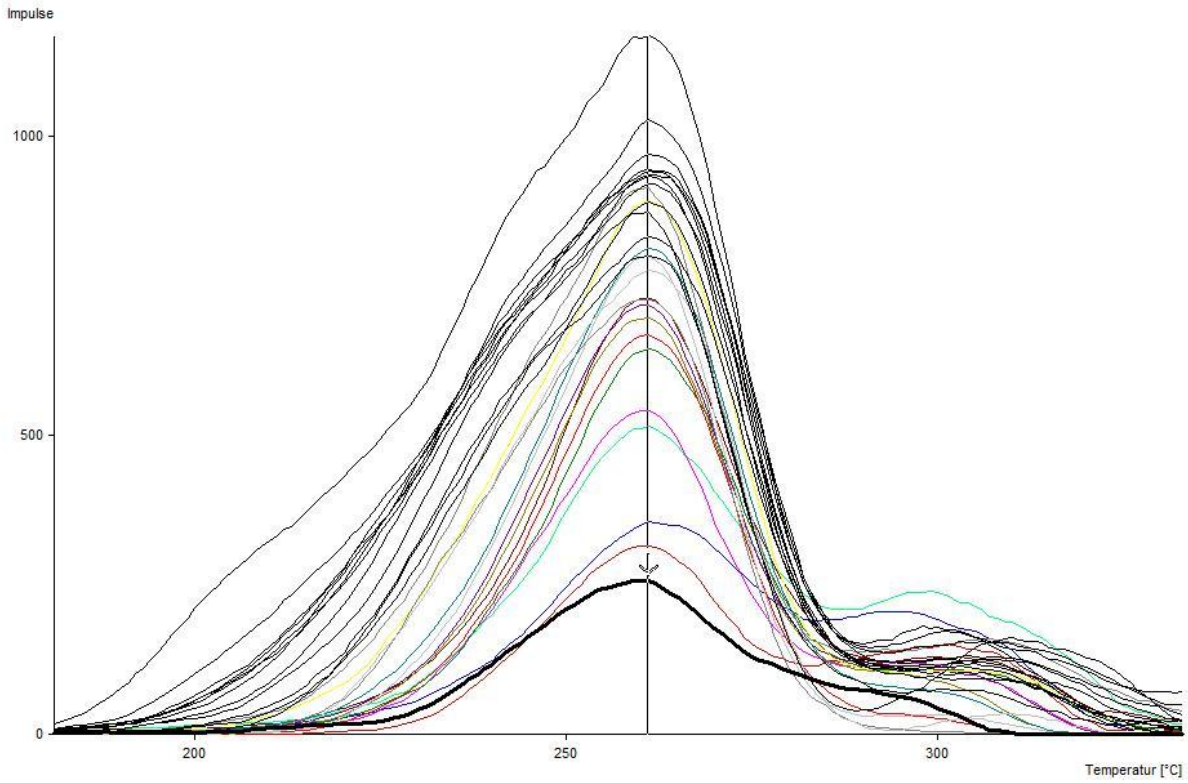

Figure IV-15: TLD-600; T_{stop} values from 206 to 262°C

Figure IV-15 shows the temperature range from T_{stop} = 206 to 262°C. The aligning temperature was 261°C. The bold black curve again represents the cut-off condition. It seems that another peak can be seen here in the region between 230 and 240°C. This peak will only be resolved by means of the deconvolution method. Since the TL intensity in this region is rather low, the statistical uncertainty will be very high.

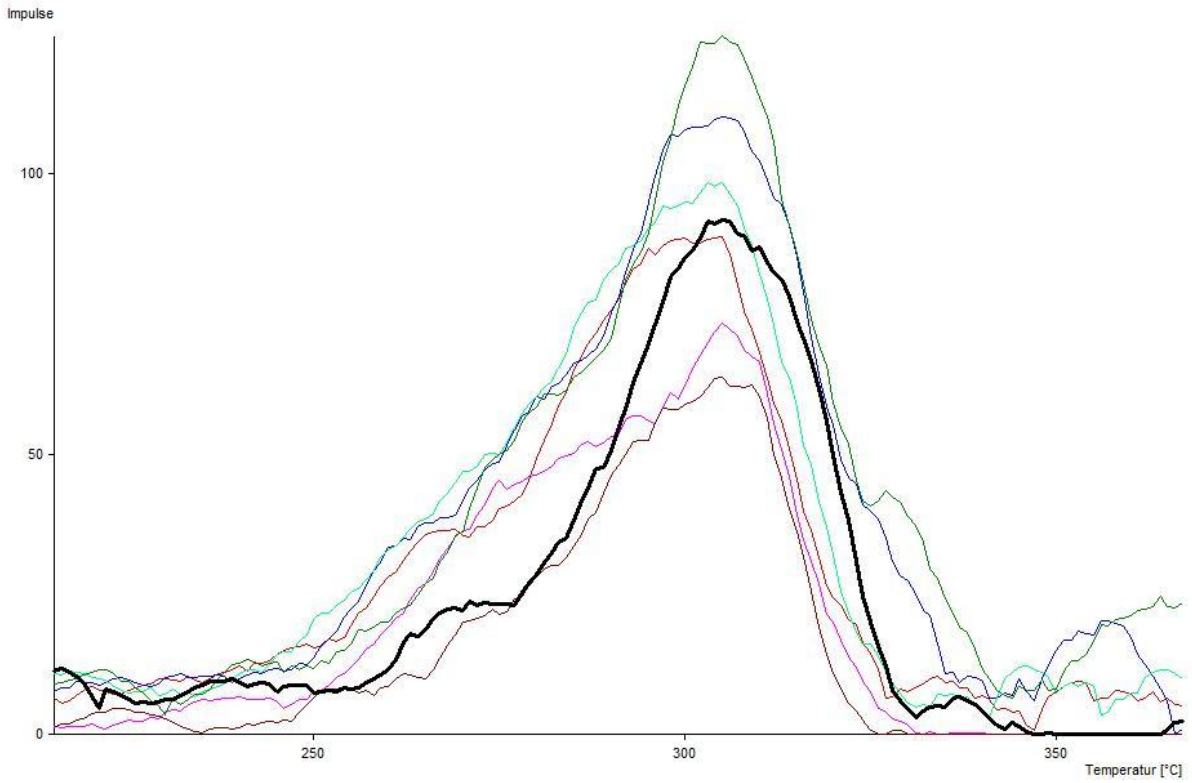

Figure IV-16: TLD-600; T_{stop} values from 276 to 288°C

The curves in figure IV-16 represent the measurements with the highest T_{stop} temperatures for the TLD-600 chip type (T_{stop} from 276 to 288°C). A definite maximum develops at ~305°C, however, since the TL intensity is very low for the applied dose (8,06 mGy), the TL intensities fluctuate wildly, as can be seen from the bold black curve which should show the lowest intensity as it corresponds to the highest T_{stop} temperature applied. In addition, the temperature shift needed to present these curves in figure IV-16 is also high (-7 to +5°C). This means that the statistical uncertainty in this region will be considerable.

IV.2.3.1 Local Maximum Method T_m–T_{stop} Diagram

If the local maxima of all the curves shown before are noted, the following T_m–T_{stop} diagram can be plotted.

Identified peaks for TLD-600 using the local maximum method

Peak 1	114,2°C ± 0,98°C
Peak 2	197,9°C ± 2,16°C
Peak 3	262,9°C ± 4,3°C
Peak 4	305°C ± 3,38°C

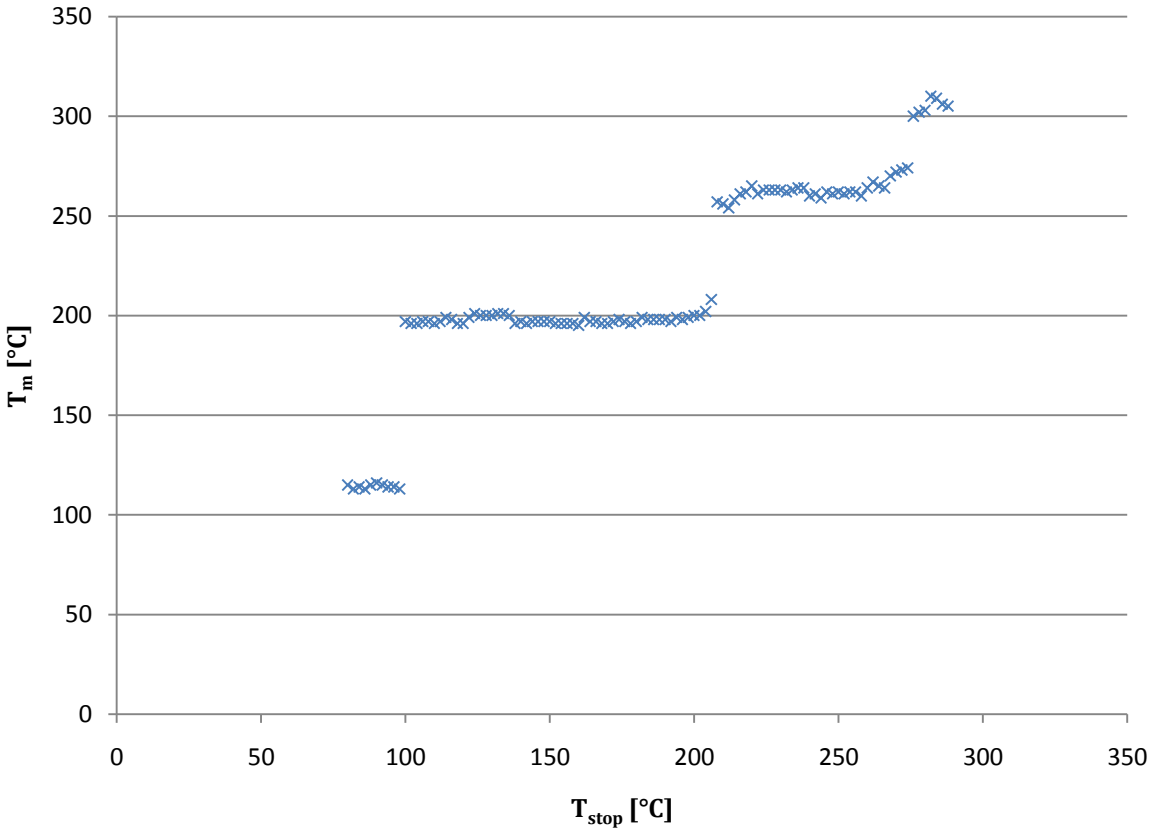

Figure IV-17: T_m-T_{stop} (80-290°C) diagram for the TLD-600 phosphor using the local maximum method

As mentioned before, the long plateau beginning at T_{stop}=104°C and ending beyond 200°C "hides" several peaks which cannot be resolved with this method. The high-temperature peak at T_m=305°C is definitely resolved but fluctuates due to poor TL intensity at this temperature.

IV.2.4 Annealed Peak Method

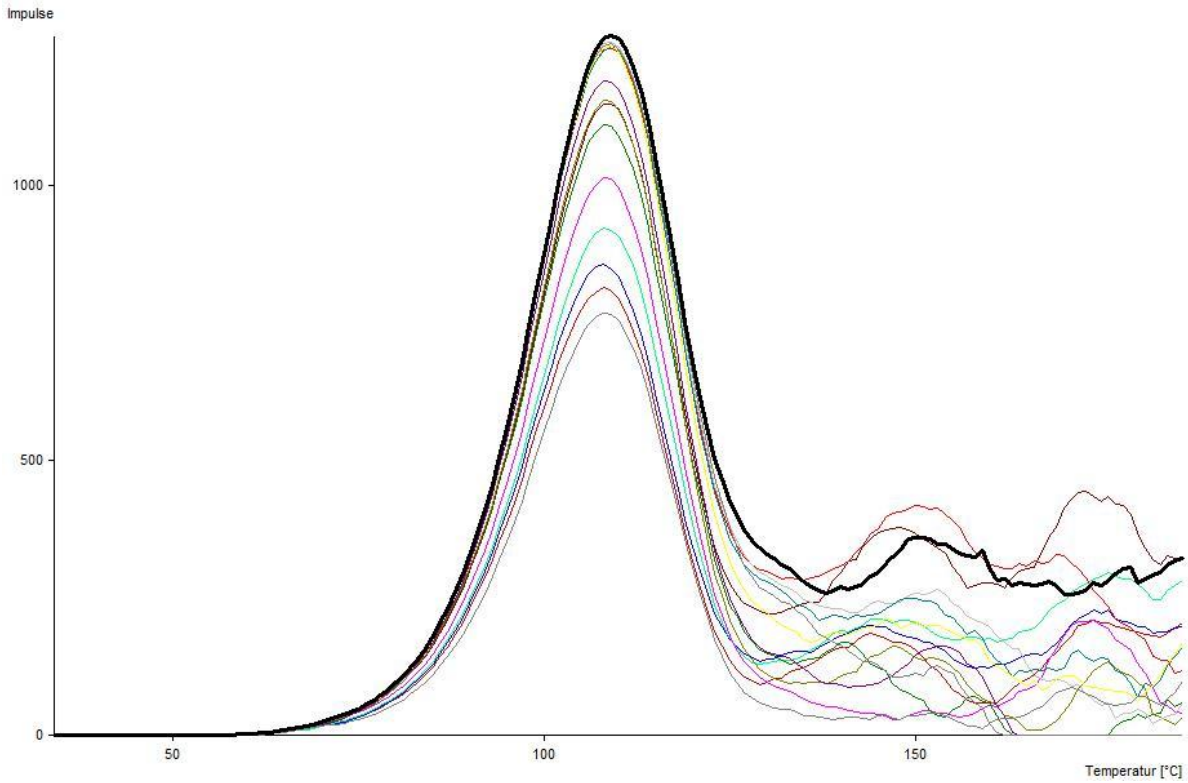

Figure IV-18: TLD-600; annealed peak method; T_{stop} values from 100 to 128°C

The curves shown in figure IV-18 represent the first maximum which can be identified with the annealed peak method. Not all measured curves are shown, however, since the first measurement started at a T_{stop} value of 80°C. They were discarded for this picture, since, after subtraction from the reference curve, they showed no residual glow curve. T_{stop} is still too low to have a significant influence on the first peak.

The bold black curve again shows the cut-off condition for this peak, since the peak increase rate stalls and the next peak at ~150°C can already be seen.

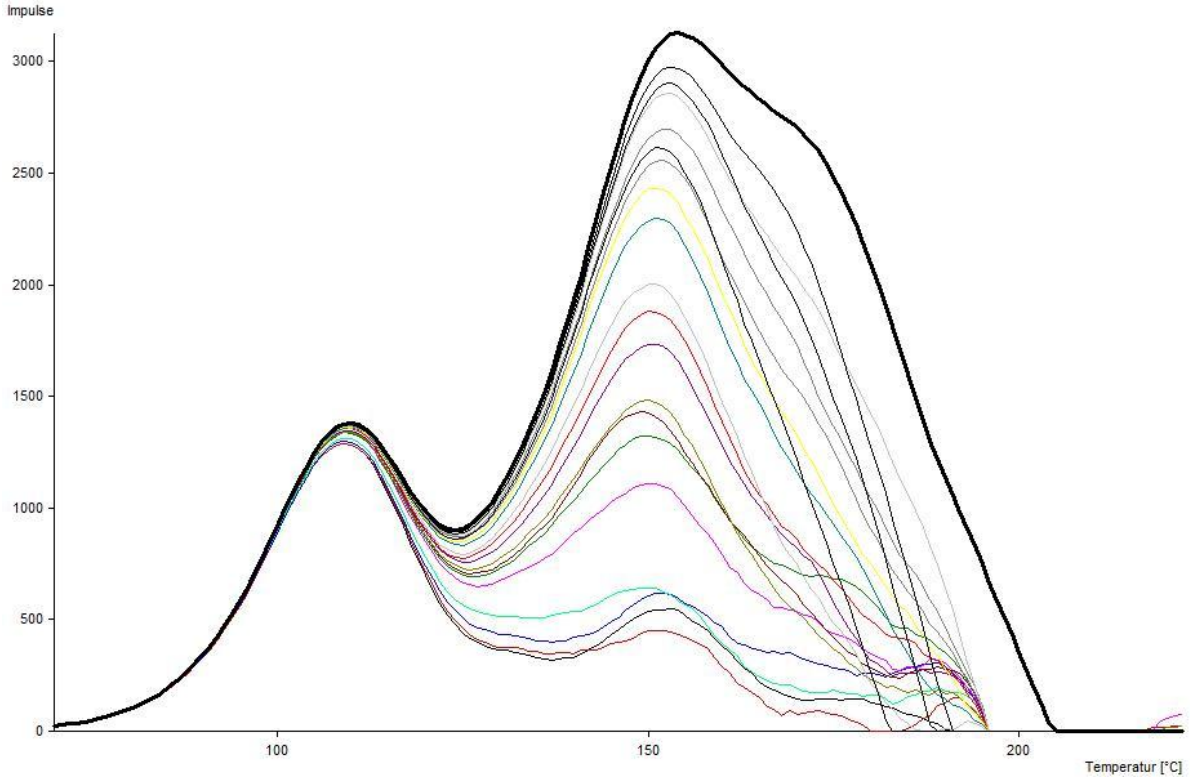

Figure IV-19: TLD-600; annealed peak method; T_{stop} values from 130 to 168°C

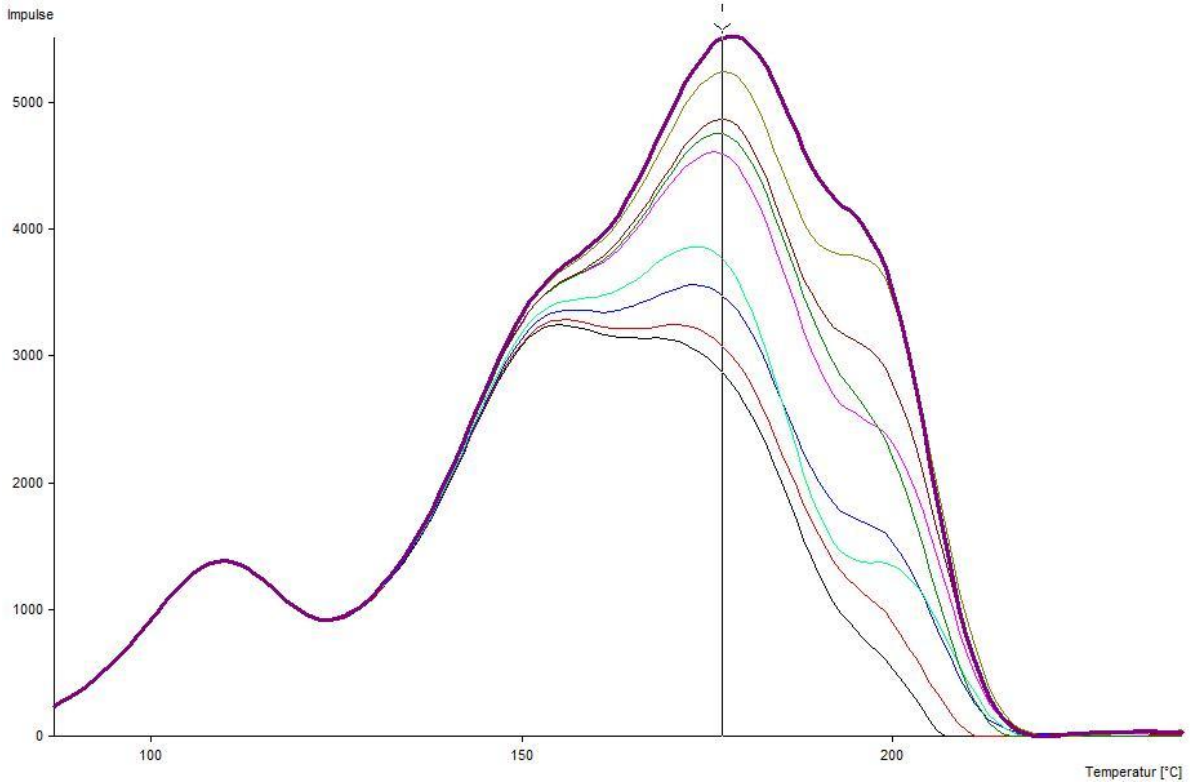

Figure IV-20: TLD-600; annealed peak method; T_{stop} values from 170 to 186°C

Figures IV-19 and IV-20 show the development of the next two peaks using T_{stop} = 130 to 168°C (IV-19) and T_{stop} = 170 to 186°C (IV-20). As good as these peaks can be differentiated because

of these graphs, there is also the biggest problem evident when using the local maximum rule to identify peaks. Especially from figure IV-20 it is obvious that the position of the maximum shifts in dependence on the intensity with respect to the neighboring peaks. So the peak starts to move from the left of the cursor to the right of it.

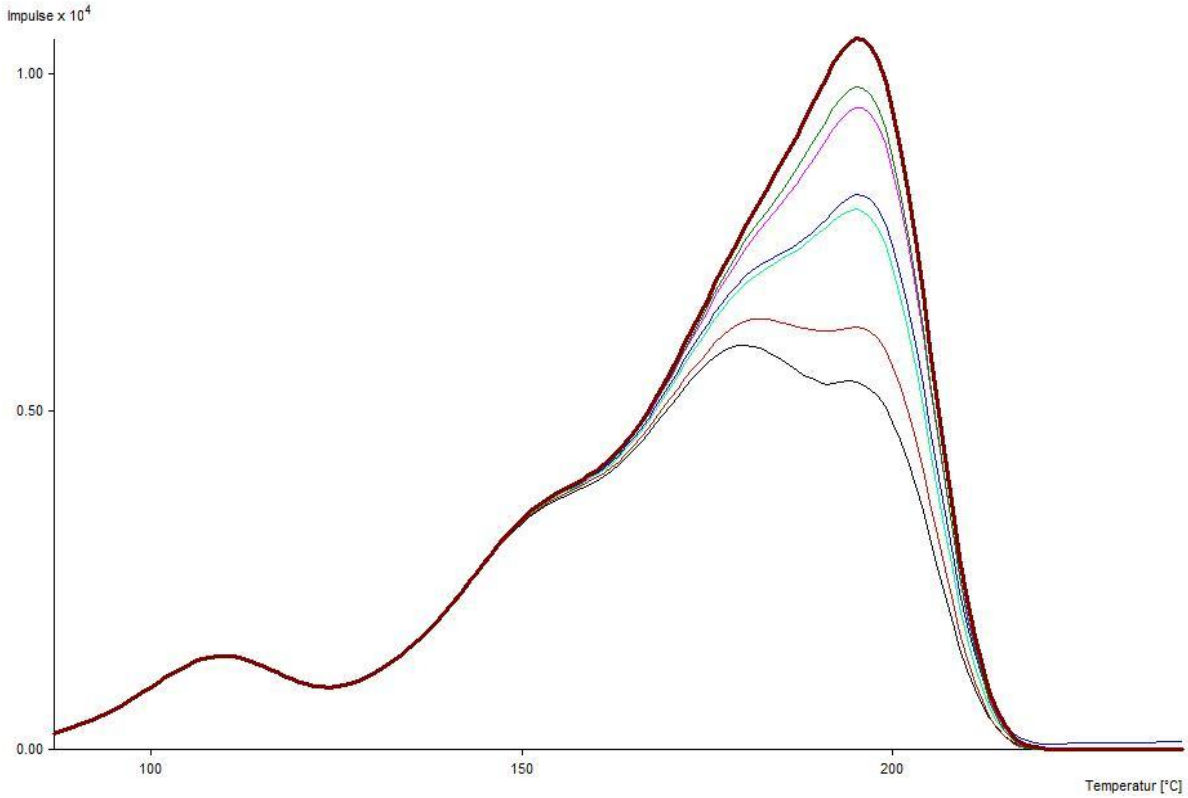

Figure IV-21: TLD-600; annealed peak method; T_{stop} values from 188 to 200°C

Figure IV-21 shows the last peak that can be found with this method. The curves shown are for T_{stop} values from 188 to 200°C.

IV.2.4.1 Annealed Peak Method T_m–T_{stop} Diagram

Using all the data from the annealed peak method, four peaks can be identified. Since additional subtraction is necessary to obtain these curves the statistical uncertainty is higher than with the conventional method. It is only possible to use this method up to its most prominent peak, hence the peaks beyond peak 4 cannot be identified here.

Identified peaks for TLD-600 using the annealed peak method

Peak 1	108,5°C ± 2,85°C
Peak 2	151,2°C ± 3,61°C
Peak 3	174,2°C ± 4,79°C
Peak 4	194,9°C ± 2,94°C

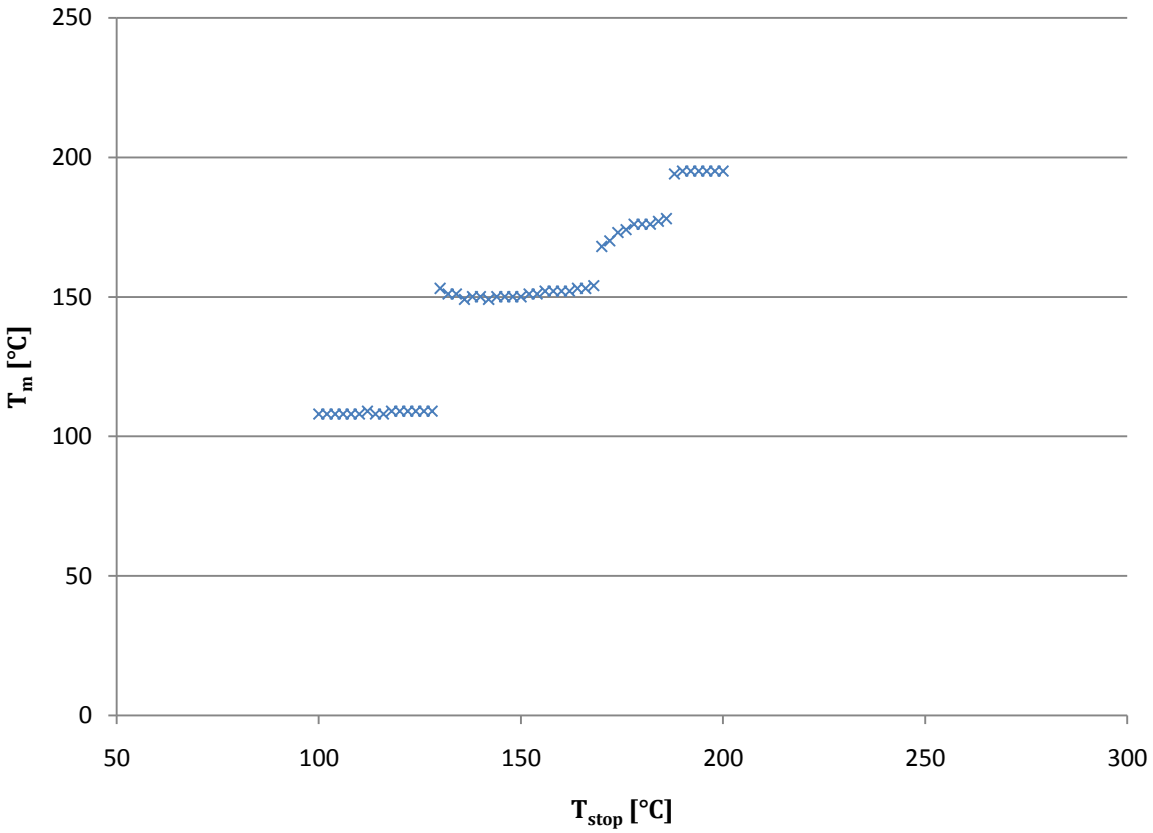

Figure IV-22: T_m-T_{stop} (100-200°C) diagram for the TLD-600 phosphor using the annealed peak method

The first four points for the third plateau (peak 3) are responsible for the bigger statistical uncertainty of this peak, compared to the other peaks. The reason for this can be seen in figure IV-20. The intensity of peak 2 and peak 3 are at this temperature almost equal. This accounts for the observed peak position shift. As peak 3 gains in intensity with increasing T_{stop} values the influence of peak 2 lessens, resulting in a more stable plateau.

IV.2.5 Deconvolution Method

With the deconvolution software GLOW FIT seven peaks can be identified on the basis of 105 measurements. Like with TLD-300, the peaks at higher temperatures have a high statistical uncertainty, due to low TL intensity.

Identified peaks for TLD-600 using GLOW FIT

Peak 1	112,6°C ± 1,67°C
Peak 2	152,7°C ± 1,56°C
Peak 3	175,5°C ± 1,05°C
Peak 4	198,9°C ± 2,6°C
Peak 5	229,9°C ± 4,67°C
Peak 6	262,6°C ± 3,2°C
Peak 7	300,7°C ± 7,17°C

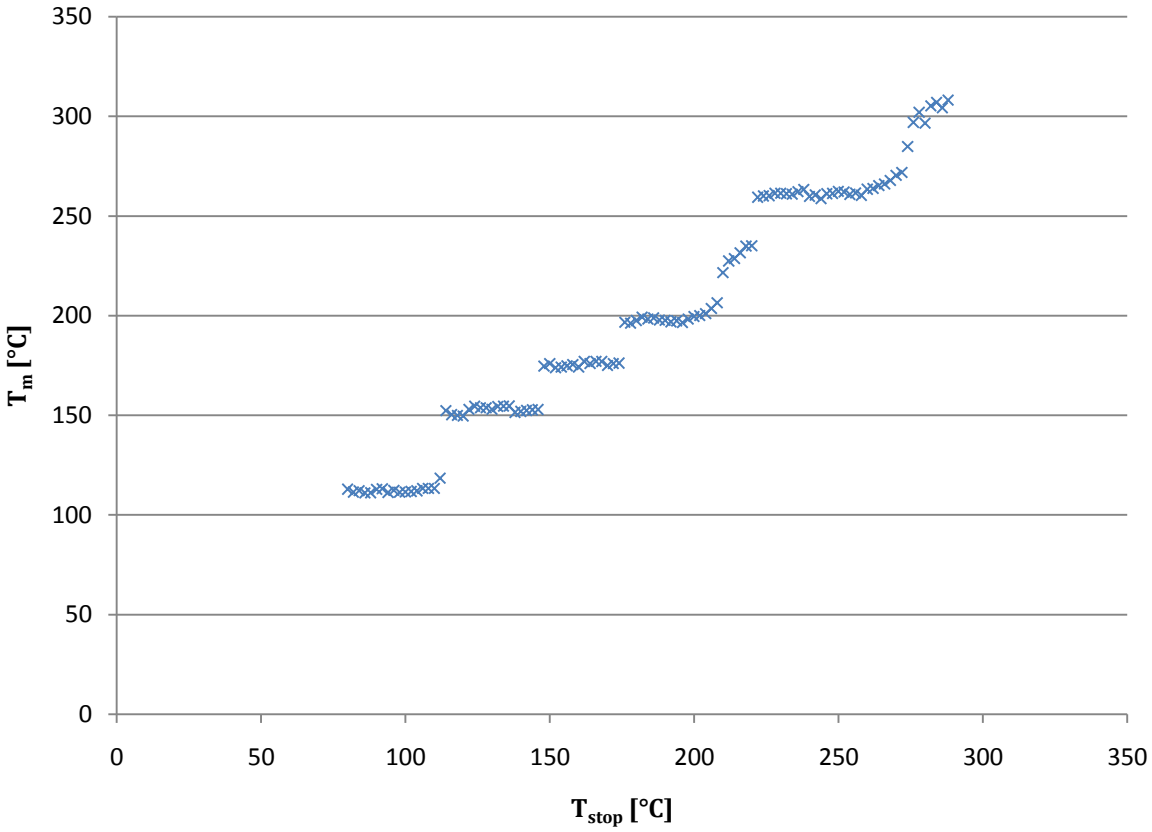

Figure IV-23: T_m-T_{stop} (80-290°C) diagram for the TLD-600 phosphor using the deconvolution software GLOW FIT

As mentioned before, the peak identified for T_{stop}=229°C is resolved with a big uncertainty and no real plateau could be

found for several measurements. One possible explanation is that this peak is of second order and cannot be resolved with GLOW FIT. However, since no similar behavior is found with the TLD-700 phosphor in this temperature region, it is probable that there is no peak at all but a measurement artifact. The same problem (see figure IV-16) can be seen for even lower TL intensity with the last peak at 300°C. The only reason why this peak can be resolved at all is that no notable peak seems to be in its vicinity, hence the reason for the statistical uncertainty is the very bad signal-to-noise ratio at this temperature.

IV.2.6 TLD-600: Results

Identified peaks for TLD-600

Local Maximum	Annealed Peak	Deconvolution
114,2°C ± 0,98°C	108,5°C ± 2,85°C	112,6°C ± 1,67°C
	151,2°C ± 3,61°C	152,7°C ± 1,56°C
C	174,2°C ± 4,79°C	175,5°C ± 1,05°C
197,9°C ± 2,16°C	194,9°C ± 2,94°C	198,9°C ± 2,6°C
		229,9°C ± 4,67°C
262,9°C ± 4,3°		262,6°C ± 3,2°C
305°C ± 3,38°C		300,7°C ± 7,17°C

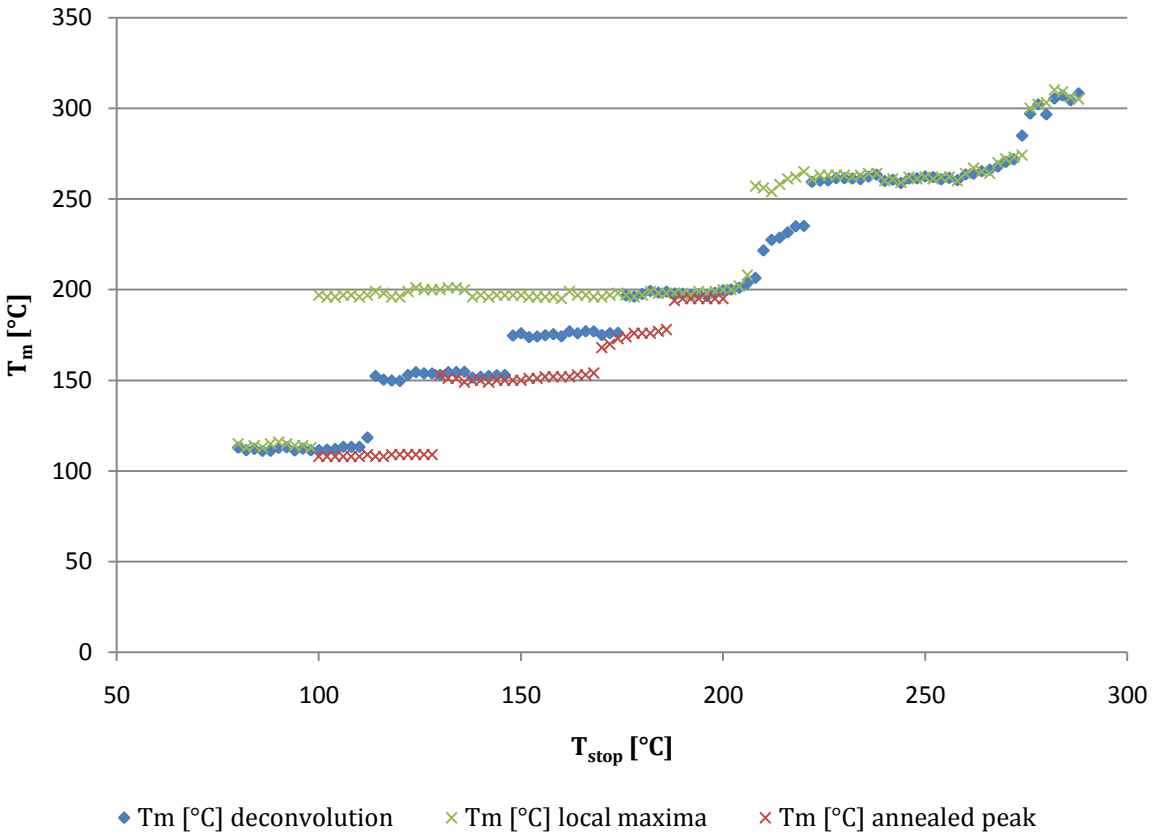

Figure IV-24: Results for the TLD-600 phosphor

Finally, all three T_m–T_{stop} graphs are shown in figure IV-24 for comparison. Again, it can be seen that the annealed peak method produces very good results compared to using just a local maximum rule to identify peaks. At higher temperatures the results from the local maximum method and deconvolution are very similar since only a few peaks are left.

IV.3 TLD-700 (^{7}LiF:Mg,Ti with ~300 ppm Mg, ~11 ppm Ti; extruded chips)

IV.3.1 Experimental Protocol

Irradiation Parameters:

distance from source	1,43 m
duration	16 h
source	Cs-137
absorbed dose	8,07 mGy
number of dosimeters	12

One day passed between irradiation and measurement. The annealing process followed the day after the measurement, and was the same as with the TLD-300, TLD-700, PF and PG dosimeters, which took 24 hours (see chapter III.1.2.3).

Measurement Parameters:

heating rate	1°Cs^{-1}
heating interval	~25°C – 420°C
T_{stop} increment	2°C
T_{stop} interval	96°C – 322°C

IV.3.2 Reference Curve

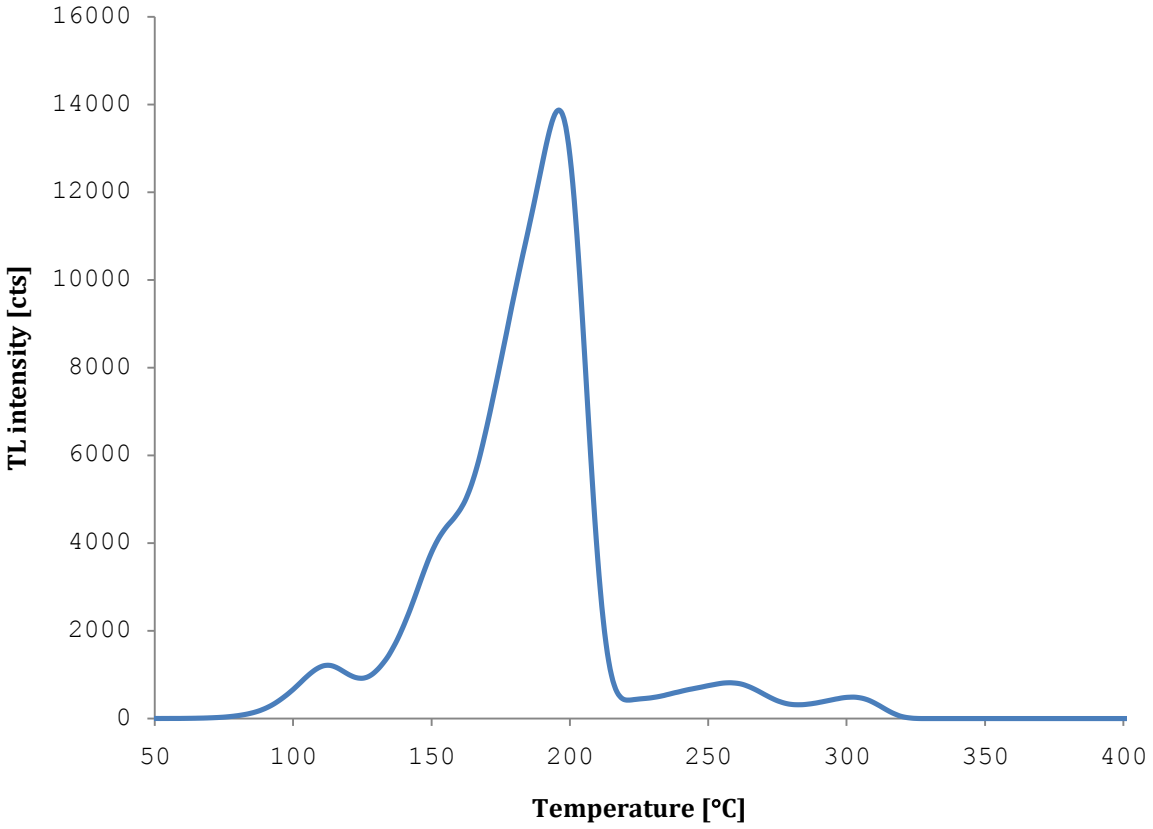

Figure IV-25: Reference curve for the TLD-700 phosphor

The curve shown in figure IV-25 was obtained from 48 reference measurements, using the same irradiation and measurement protocols. Each one of the twelve chips was measured four times. Then the arithmetic mean for the position of the highest peak intensity was calculated. All curves were then aligned at this temperature, in this case 196°C. The maximum shift was ±3°C. The final step was obtaining the normalized mean of all the curves which is the curve shown in figure IV-25. This curve will be used in the annealed peak method and is shown here for reference.

IV.3.3 Local Maximum Method

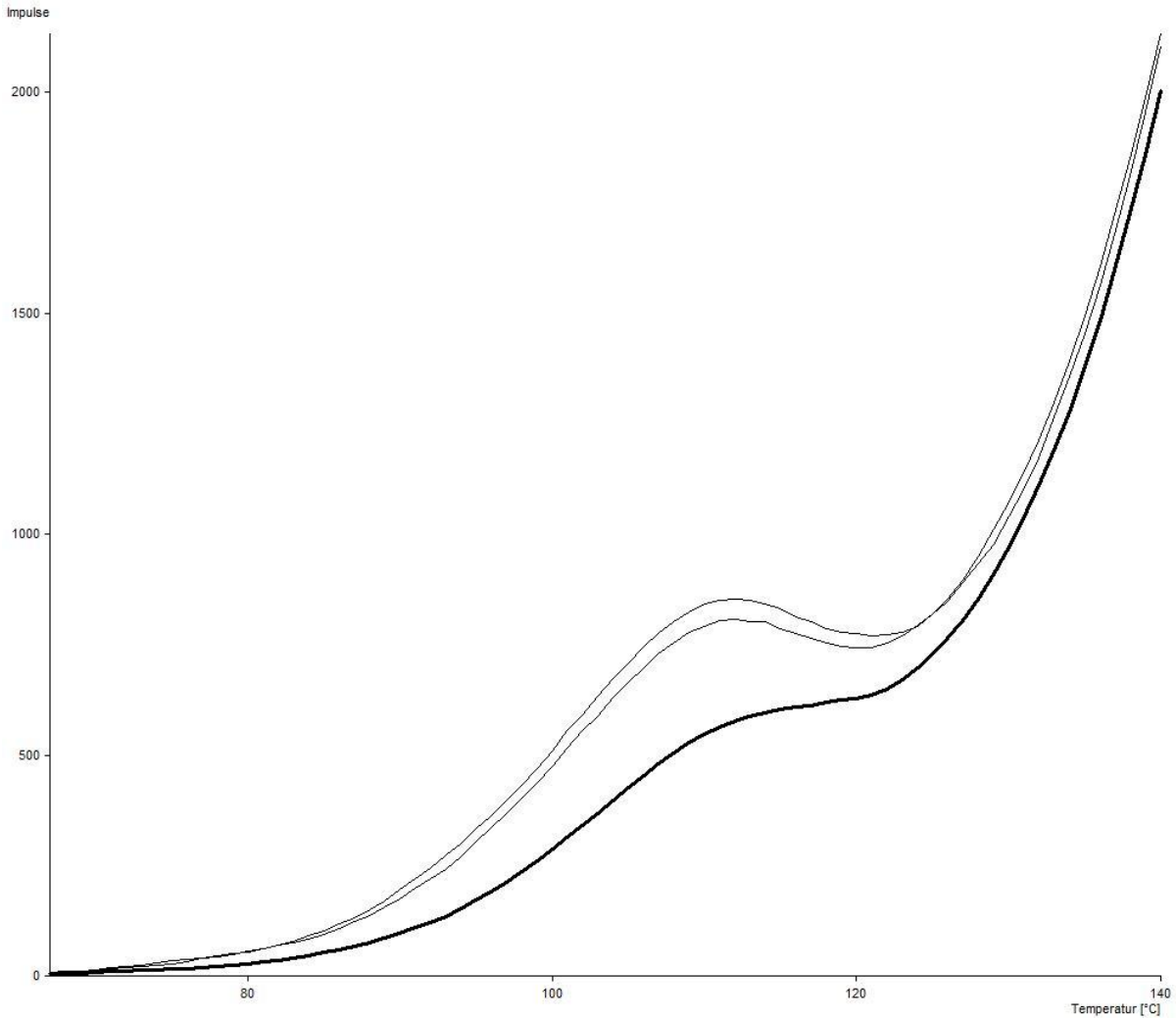

Figure IV-26: TLD-700; T_{stop} values from 96 to 100°C

Figure IV-26 shows the first maximum that can be found with the local maximum method. The curves shown are for T_{stop} = 96 to 100°C. The black curve represents the cut-off condition. In addition, these curves have been aligned at 196°C.

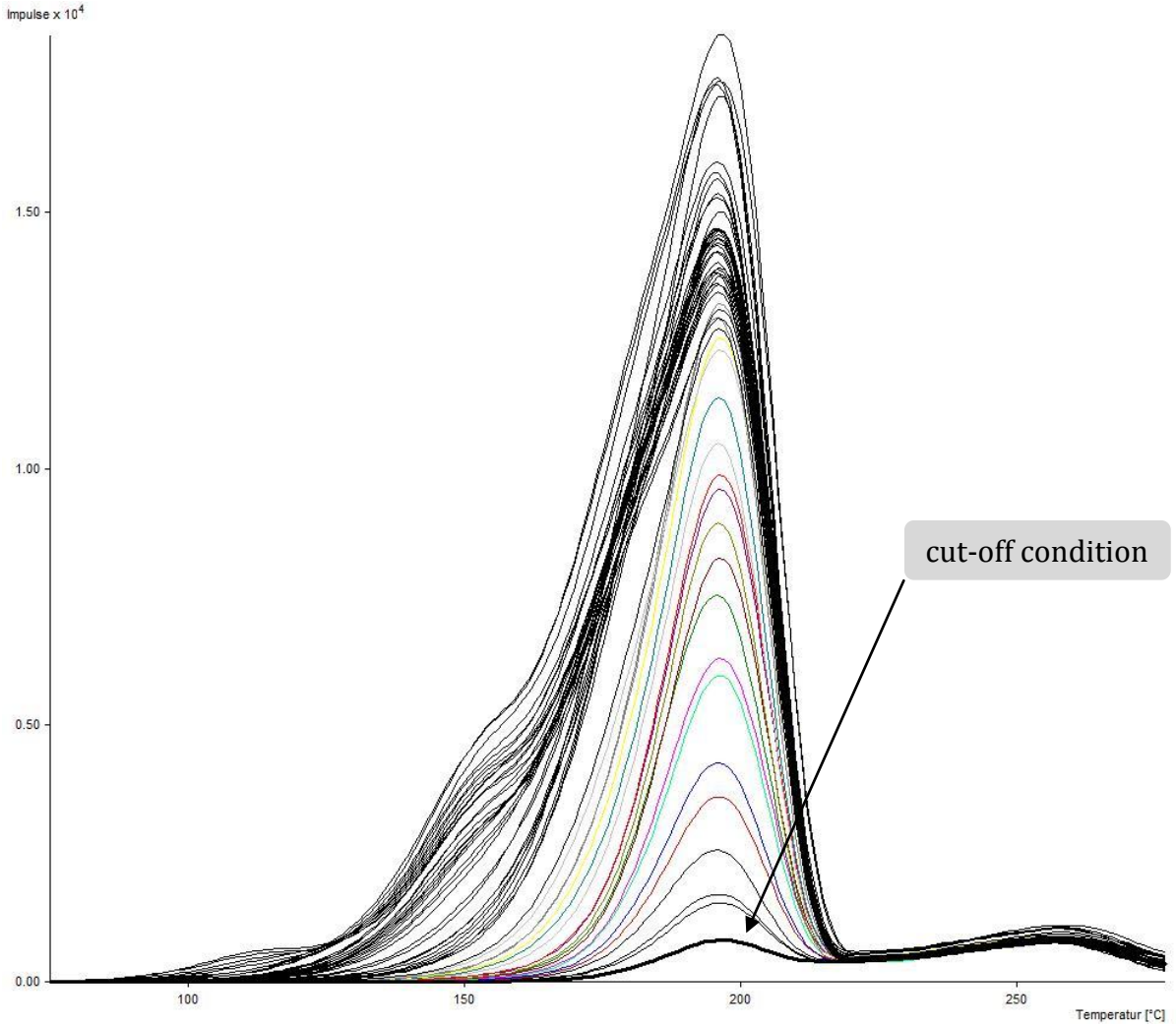

Figure IV-27: TLD-700; T_{stop} values from 102 to 208°C

The situation in figure IV-27 is very similar to the TLD-600 case. Since the next peak does not form a local maximum, it is not recorded. In addition, as with TLD-600, another peak can be seen between 170 to 180°C, its intensity, with respect to the following main peak (at 198°C), is very small. The shown curves range from T_{stop} = 102°C to 208°C. They have been aligned at 196°C. Again, the black curve is the cut-off condition.

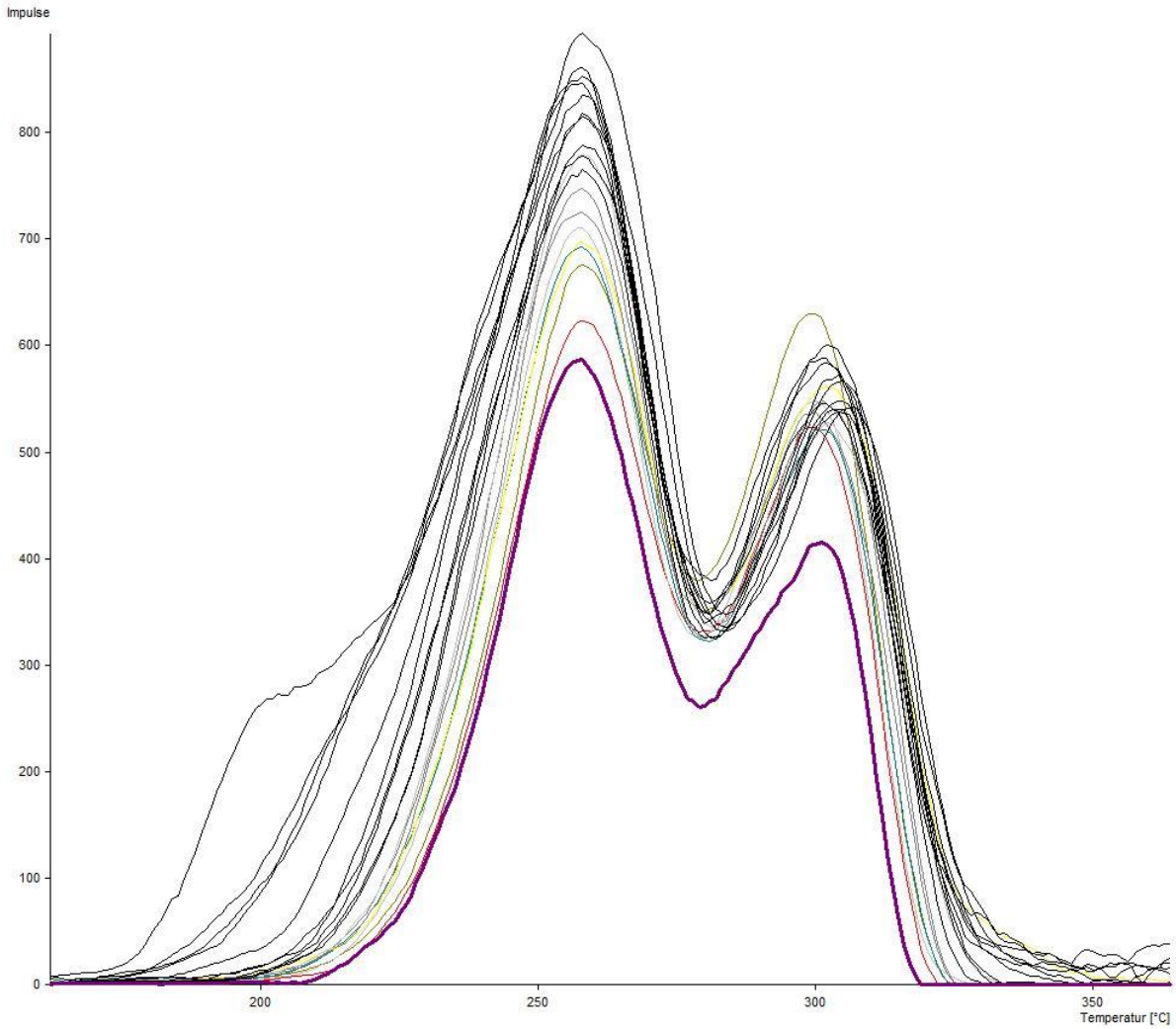

Figure IV-28: TLD-700; T_{stop} values from 212 to 248°C

Looking at higher T_{stop} values (212 to 248°C), the next peak is found (figure IV-28). What seems to be a local maximum in the T_{stop}=212°C curve is the remnant of the previous peak. The position would suggest that it is an almost completely annealed main peak (198°C). Since the TL intensity at this dose and temperature begins to fall below 500 counts, background subtraction starts to be crucial.

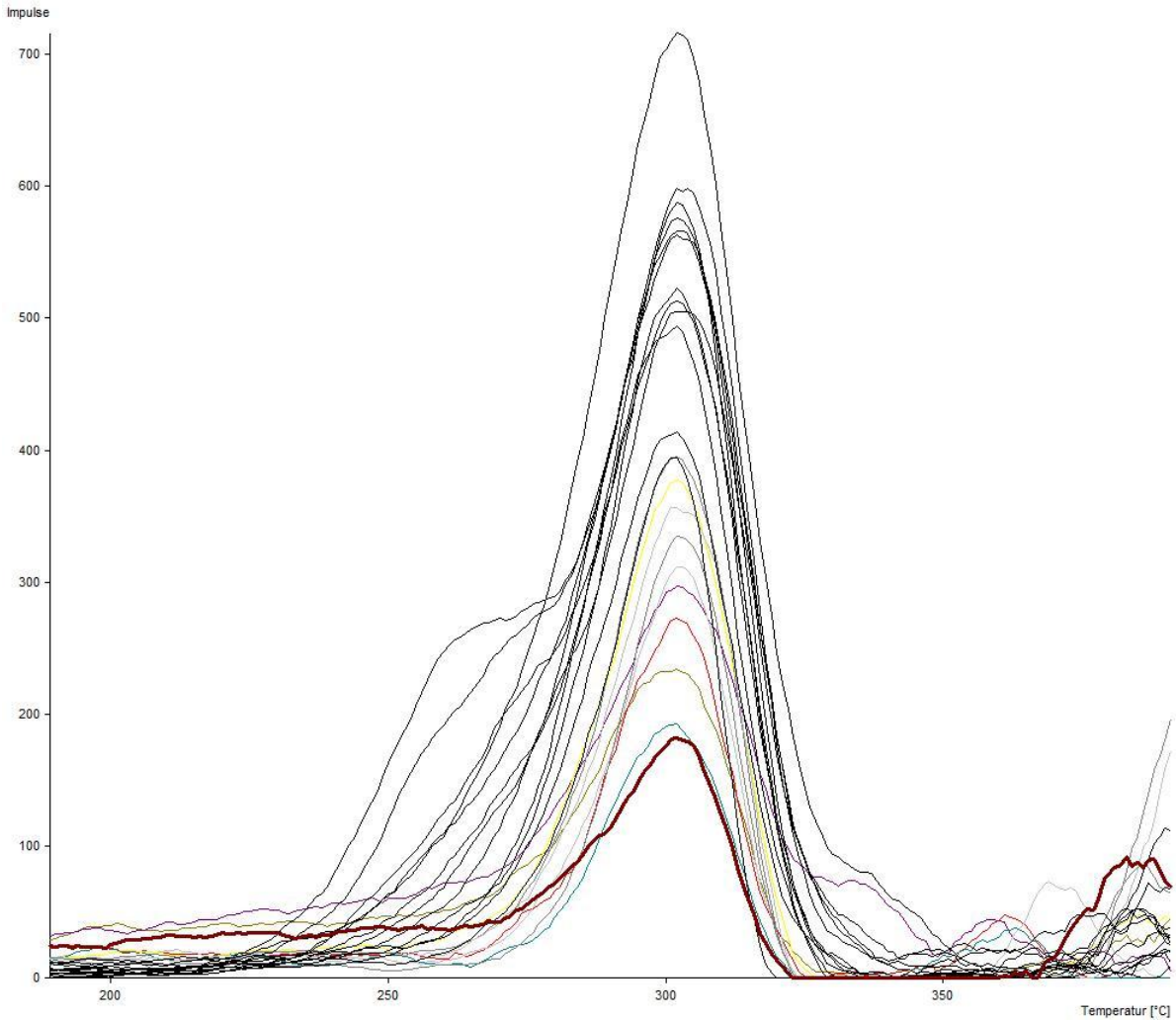

Figure IV-29: TLD-700; T_{stop} values from 266 to 310°C

The curves plotted in figure IV-29 (T_{stop} = 266 to 310°C) show the last peak obtained with this method. TL intensity gets very low, which is the reason why the measurements for temperatures T_{stop} higher than 310°C are not shown here.

IV.3.3.1 Local Maximum Method T_m–T_{stop} Diagram

The collected data from all the above maxima is used for the following T_m-T_{stop} plot (figure IV-30).

Identified peaks for TLD-700 using the local maximum method

Peak 1	115,7°C ± 0,94°C
Peak 2	198,1°C ± 2,52°C
Peak 3	262,1°C ± 4,33°C
Peak 4	306,9°C ± 2,23°C

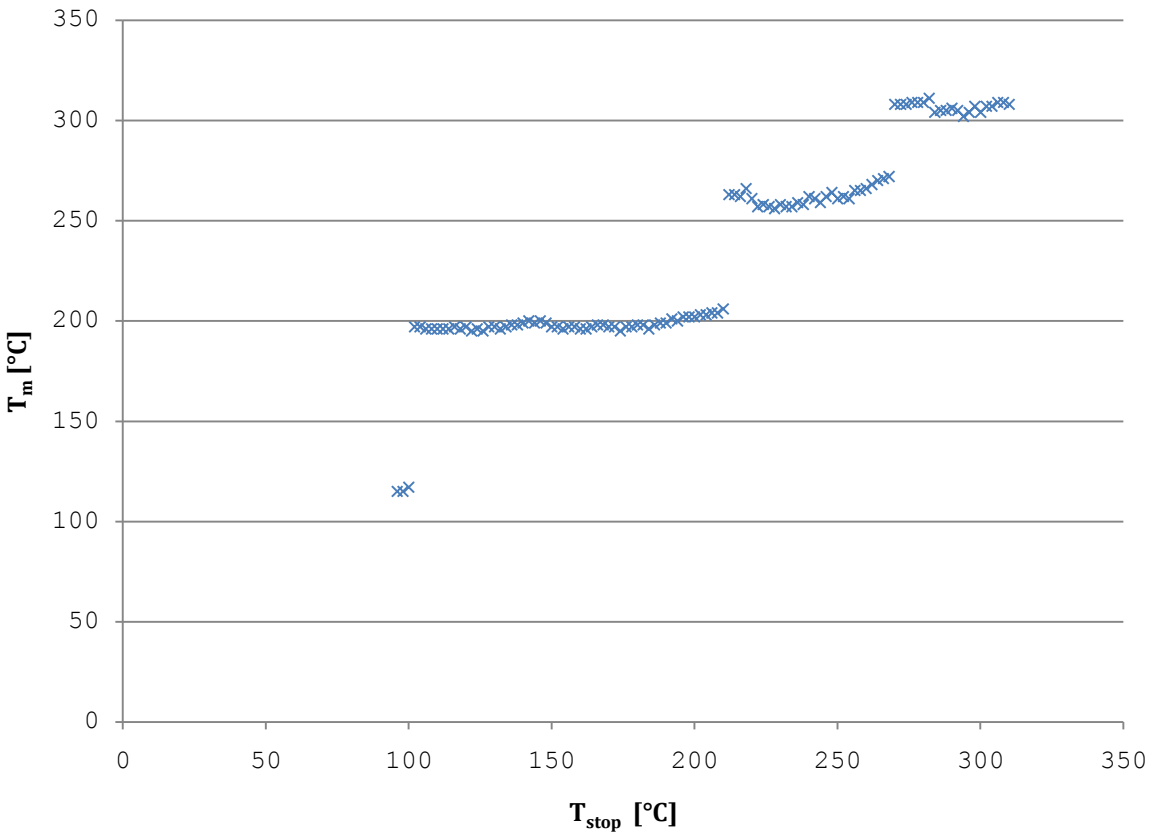

Figure IV-30: T_m-T_{stop} (96-322°C) diagram for the TLD-700 phosphor using the local maximum method

The considerable uncertainty for peak 3 results on the one hand from the similar TL intensity of peaks 3 and 4 and on the other hand from their overlap. As the intensity of peak 3 decreases step by step, with the intensity of peak 4 remaining, more or less, the same, the position of peak 3 in the glow curve begins to shift to higher temperatures.

IV.3.4 Annealed Peak Method

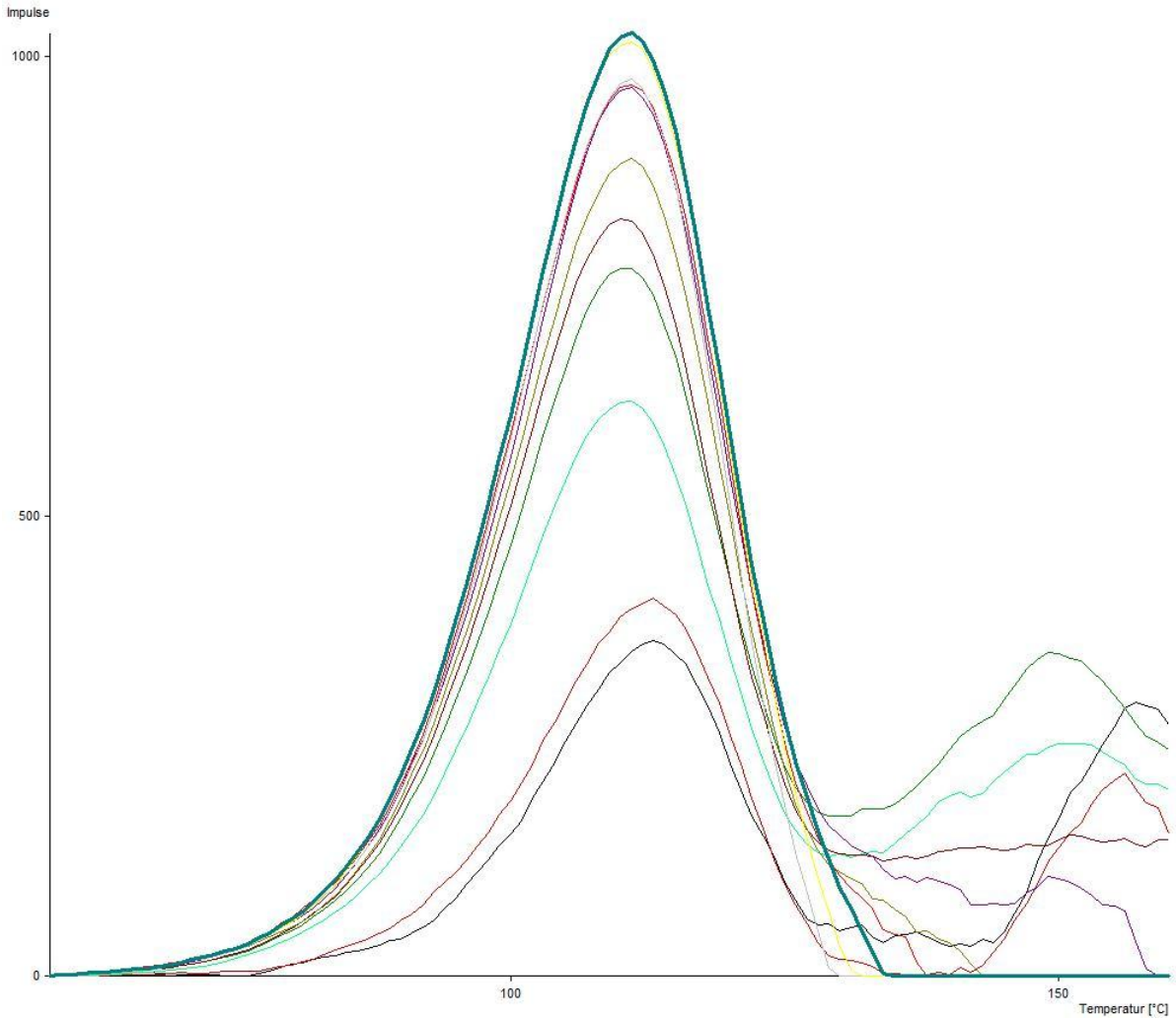

Figure IV-31: TLD-700; annealed peak method; T_{stop} values from 96 to 120°C

All the glow curves used in this method with TLD-700 have been aligned at the main peak of the reference curve (196°C), before being subtracted from it.

The first peak obtained from the annealed peak method can be seen in the T_{stop} interval from 96 to 120°C (figure IV-31). Again the curve with the highest intensity represents the highest T_{stop} value and the cut-off condition for this peak. As a characteristic of this method, the peak can still be seen at much higher T_{stop} values than with other methods.

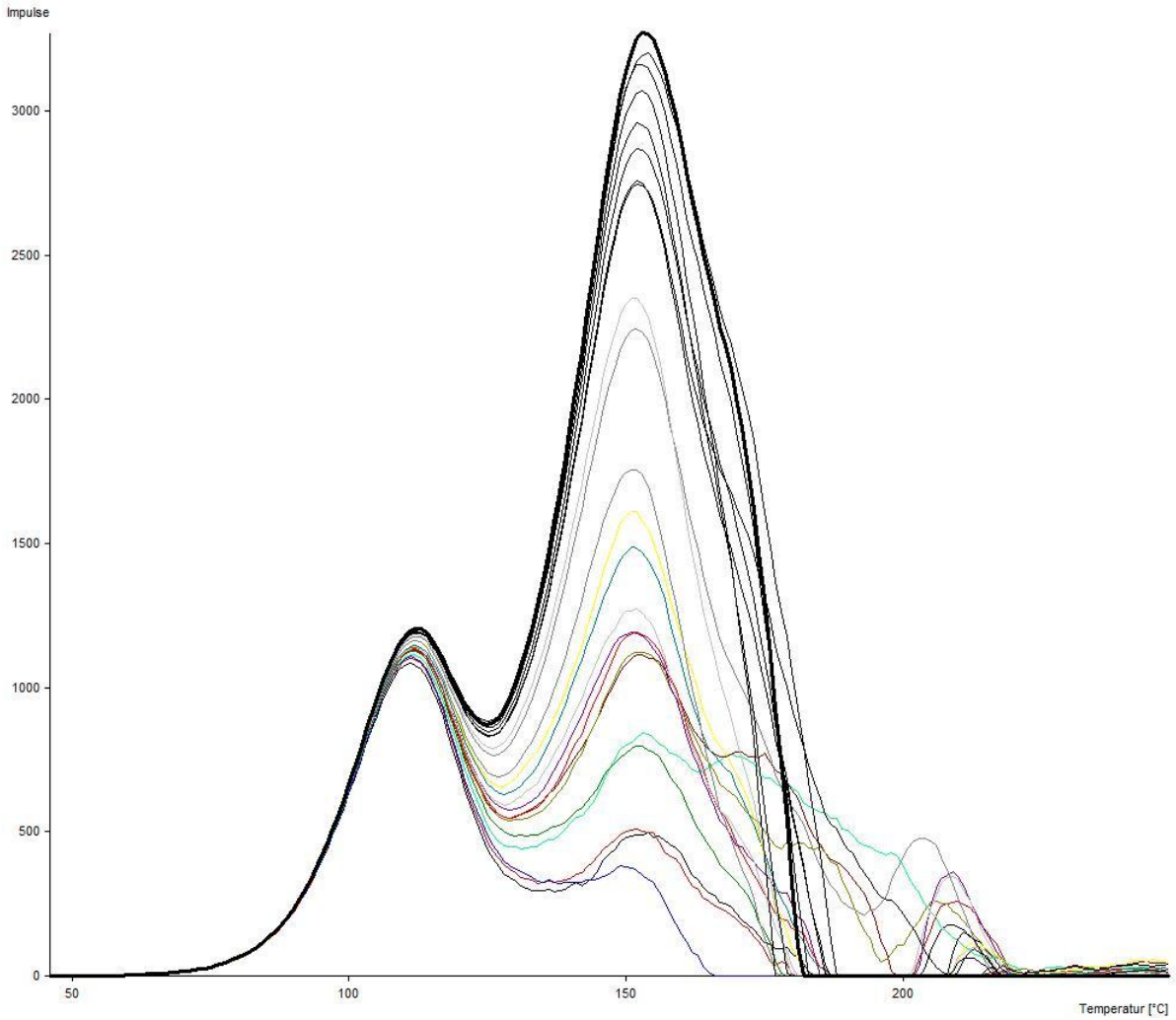

Figure IV-32: TLD-700; annealed peak method; T_{stop} values from 122 to 168°C

The next visible peak is found for T_{stop} values between 122 and 168°C (figure IV-32). Although formation of the next peak can already be seen for the upper shoulder of the glow curves, the peak remains stable, quite contrary to the next peak (figure IV-33).

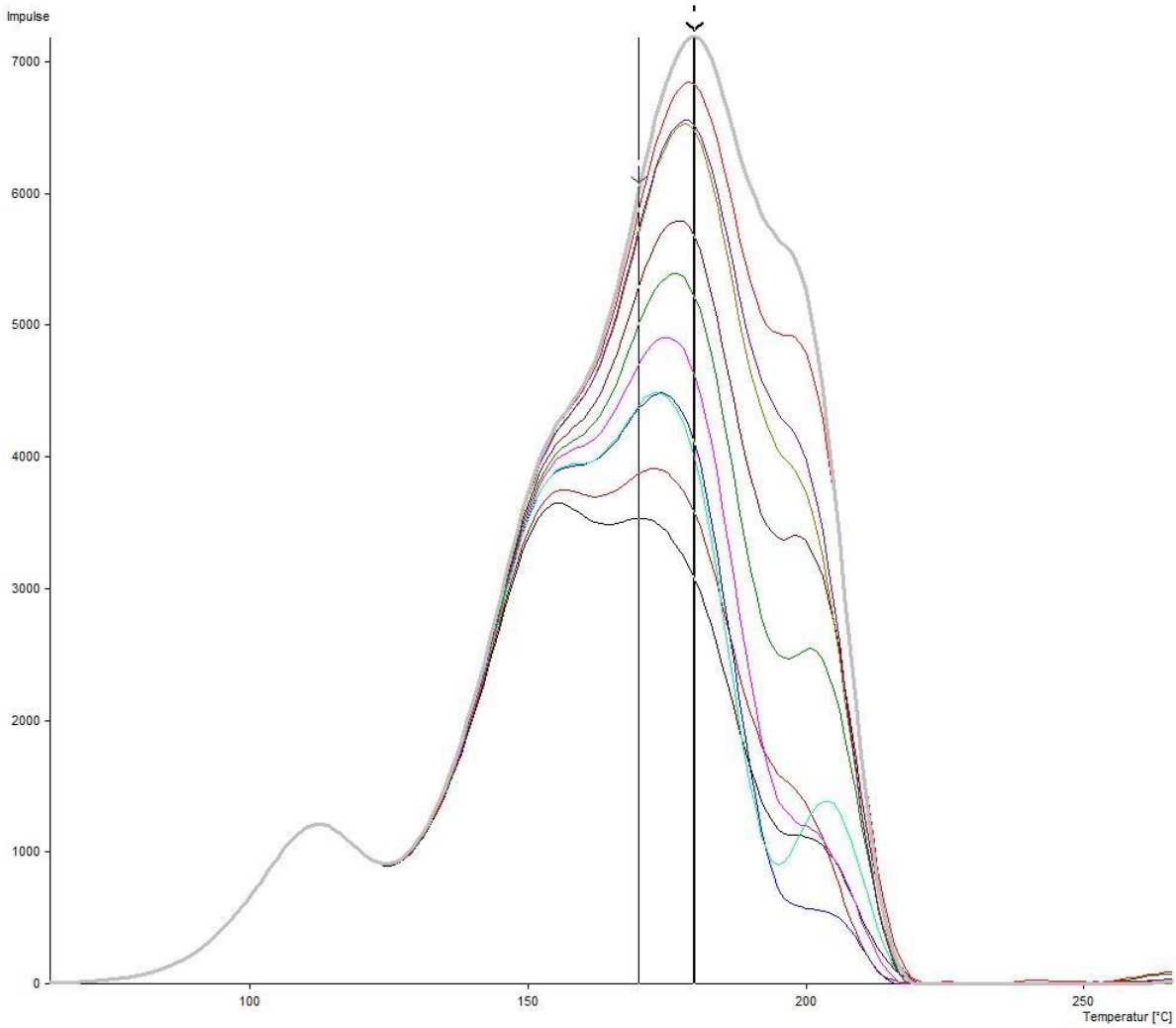

Figure IV-33: TLD-700; annealed peak method; T_{stop} values from 170 to 190°C

The T_{stop} interval for figure IV-33 is 170 to 190°C. This picture shows the shift of the third peak (marked by both cursors) found with the annealed peak method for T_{stop} from 170 to 180°C. Here, both the advantage of the annealed peak method and the disadvantage of using local maxima to identify peaks can be seen very well.

The situation is very similar to that of TLD-600, but expressed even better. In addition, the main peak can already be seen from the upper shoulder of the glow curves.

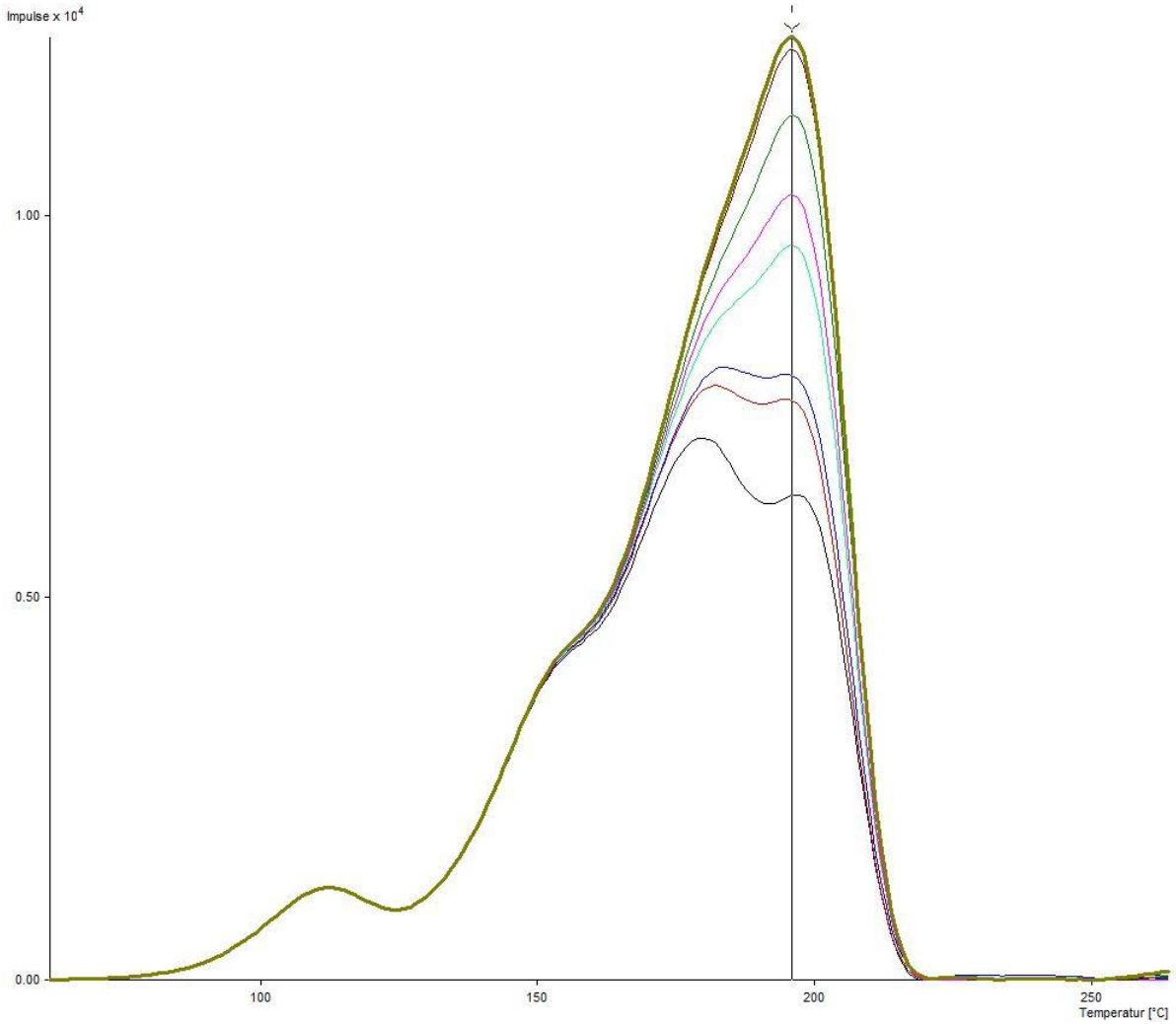

Figure IV-34: TLD-700; annealed peak method; T_{stop} values from 192 to 206°C

Finally (figure IV-34), the main peak develops (T_{stop} from 192 to 206°C) and marks the last peak detectable with this method. The cursor shows that there is almost no shift as the main peak increases in intensity. This is the result of the aligning process prior to the subtraction.

IV.3.4.1 Annealed Peak Method T_m–T_{stop} Diagram

Using all the data from the annealed peak curves, four peaks can be identified. Again, additional subtraction is necessary to obtain these curves and, therefore, the statistical uncertainty is higher.

Identified peaks for TLD-700 using the annealed peak method

Peak 1	111°C ± 2,45°C
Peak 2	152,1°C ± 2,97°C
Peak 3	175,8°C ± 4,73°C
Peak 4	195,9°C ± 6,84°C

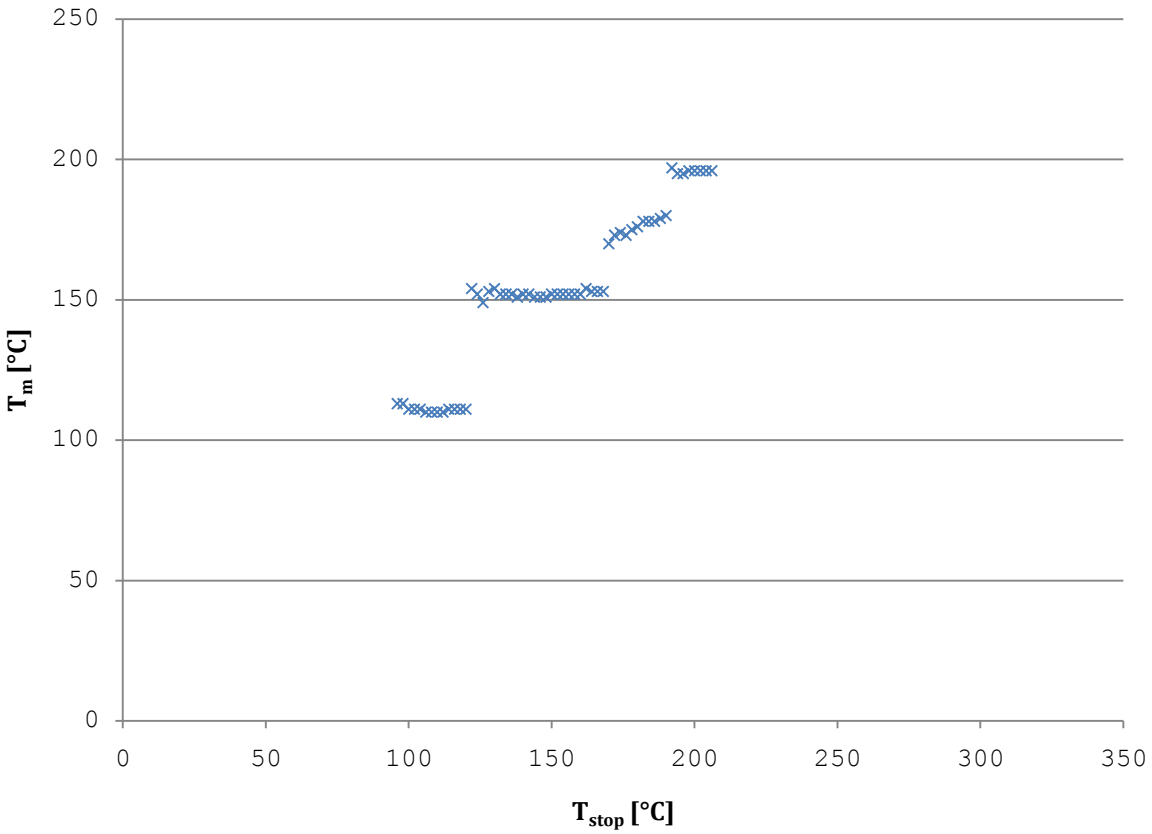

Figure IV-35: T_m-T_{stop} (96-206°C) diagram for the TLD-700 phosphor using the annealed peak method

This uncertainty can be seen for peak 4, which does shift very little in figure IV-34. However, the initial aligning before the subtraction was very high for this peak and, therefore, is the uncertainty. The glow curves responsible for this situation can be seen in figure IV-27 as the eight lowest-

intensity curves. Since, as mentioned before, peak 4 is very narrow, increasing T_{stop} beyond the corresponding T_m value results in rapidly decreasing TL intensity (considering a first-order peak), which leads to the resulting poor accuracy.

IV.3.5 Deconvolution Method

Using the deconvolution software GLOW FIT, six peaks could be identified from 113 measurements. The results from the GLOW FIT software agree well with the T_m values found with the other methods. The only peak with a rather big statistical uncertainty is peak 5 which could be explained by the presence of another peak not found in this work, but since intensity values were very low at this temperature (compare figure IV-28 and IV-29) no definite conclusion could be drawn.

Identified peaks for TLD-700 using GLOW FIT

Peak 1	115,2°C ± 1,37°C
Peak 2	152,6°C ± 2,22°C
Peak 3	177,5°C ± 0,79°C
Peak 4	199,9°C ± 2,71°C
Peak 5	262°C ± 5,17°C
Peak 6	306,6°C ± 1,98°C

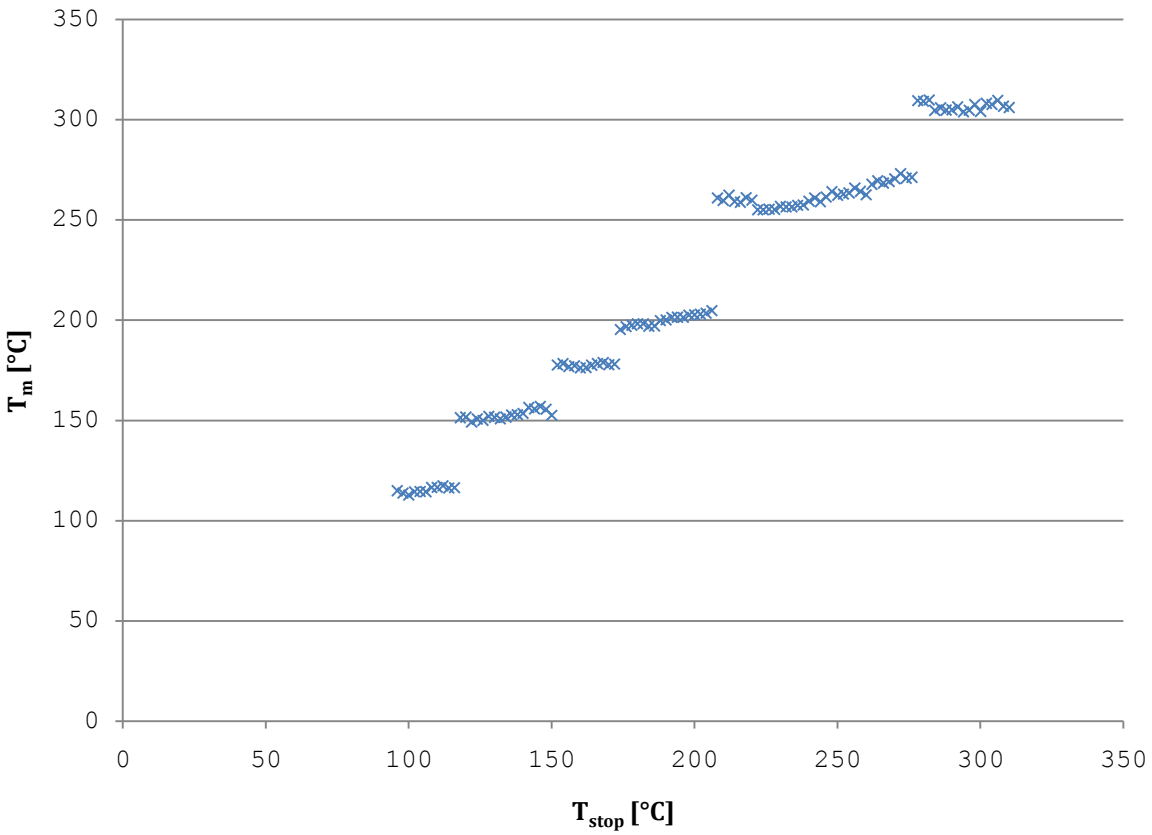

Figure IV-36: T_m-T_{stop} (96-322°C) diagram for the TLD-700 phosphor using the deconvolution software GLOW FIT

IV.3.6 TLD-700: Results

Identified peaks for TLD-700

Local Maximum	Annealed Peak	Deconvolution
115,7°C ± 0,94°C	111°C ± 2,45°C	115,2°C ± 1,37°C
	152,1°C ± 2,97°C	152,6°C ± 2,22°C
	175,8°C ± 4,73°C	177,5°C ± 0,79°C
198,1°C ± 2,52°C	195,9°C ± 6,84°C	199,9°C ± 2,71°C
262,1°C ± 4,33°C		262°C ± 5,17°C
306,9°C ± 2,23°C		306,6°C ± 1,98°C

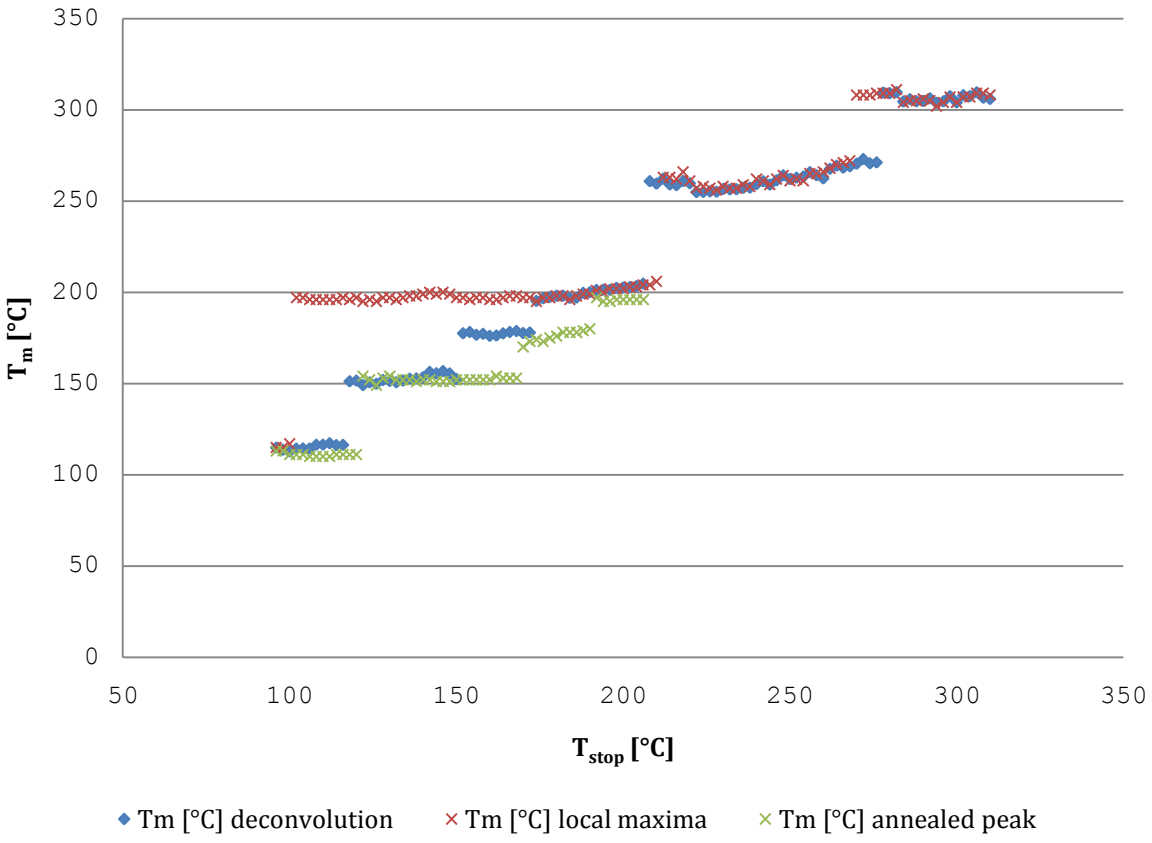

Figure IV-37: Results for the TLD-700 phosphor

Figure IV-37 shows the results for all three methods in one graph. As can be seen, the results agree very well and the results from the annealed peak method give the same T_m values as the deconvolution, but at a higher T_{stop}. Comparing these results with those from the TLD-600 phosphor class, the missing peak at about 230°C is of note. Since the phosphor types 600 and 700 are very similar (the only difference is the

used isotope: ^{7}Li for 700 and ^{6}Li for 600), the conclusion is strengthened that the “peak” at 230°C is not a second order peak but a measuring artifact.

IV.4 MTT-7 (^{7}LiF:Mg,Ti with ~50 ppm Mg, ~120 ppm Ti; extruded chips)

IV.4.1 Experimental Protocol

Irradiation Parameters:

distance from source	1 m
duration	22 h
source	Cs-137
absorbed dose	22,66 mGy
number of dosimeters	9

One day passed between irradiation and measurement. The annealing process was performed subsequent to the measurement in the LAB 01/400 (see chapter III.1.2.3).

Measurement Parameters:

heating rate	1°Cs^{-1}
heating interval	~25°C – 400°C
T_{stop} increment	2°C
T_{stop} interval	94°C – 270°C

IV.4.2 Reference Curve

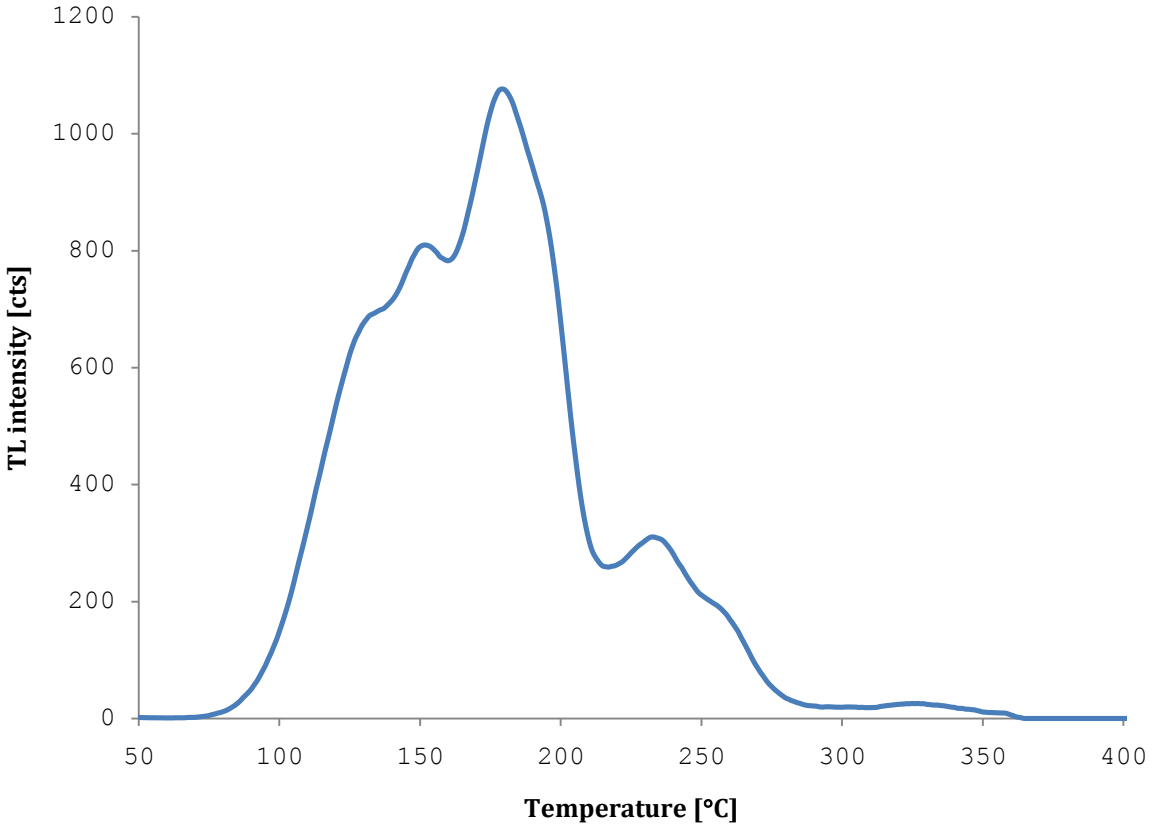

Figure IV-38: Reference curve for the MTT-7 TLD

The reference curve (figure IV-38) was obtained from 27 measurements. Each chip was measured three times. The arithmetic mean for the position of the highest peak intensity was calculated. All curves were then aligned at this temperature, in this case 179°C. The maximum shift was ±4°C. The final step was obtaining the normalized mean of all the curves which is the curve shown in figure IV-38. This curve will be used in the annealed peak method and is shown here as a reference.

The MTT-7 TLDs proved difficult to evaluate. Not only did they show variations in dose response, but also in the glow curve structure, which made comparing results from different chips very difficult. In addition, several phosphors did not withstand the measurements and broke into several pieces.

IV.4.3 Local Maximum Method

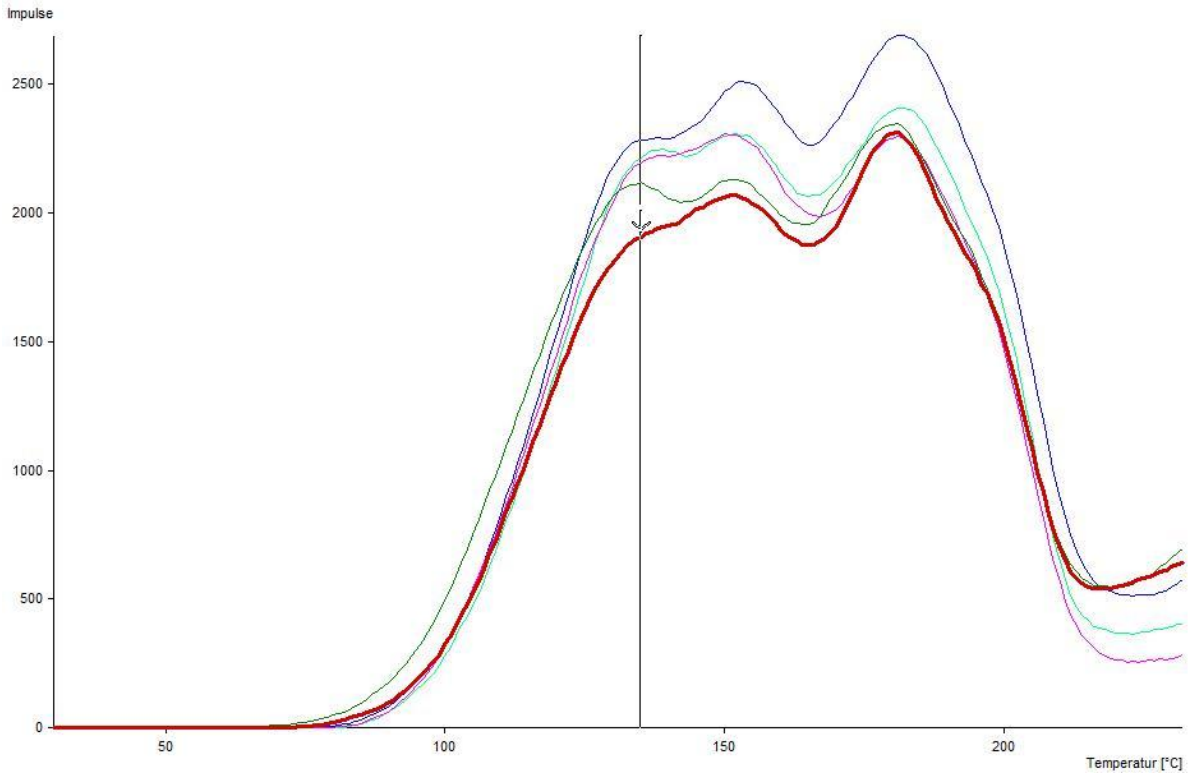

Figure IV-39: MTT-7 TLD; T_{stop} values from 94 to 102°C

The glow curves shown in figure IV-39 represent T_{stop} values from 94 to 102°C. They were aligned at 182°C. The intensity variations for the main peak at 182°C are due to batch variations.

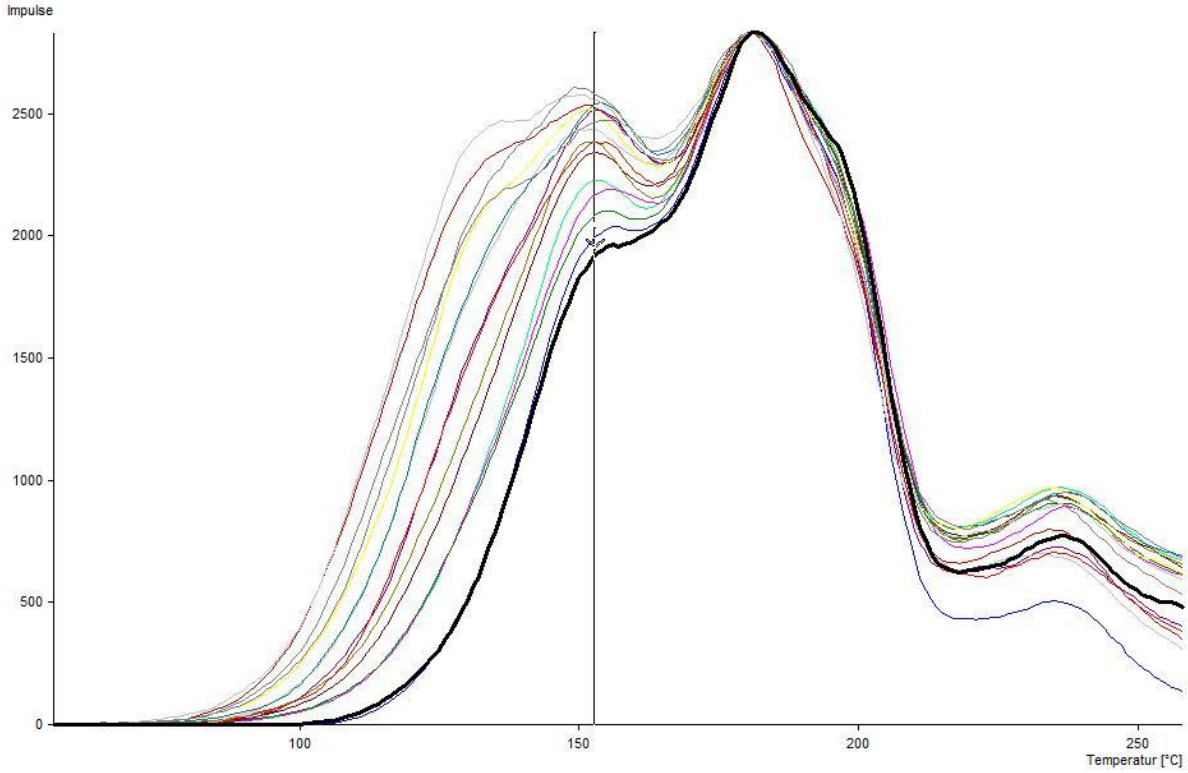

Figure IV-40: MTT-7 TLD; T_{stop} values from 102 to 132°C

Figure IV-40 shows curves for the T_{stop} interval from 102 to 132°C. Here, the bold curve again shows the cut-off condition for this peak. The curves were aligned at 182°C. To better view the different T_{stop} steps the curves were normalized to the main peak. This normalization causes the peak intensity variations seen at ~240°C.

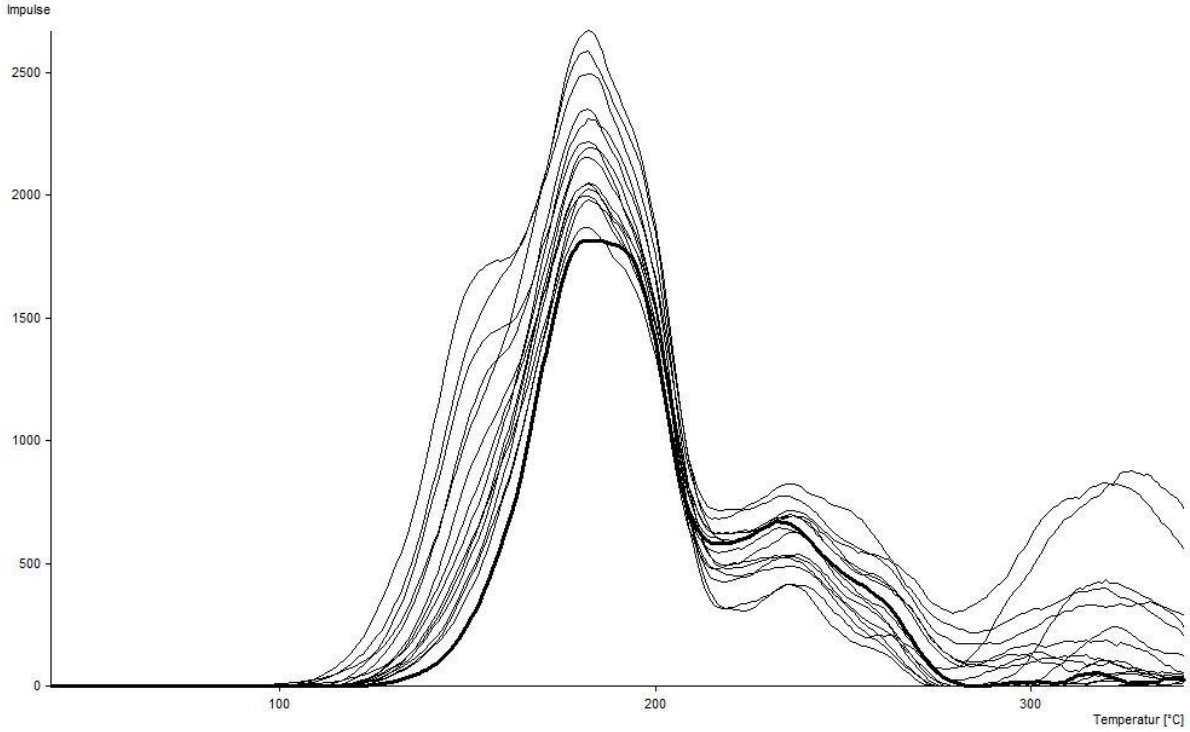

Figure IV-41: MTT-7 TLD; T_{stop} values from 134 to 162°C

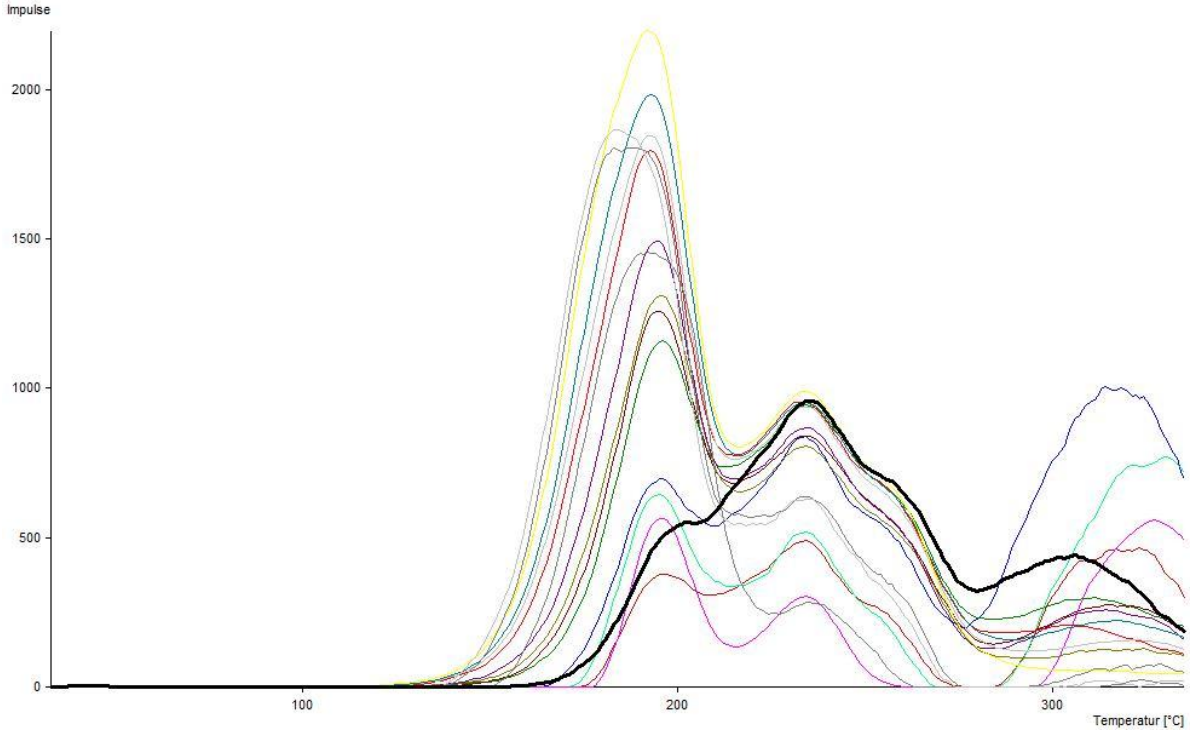

Figure IV-42: MTT-7 TLD; T_{stop} values from 164 to 194°C

Figures IV-41 and IV-42 (IV-41: T_{stop} from 134 to 162°C, aligned at 182°C; IV-42: T_{stop} from 164 to 194°C aligned at 234°C) show the closest peak transition resolved within this work using the local maximum method. This is only possible because both peaks appear to be very narrow. The cut-off condition in

figure IV-41 shows this best, as here both peaks form a plateau and appear to be at exactly the same intensity at this T_{stop} temperature (194°C).

The bold black curve in figure IV-42 was measured with the highest T_{stop} temperature, but due to the aforementioned sensitivity variations of the MTT-7 TLDs it does not represent the curve with the lowest intensity of the residual glow curve.

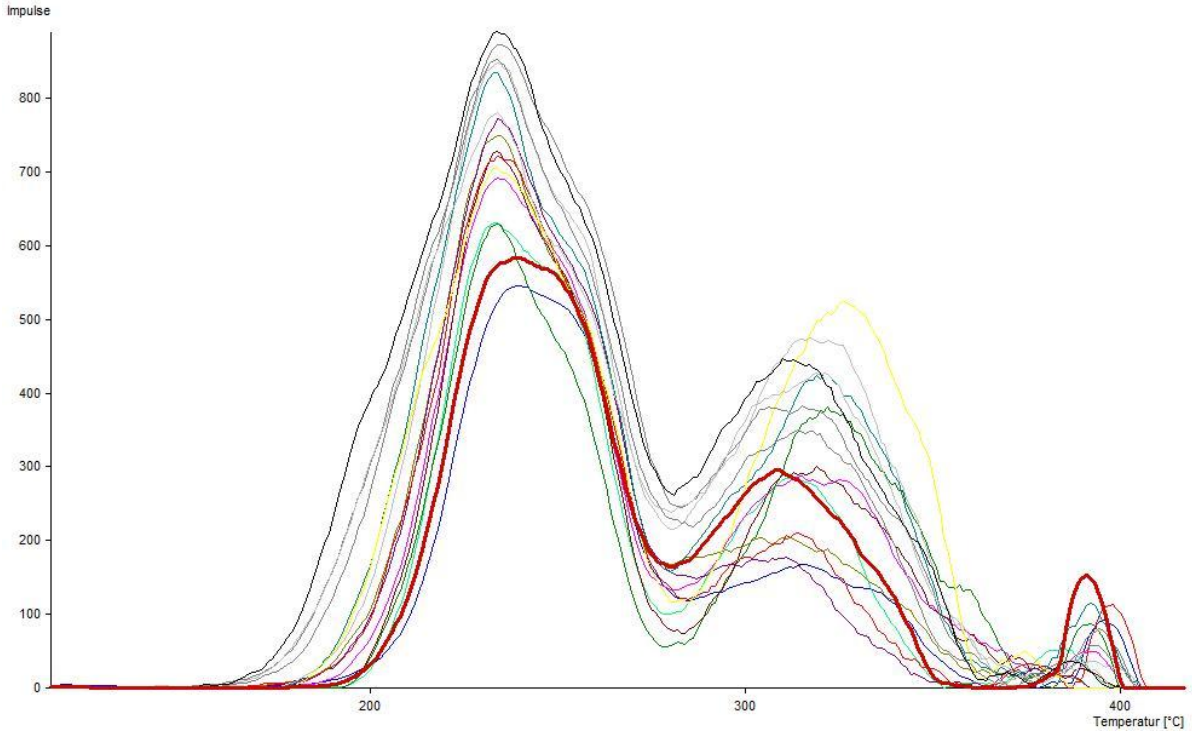

Figure IV-43: MTT-7 TLD; T_{stop} values from 196 to 226°C

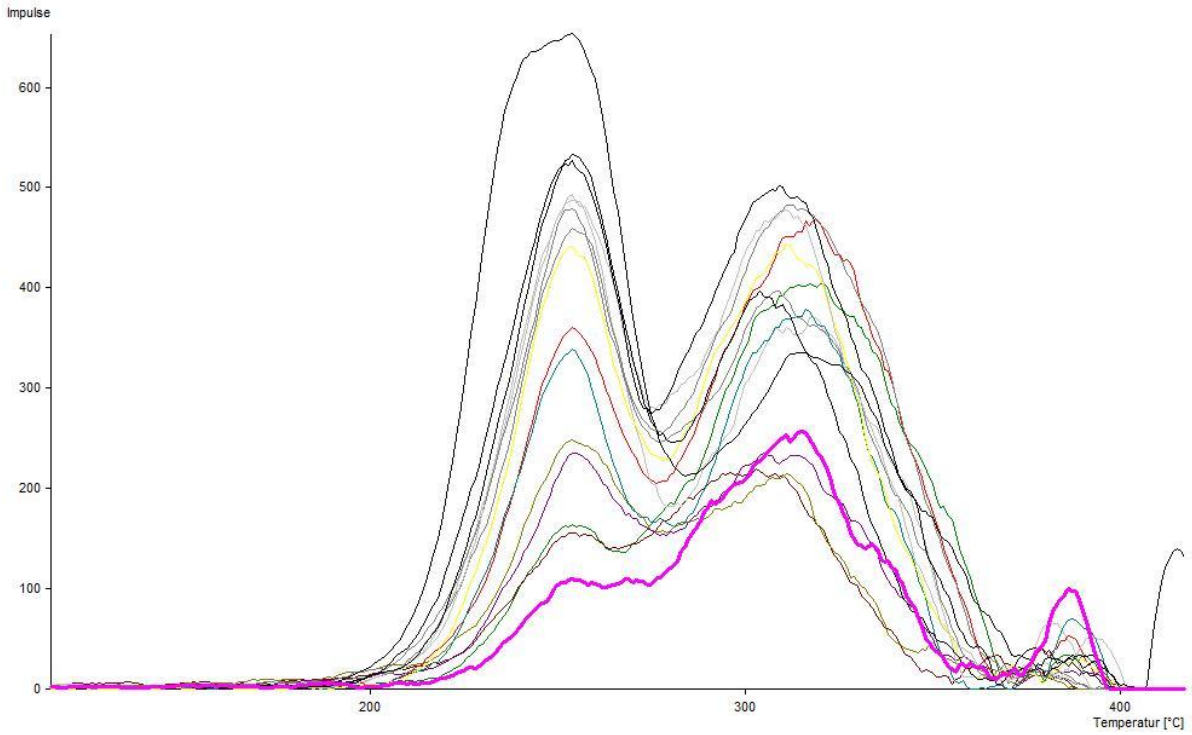

Figure IV-44: MTT-7 TLD; T_{stop} values from 228 to 262°C

Another peak transition resolved with the local maximum method can be seen from figure IV-43 and IV-44. Figure IV-43 shows T_{stop} values ranging from 196 to 226°C, aligned at 234°C. The T_{stop} values for Figure IV-44 are between 228 and 262°C, aligned at 254°C.

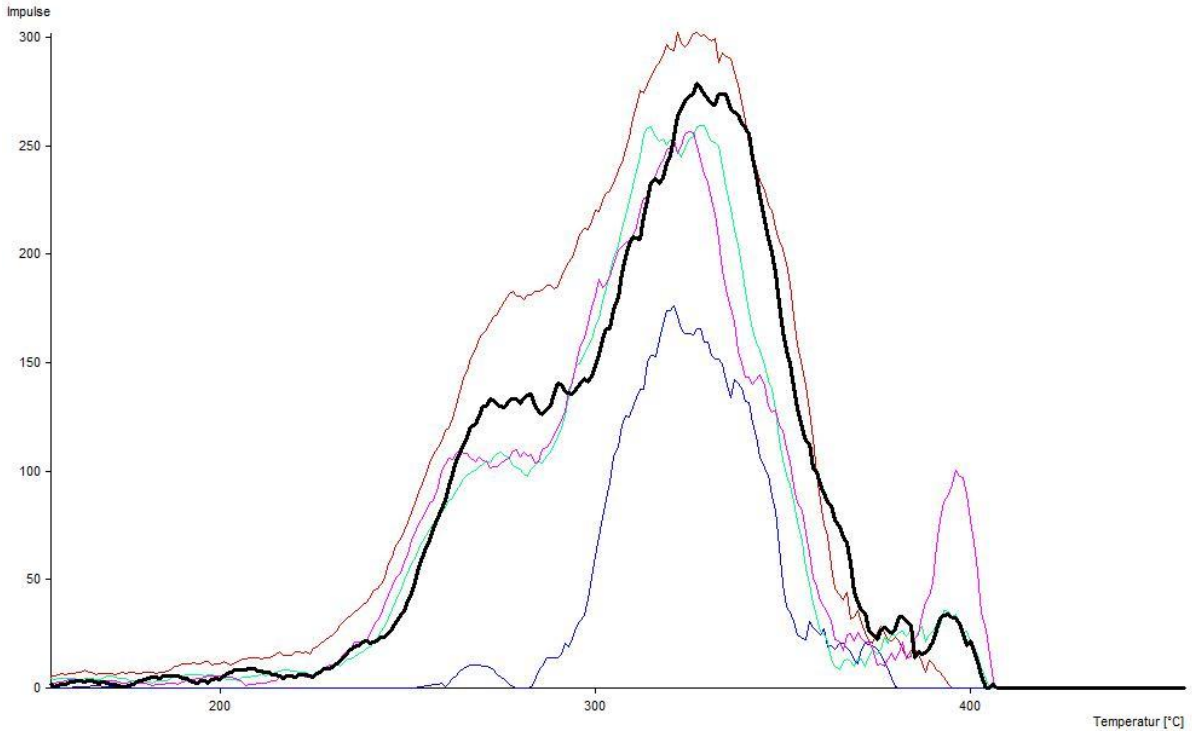

Figure IV-45: MTT-7 TLD; T_{stop} values from 264 to 270°C

The glow curves shown in figure IV-45 (T_{stop} from 264 to 270°C) were not aligned. The TL intensity is very low, nonetheless with the local maximum method the highest-temperature peak for the MTT-7 chip can be found. Because the peak positions are quite close, the statistical uncertainty is smaller than expected. However, since the intensity is so low, this position needs to be confirmed by other methods (see deconvolution below).

IV.4.3.1 Local Maximum Method T_m–T_{stop} Diagram

The collected peak information is shown in figure IV-46. Seven peaks could be identified with the local maximum method which is the highest number of all investigated phosphors. Although the MTT-7 TLD has a very complex glow curve structure, it seems that most of these peaks (at this absorbed dose) are of almost the same intensity and are separated sufficiently for local maxima to develop, instead of being overshadowed by a large peak as it is often the case with other TLD substances.

Identified peaks for the MTT-7 TLD using the local maximum method

Peak 1	137°C ± 0,71°C
Peak 2	150,4°C ± 1,8°C
Peak 3	180,8°C ± 2,65°C
Peak 4	193,1°C ± 3,87°C
Peak 5	236,8°C ± 2,9°C
Peak 6	259,6°C ± 5,72°C
Peak 7	323,3°C ± 2,63°C

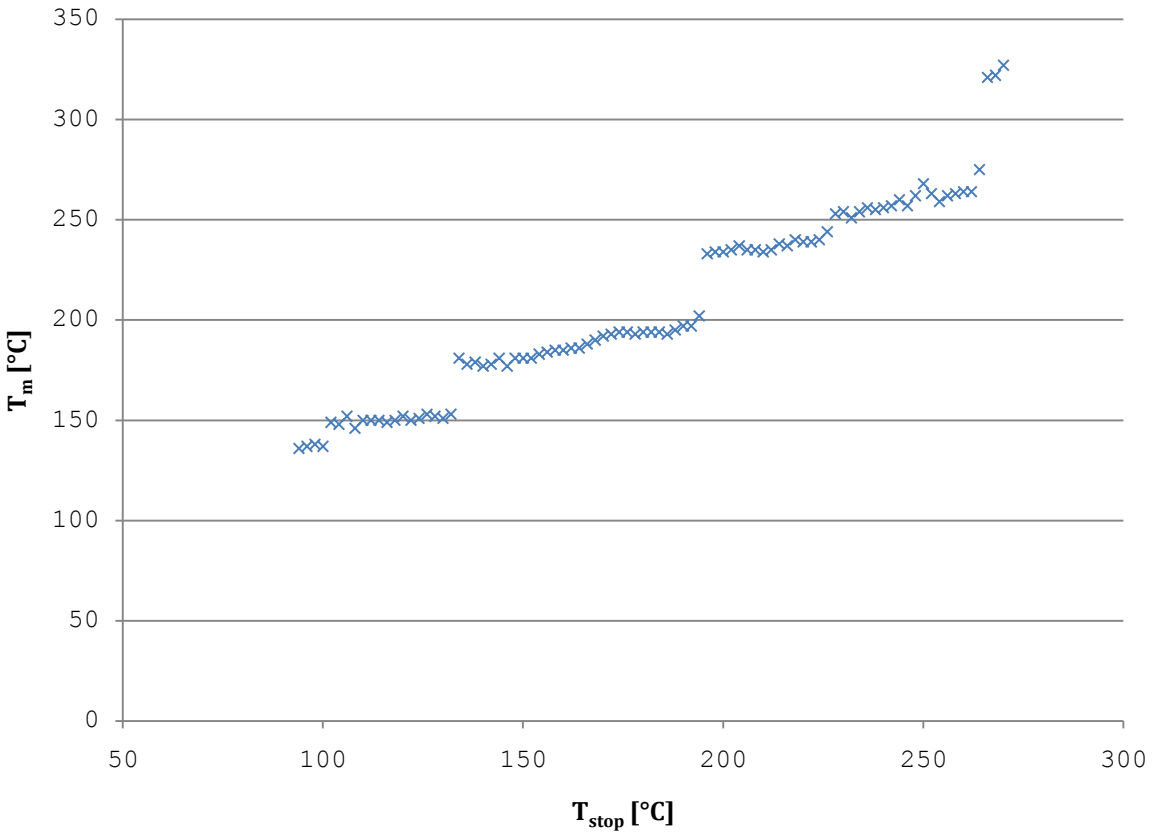

Figure IV-46: T_m-T_{stop} (94-270°C) diagram for the MTT-7 TLD using the local maximum method

The continuous transition from peak 3 to 4 seems not to suggest a second peak. However, the two separated visible plateaus indicate that indeed there are two separated peaks. A similar situation is found with peaks 5 and 6. These peaks seem to be separated sufficiently for a noticeable step to occur in the T_m–T_{stop} diagram.

IV.4.4 Annealed Peak Method

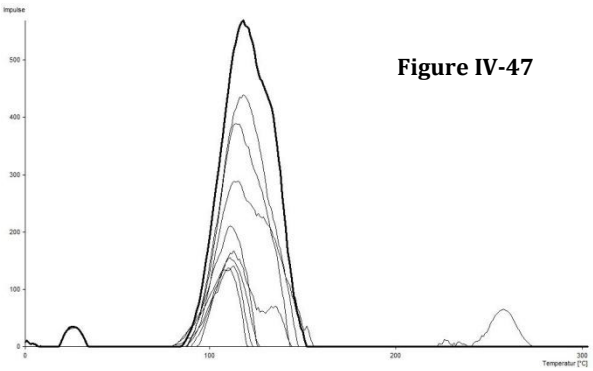

Figure IV-47

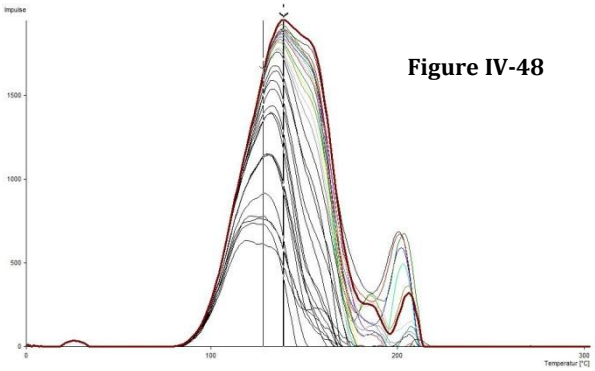

Figure IV-48

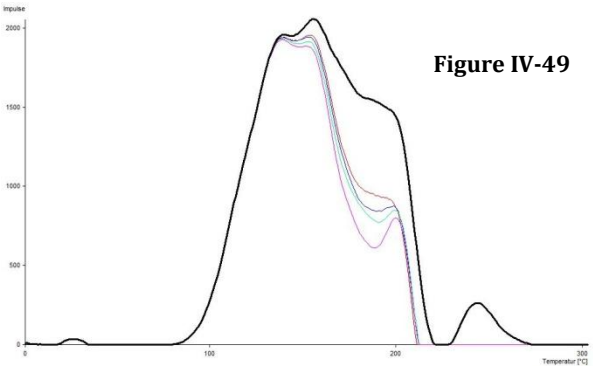

Figure IV-49

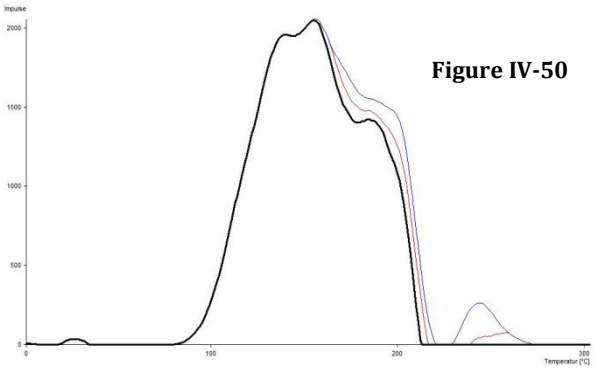

Figure IV-50

As explained in chapter II.4.2 (Visualizing T_m-T_{stop}), the annealed peak method works best when low-intensity peaks are followed by high-intensity peaks with increasing temperature. Since the MTT-7 glow curves do not have such a structure, this method does not work well with these glow curves. It is shown here for completeness. The huge statistical uncertainties can be explained to be due to the impossibility to align the curves with high accuracy at the main peak.

IV.4.4.1 Annealed Peak Method T_m–T_{stop} Diagram

From the depicted (figures IV-47 to IV-50) glow curves, four peaks can be identified. The results from the annealed peak method correspond with the deconvolution results, but, as mentioned before, the statistical uncertainties make these results almost meaningless.

Identified peaks for the MTT-7 TLD using the annealed peak method

Peak 1	113,6°C ± 9,02°C
Peak 2	133,6°C ± 11,28°C
Peak 3	153,4°C ± 10,31°C
Peak 4	184,5°C ± 11,55°C

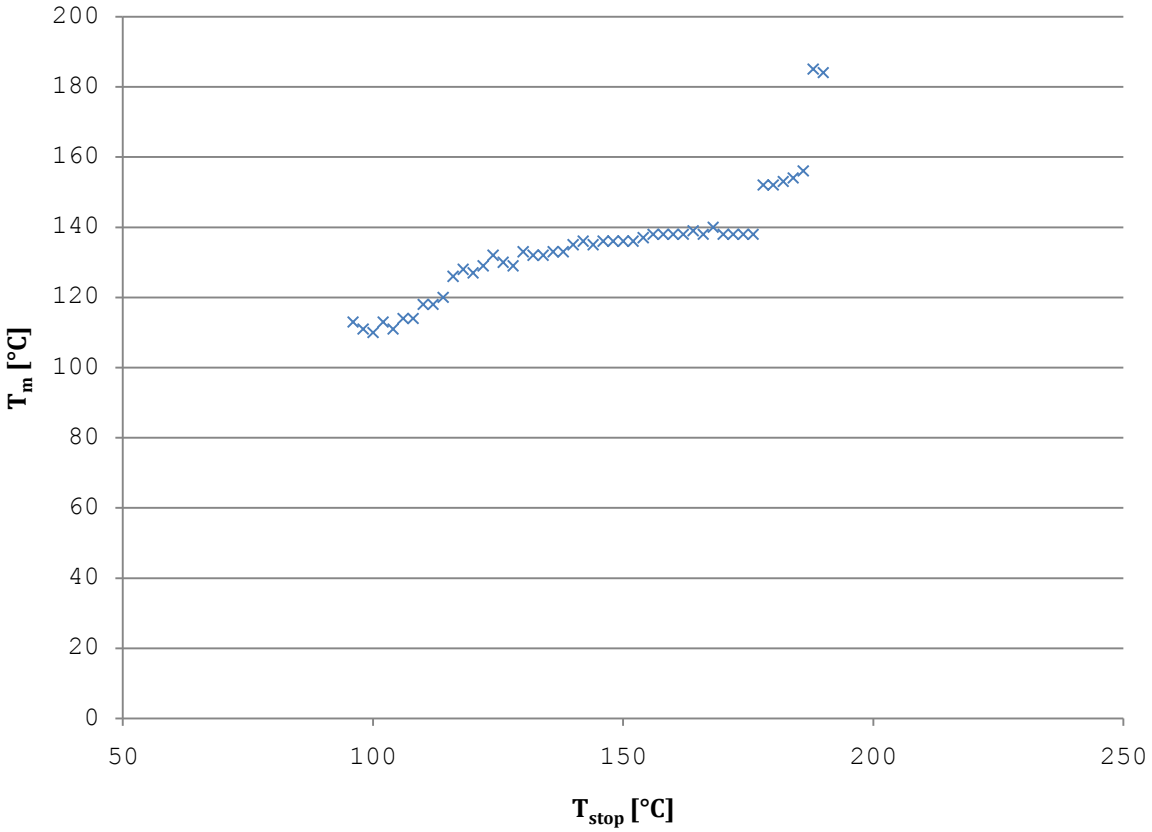

Figure IV-51: T_m-T_{stop} (96-190°C) diagram for the MTT-7 TLD using the annealed peak method

IV.4.5 Deconvolution Method

The deconvolution of 88 measured glow curves with GLOW FIT identified ten peaks (figure IV-52). The statistical uncertainties were higher than with other phosphors.

Identified peaks for the MTT-7 TLD using GLOW FIT

Peak 1	112,8°C ± 0,67°C
Peak 2	127,3°C ± 1,5°C
Peak 3	147,8°C ± 1,28°C
Peak 4	177,2°C ± 2,47°C
Peak 5	195,2°C ± 1,66°C
Peak 6	213,6°C ± 3,15°C
Peak 7	234°C ± 2,03°C
Peak 8	255°C ± 4,09°C
Peak 9	262°C ± 2,39°C
Peak 10	330,1°C ± 3,13°C

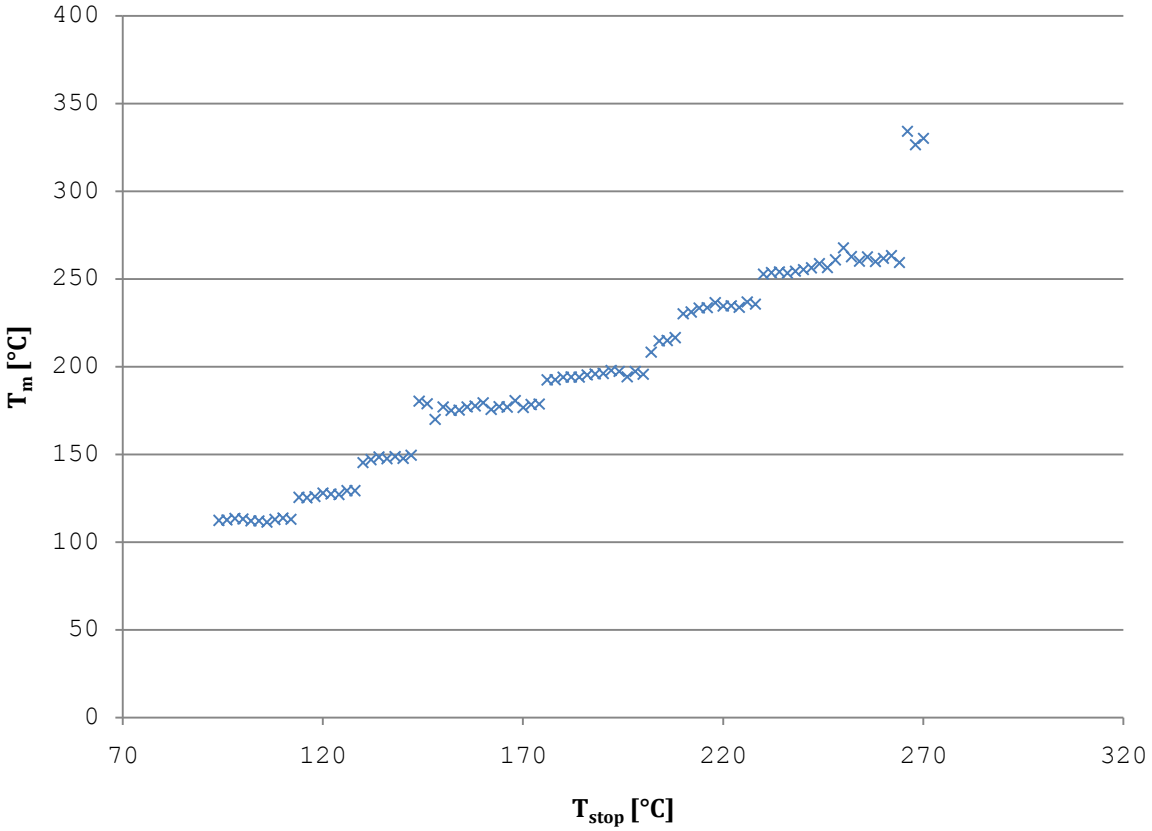

Figure IV-52: T_m-T_{stop} (94-270°C) diagram for the MTT-7 TLD using the deconvolution software GLOW FIT

IV.4.6 MTT-7: Results

Identified peaks for MTT-7

Local Maximum	Annealed Peak	Deconvolution
	113,6°C ± 9,02°C	112,8°C ± 0,67°C
137°C ± 0,71°C	133,6°C ± 11,28°C	127,3°C ± 1,5°C
150,4°C ± 1,8°C	153,4°C ± 10,31°C	147,8°C ± 1,28°C
180,8°C ± 2,65°C	184,5°C ± 11,55°C	177,2°C ± 2,47°C
193,1°C ± 3,87°C		195,2°C ± 1,66°C
		213,6°C ± 3,15°C
236,8°C ± 2,9°C		234°C ± 2,03°C
		255°C ± 4,09°C
259,6°C ± 5,72°C		262°C ± 2,39°C
323,3°C ± 2,63°C		330,1°C ± 3,13°C

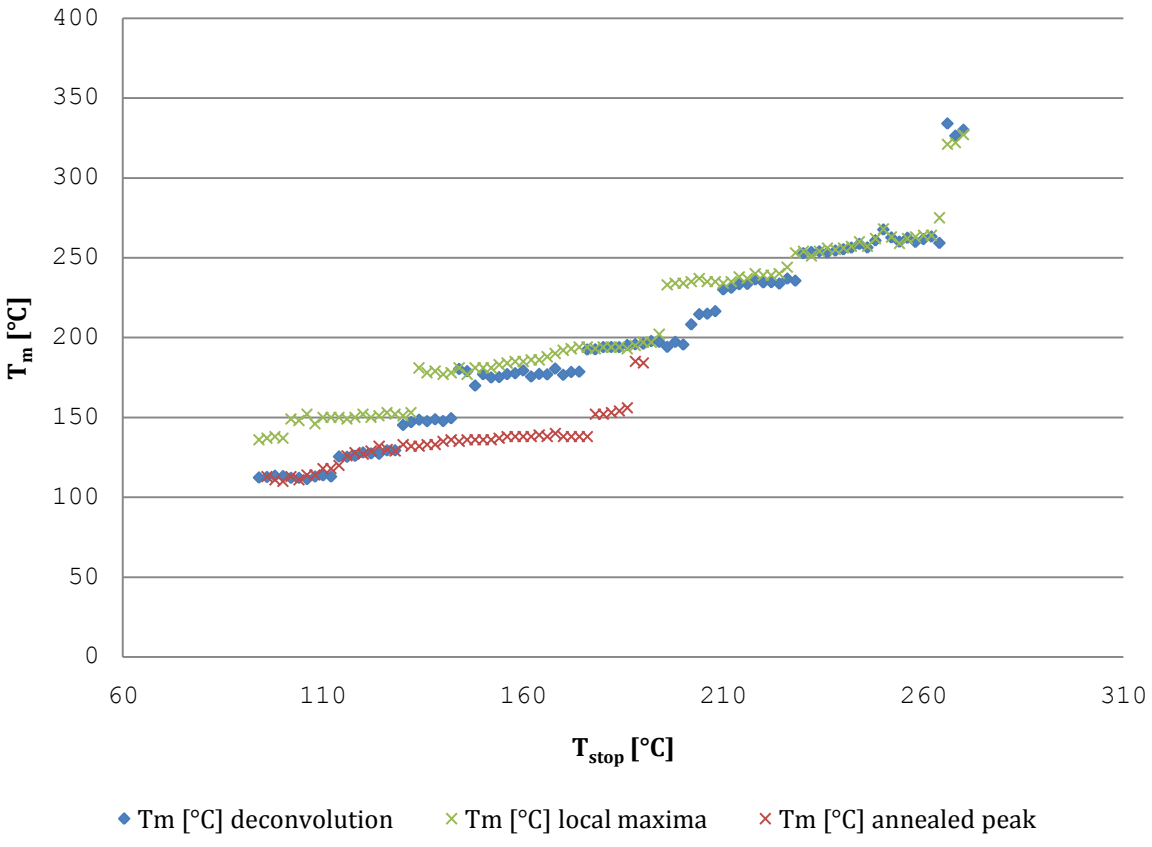

Figure IV-53: Results for the MTT-7 TLD

The results obtained from the deconvolution confirm the results from the local maximum method. So, the small separation of peaks 4 and 5 as well as the peak at T_m=330°C are

found within the statistical uncertainty, as is shown in figure IV-53. The poor resolution of the annealed peak method for this glow curve type is shown as well.

IV.5 Tempered MTT-7 (^{7}LiF:Mg,Ti with ~50 ppm Mg, ~120 ppm Ti; extruded chips)

IV.5.1 Experimental Protocol

Irradiation Parameters:	
distance from source	1 m
duration	22 h
source	Cs-137
absorbed dose	22,66 mGy
number of dosimeters	9

One day passed between irradiation and measurement. Prior to the measurement the MTT-7 TLDs were being pre-heated (figure IV-54) at 120°C for 30 minutes.

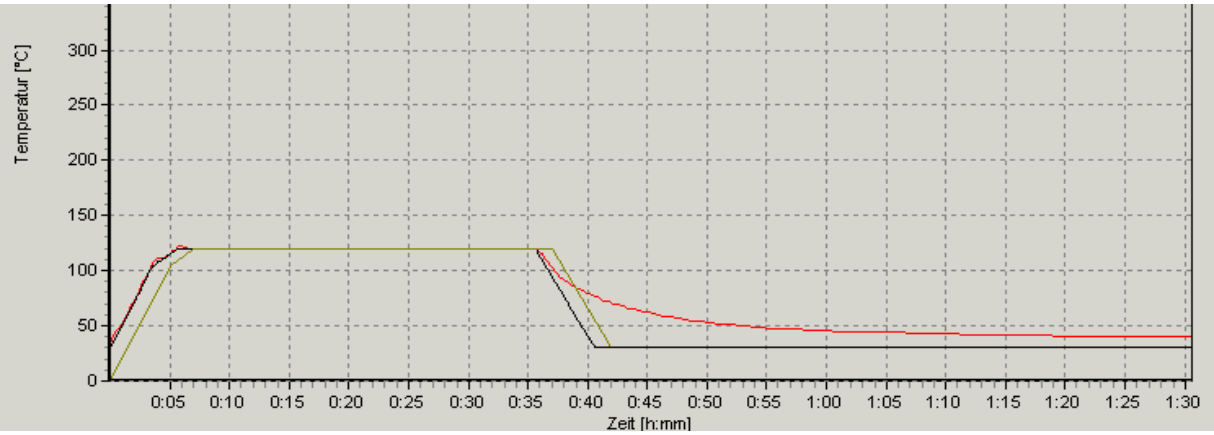

Figure IV-54: tempering process; the red curve depicts the real temperature whereas the black shows the preprogrammed temperature.

This procedure effectively annealed the low-temperature peaks (compare the reference curves IV-38 and IV-55). The annealing process was performed subsequent to the measurement in the LAB 01/400 (see chapter III.1.2.3).

Measurement Parameters:	
heating rate	1°Cs^{-1}
heating interval	~25°C – 400°C
T_{stop} increment	2°C
T_{stop} interval	140°C – 296°C

IV.5.2 Reference Curve

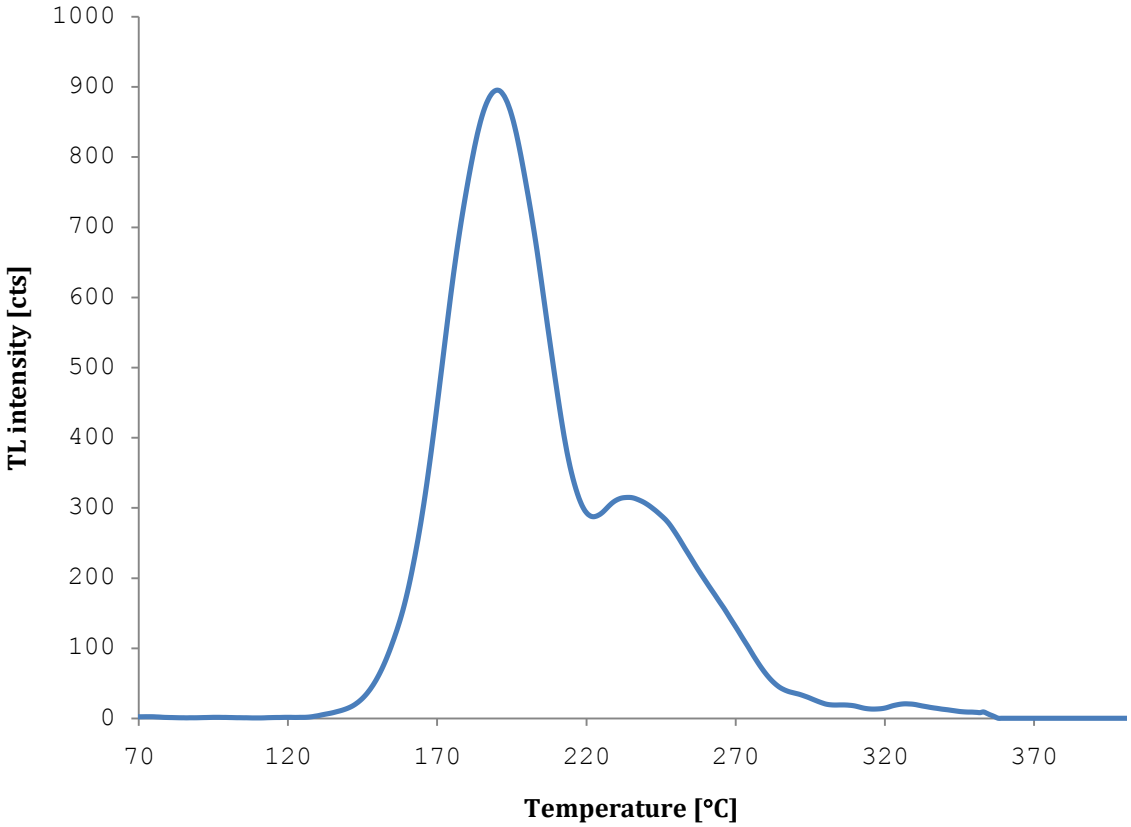

Figure IV-55: Reference curve for the tempered MTT-7 TLD

The reference curve (figure IV-55) was obtained from 27 measurements. Each chip was measured three times. The arithmetic mean for the position of the highest peak intensity was calculated. All curves were then aligned at this temperature, in this case 190°C. The maximum shifts were -2°C and +7°C. The final step was obtaining the normalized mean of all the curves which is the curve shown in figure IV-55. This curve will be used in the annealed peak method and is shown here as a reference.

IV.5.3 Local Maximum Method

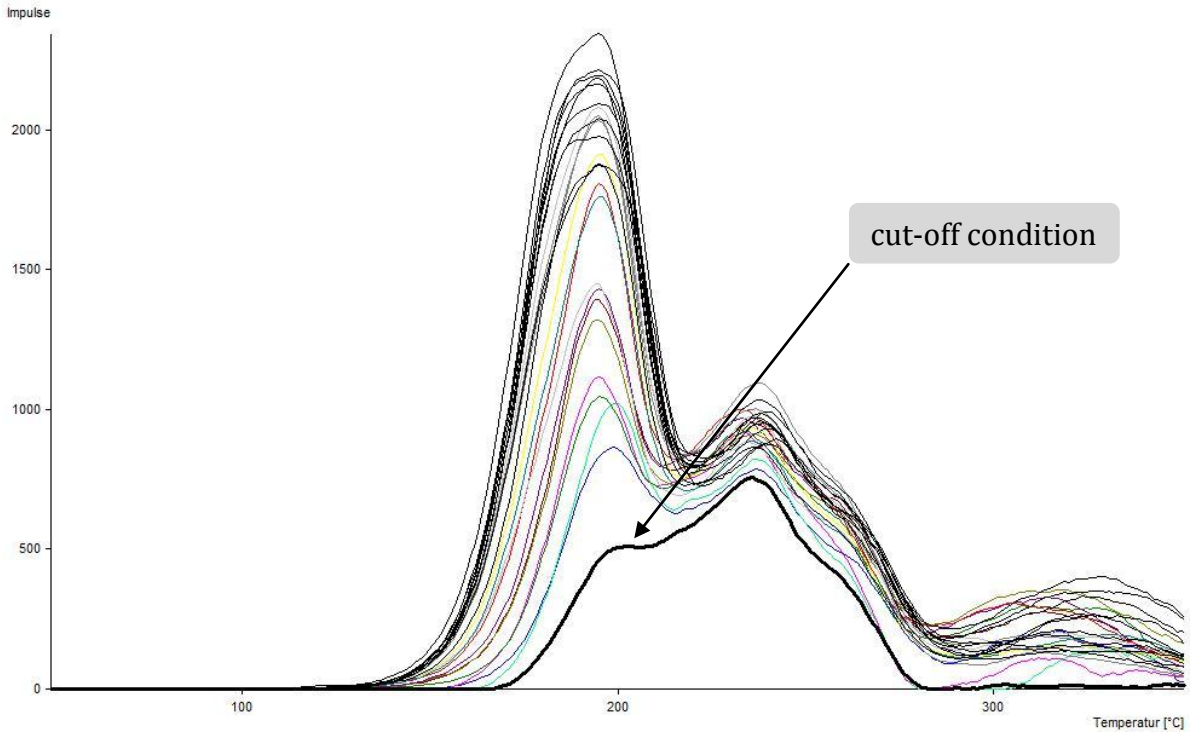

Figure IV-56: tempered MTT-7 TLD; T_{stop} values from 104 to 196°C

Figure IV-56 shows the glow curves for T_{stop} values from 104 to 196°C. The curves were aligned at 195°C for better visibility. The glow curves of higher TL intensity suggest that the main peak is composed of two peaks. However, with the local maximum method no second peak could be found. The bold black curve represents the cut-off condition.

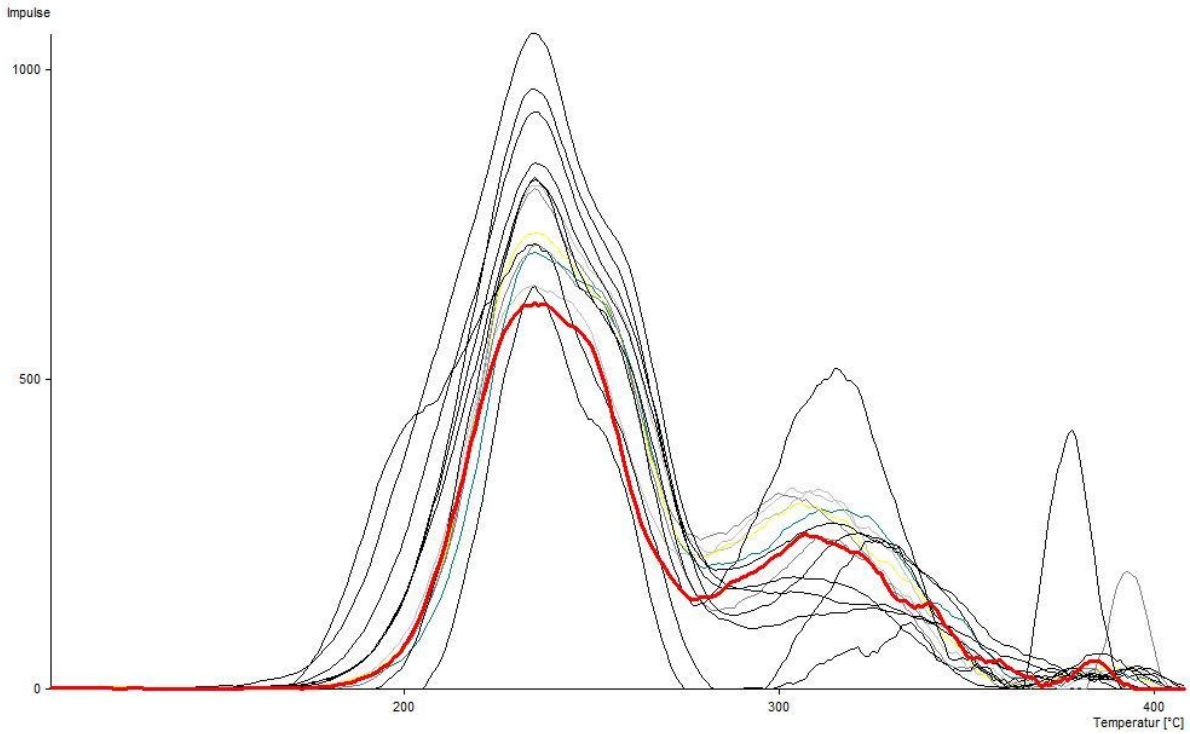

Figure IV-57: tempered MTT-7 TLD; T_{stop} values from 198 to 228°C

The next peak (figure IV-57) found with the local maximum method can be seen at T_{stop} values from 198 to 228°C. The shown glow curves were aligned at 235°C.

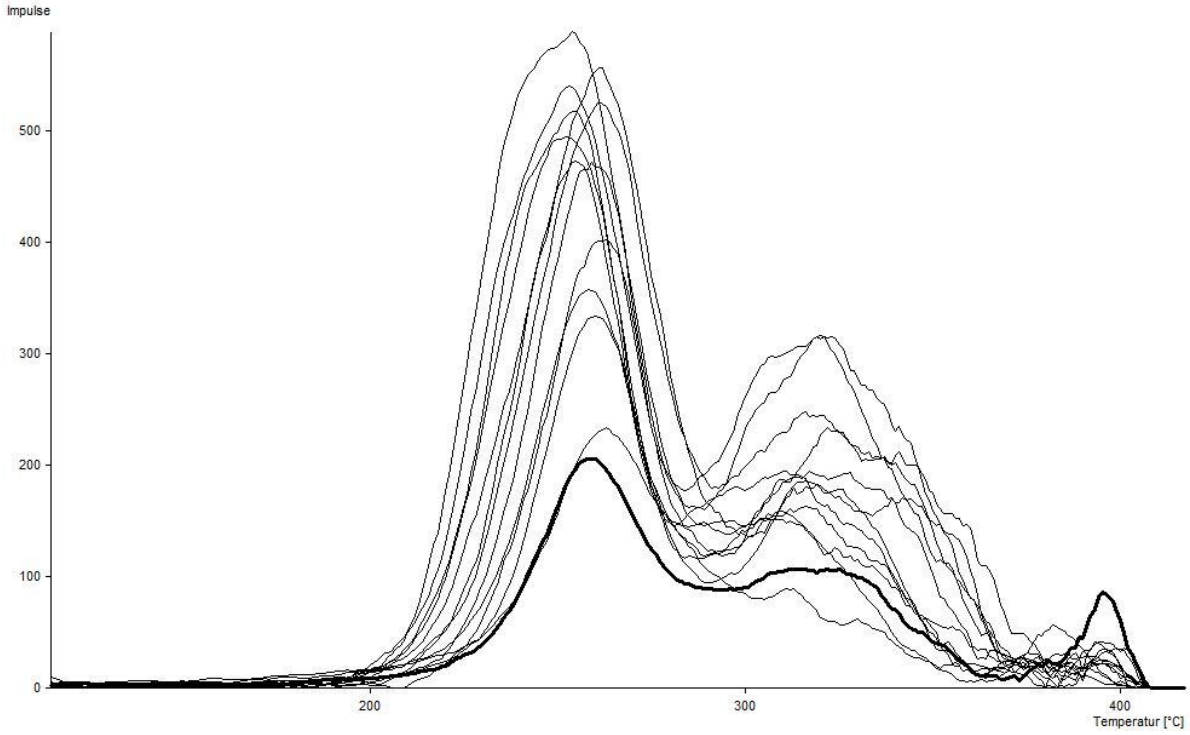

Figure IV-58: tempered MTT-7 TLD; T_{stop} values from 230 to 258°C

The glow curves shown in figure IV-58 were obtained for T_{stop} values from 230 to 258°C. These curves have not been aligned. The next visible peak at ~320°C could not be identified with this method as the TL intensity got very low for T_{stop} values exceeding 258°C. Because of this, the measurements above 258°C had to be discarded.

IV.5.3.1 Local Maximum Method T_m–T_{stop} Diagram

Three peaks could be identified with this method (figure IV-59). Although two more peaks might be expected, the resolution has not been sufficient to resolve these.

Identified peaks for the tempered MTT-7 TLD using the local maximum method

Peak 1	192,9°C ± 5,26°C
Peak 2	236,8°C ± 4,15°C
Peak 3	258,2°C ± 3,54°C

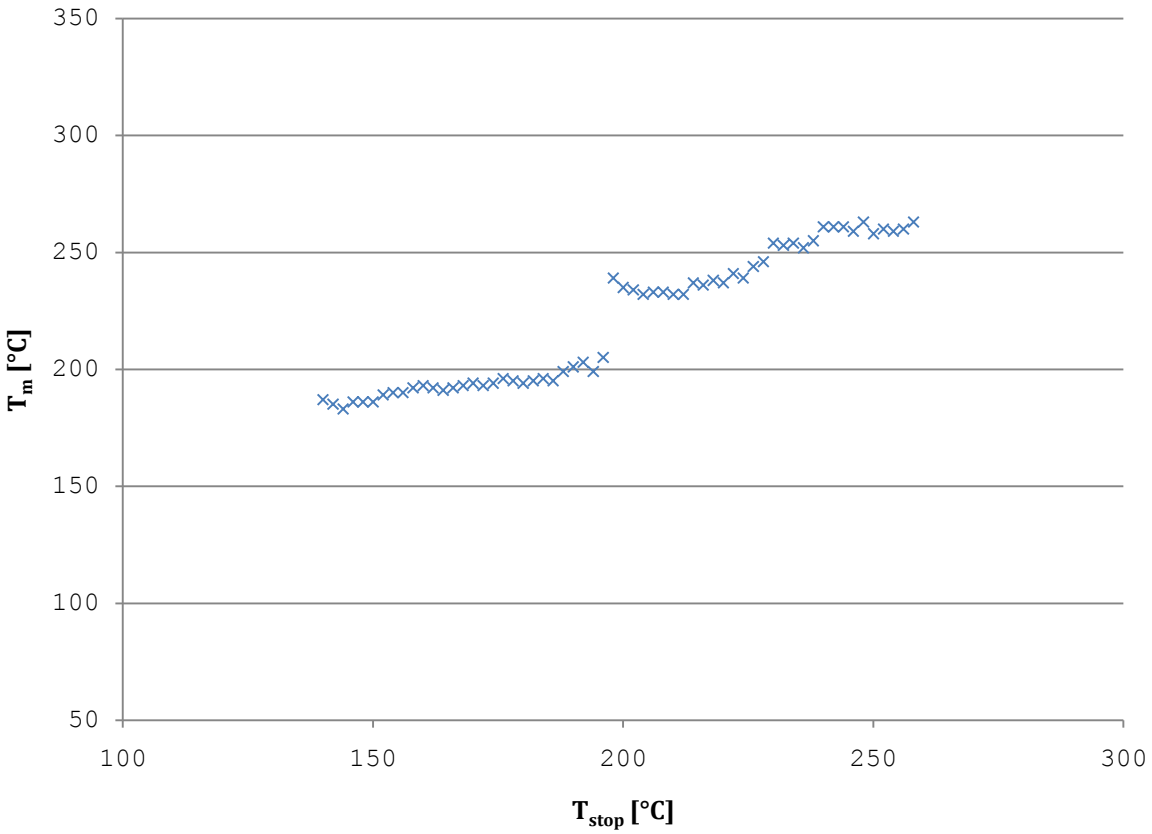

Figure IV-59: T_m-T_{stop} (140-296°C) diagram for the tempered MTT-7 TLD using the local maximum method

IV.5.4 Annealed Peak Method

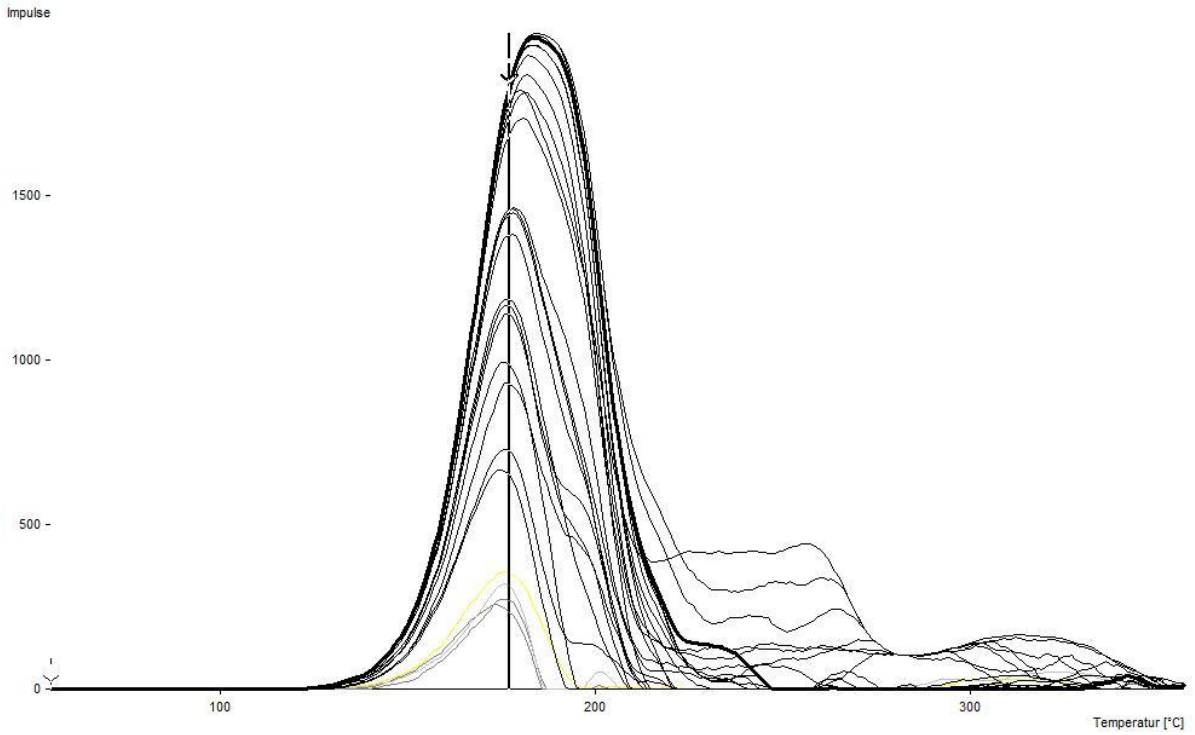

Figure IV-60: tempered MTT-7 TLD; annealed peak method

The same problems as with the non-tempered MTT-7 chips apply here. In figure IV-60, the transition from one peak to the next clearly suggests that the main peak consists in fact of at least two peaks. However, the T_{stop} temperature region where this method can be applied is too small to resolve these. Hence, in the following T_m-T_{stop} diagram only one plateau with a slight incline to a second plateau is shown. Since the statistical uncertainty found with these curves does not justify a conclusion in such a small scale, only one peak can be found.

IV.5.4.1 Annealed peak Method T_m–T_{stop} Diagram

Identified peaks for the tempered MTT-7 TLD using the annealed peak method

Peak 1	179,3°C ± 7,73°C	

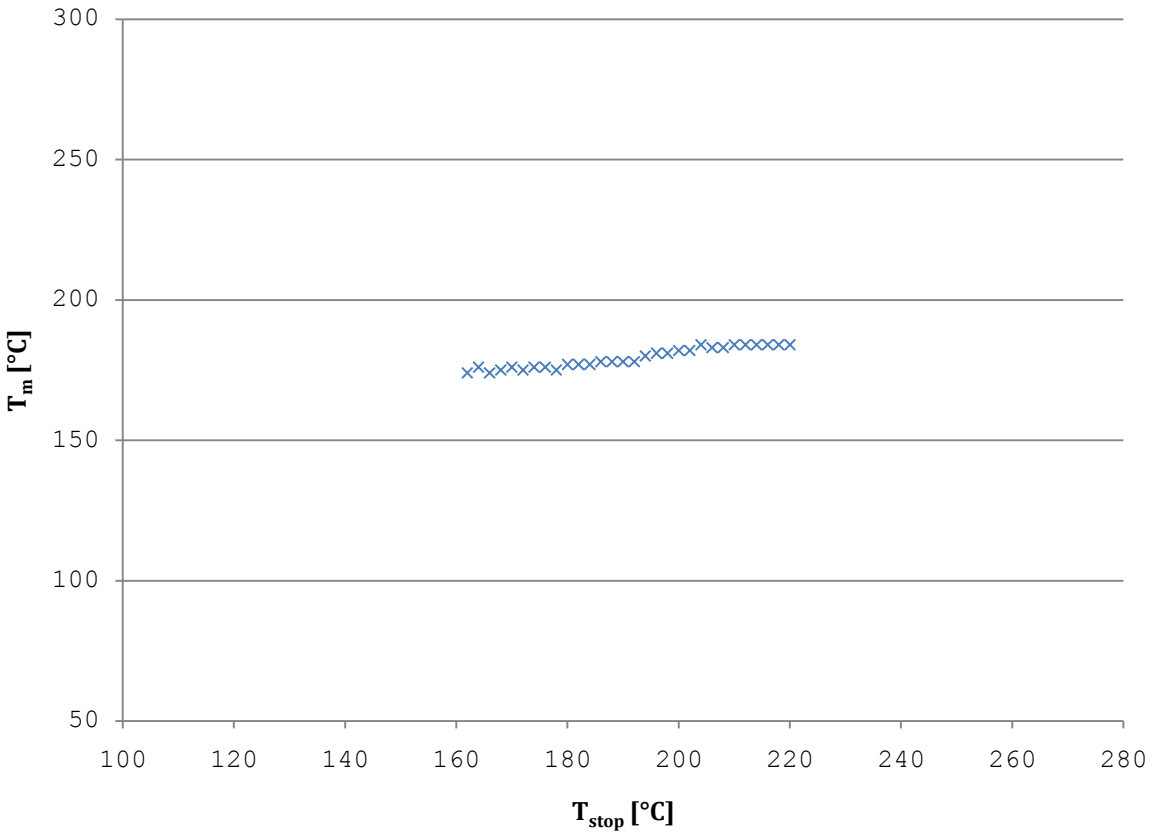

Figure IV-61: T_m-T_{stop} (162-220°C) diagram for the tempered MTT-7 TLD using the annealed peak method

The inability to resolve these peaks can be explained by the need to align the glow curves at a prominent maximum. Since no pronounced peak exists (the main peak is composed of at least two peaks with about equal intensity), the aligning process introduced a bigger than usual error which effectively lead to the shown T_m-T_{stop} diagram.

IV.5.5 Deconvolution Method

The deconvolution of the 78 measured glow curves yielded five peaks. These are shown in figure IV-62. Important to note that the TL intensity was very low for these measurements, therefore the reliability is low. It is all the more surprising that the detected peaks were computed with a smaller than usual statistical uncertainty.

Identified peaks for the tempered MTT-7 TLD using GLOW FIT

Peak 1	175,9°C ± 1,62°C
Peak 2	196,6°C ± 3,85°C
Peak 3	232,6°C ± 3,41°C
Peak 4	253,1°C ± 0,64°C
Peak 5	260,7°C ± 0,91°C

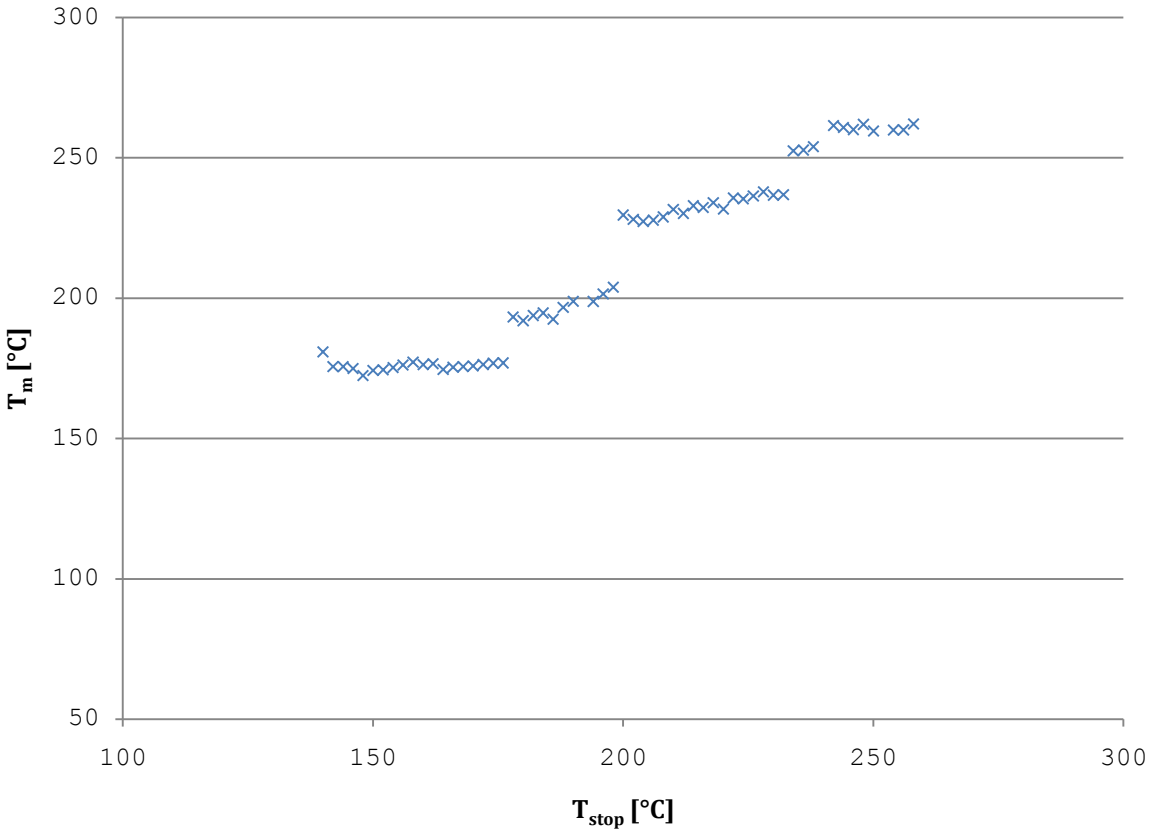

Figure IV-62: T_m-T_{stop} (140-296°C) diagram for the tempered MTT-7 TLD using the deconvolution software GLOW FIT

Using the deconvolution technique, all the previously suspected, but unresolvable peaks could be found (figure

IV-62). However, if the results of the tempered MTT-7 are compared with the non-tempered equivalent, it seems that peak 6 found for the non-tempered case at 259,6°C ± 5,72°C (see figure IV-44) appears as two peaks in the tempered case at 253,1°C ± 0,64°C and 260,7°C ± 0,91°C respectively (see figure IV-58). Still, since the TL intensities have been very low in this temperature region (compare figure IV-44 and IV-58), it is not possible to make a decisive statement.

IV.5.6 Tempered MTT-7: Results

Identified peaks for MTT-7 (tempered)

Local Maximum	Annealed Peak	Deconvolution
	179,3°C ± 7,73°C	175,9°C ± 1,62°C
192,9°C ± 5,26°C		196,6°C ± 3,85°C
236,8°C ± 4,15°C		232,6°C ± 3,41°C
		253,1°C ± 0,64°C
258,2°C ± 3,54°C		260,7°C ± 0,91°C

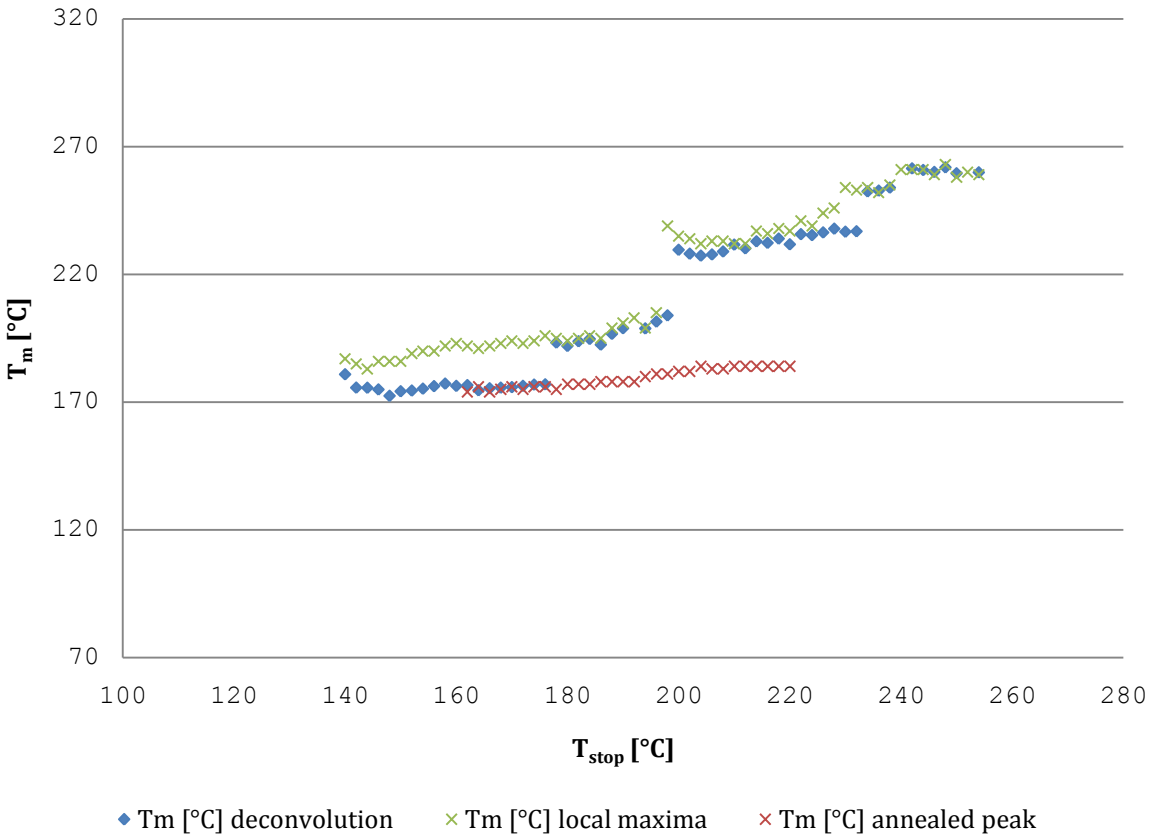

Figure IV-63: Results for the tempered MTT-7 TLD

All results for the tempered MTT-7 TLDs are shown in figure IV-63. Here, it is also easy to see that the annealed peak method does not work for glow curves of this type.

IV.6 PF (LiF:Mg,Ti with ~151 ppm Mg, ~11,5 ppm Ti, natural Li isotopic ratio; single crystals)

IV.6.1 Experimental Protocol

Irradiation Parameters:

distance from source	1,43 m
duration	16 h
source	Cs-137
absorbed dose	8,07 mGy
number of dosimeters	12

One day passed between radiation and measurement. The annealing process followed the day after the measurement, and was the same as with the TLD-300, TLD-600, TLD-700 and PG dosimeters, which took 24 hours (see chapter III.1.2.3).

Measurement Parameters:

heating rate	$1°Cs^{-1}$
heating interval	~25°C – 420°C
T_{stop} increment	2°C
T_{stop} interval	100°C – 290°C

IV.6.2 Reference Curve

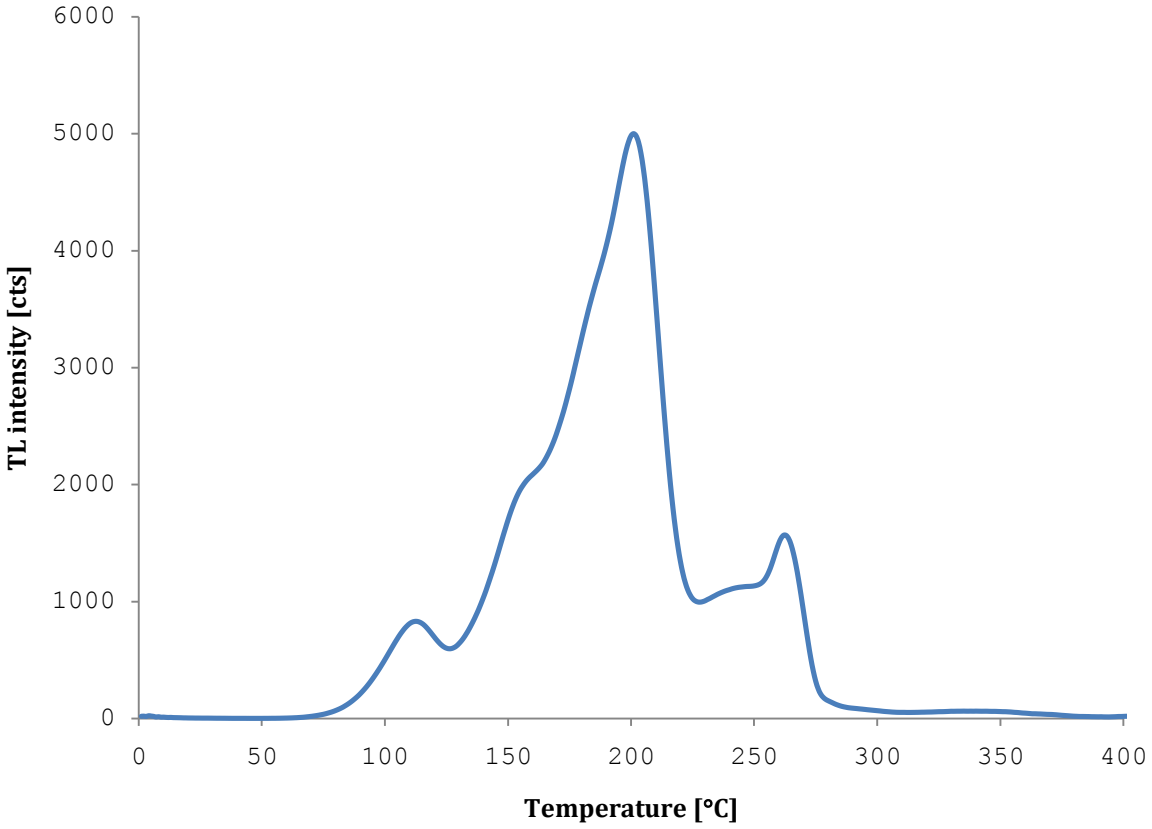

Figure IV-64: Reference curve for the PF-TLD

The reference curve (figure IV-64) was obtained from 36 measurements. Each of the twelve TLDs was measured three times, and then the arithmetic mean for the position of the highest peak intensity was calculated. All curves were aligned at this temperature, in this case 199°C. The maximum shifts were -3°C and +4°C. The final step was obtaining the normalized mean of all the curves which is the curve shown in figure IV-64. This curve will be used in the annealed peak method and is shown here as a reference.

IV.6.3 Local Maximum Method

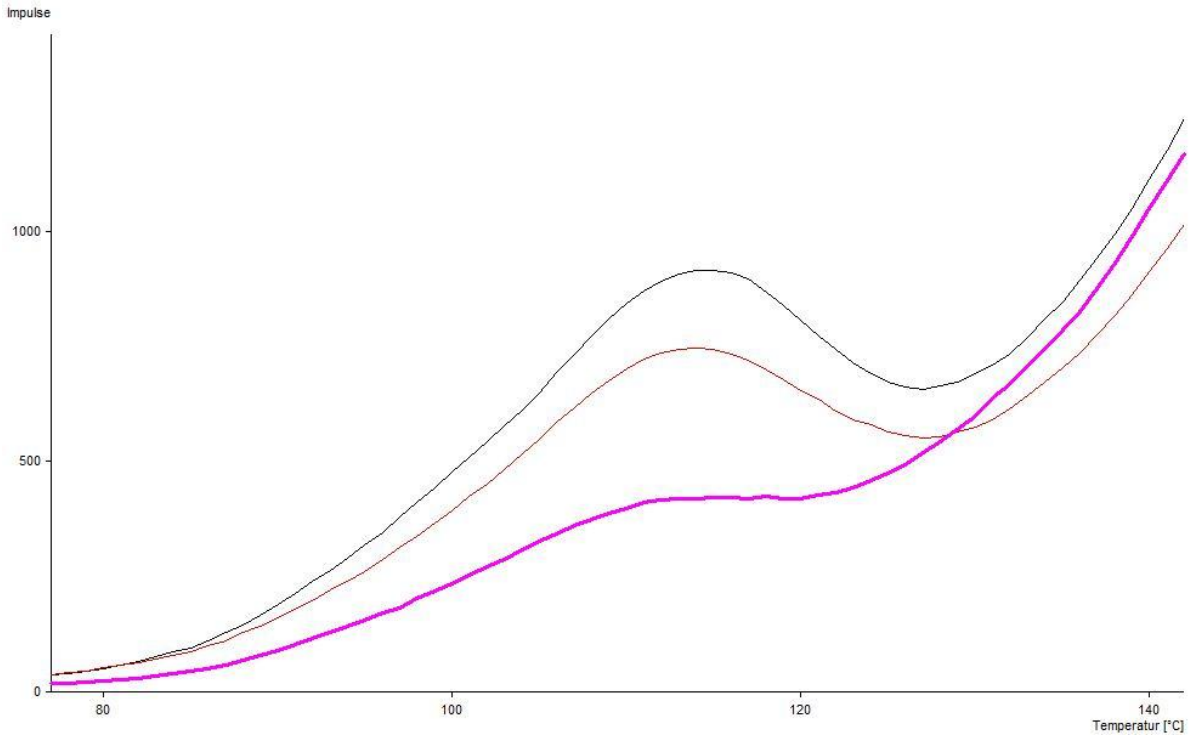

Figure IV-65: PF-TLD; T_{stop} values from 100 to 104°C

The first local maximum develops into a saddle point as T_{stop} increases quickly within two T_{stop} increments (4 °C). The curves (figure IV-65) show the first three values for T_{stop} (100 to 104°C).

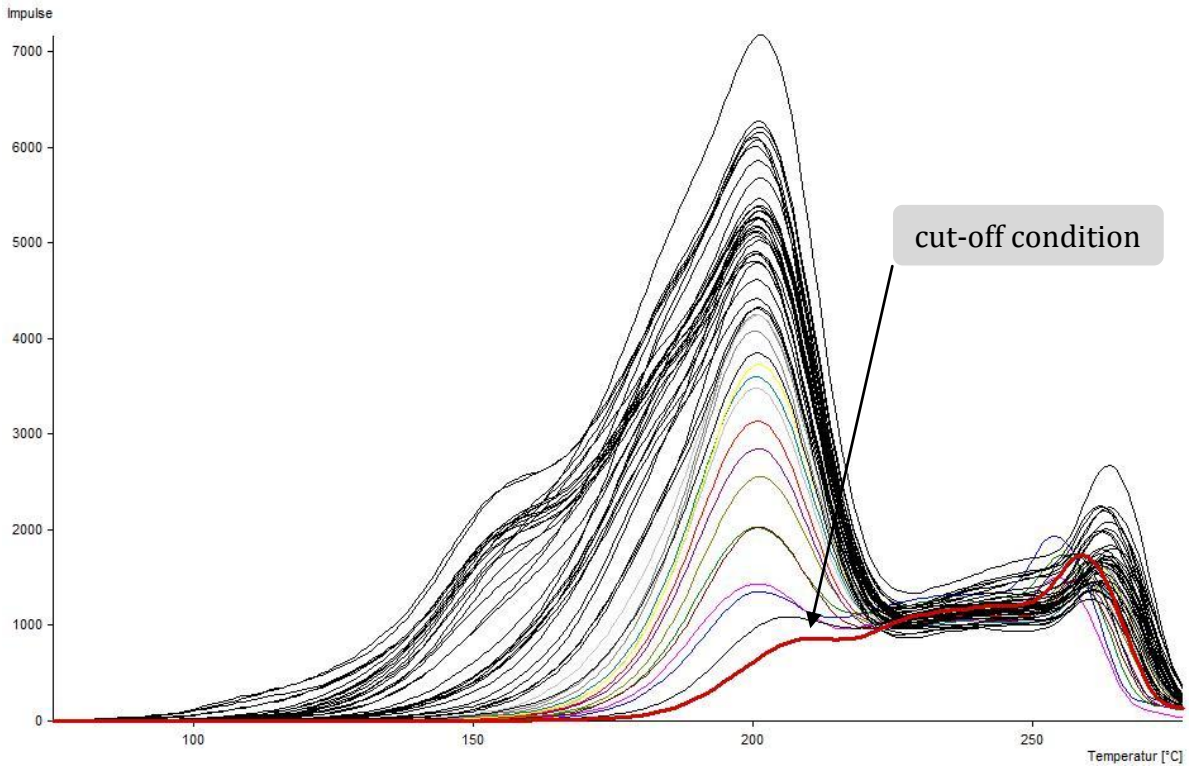

Figure IV-66: PF-TLD; T_{stop} values from 106 to 206°C

After the first peak has been annealed, the local maximum method "jumps" already to the main peak which gets annealed for T_{stop} values above 206°C. All the plotted glow curves (figure IV-66) are aligned at 201°C. At least two peaks (~160°C and ~180°C) can be suspected not to form local maxima.

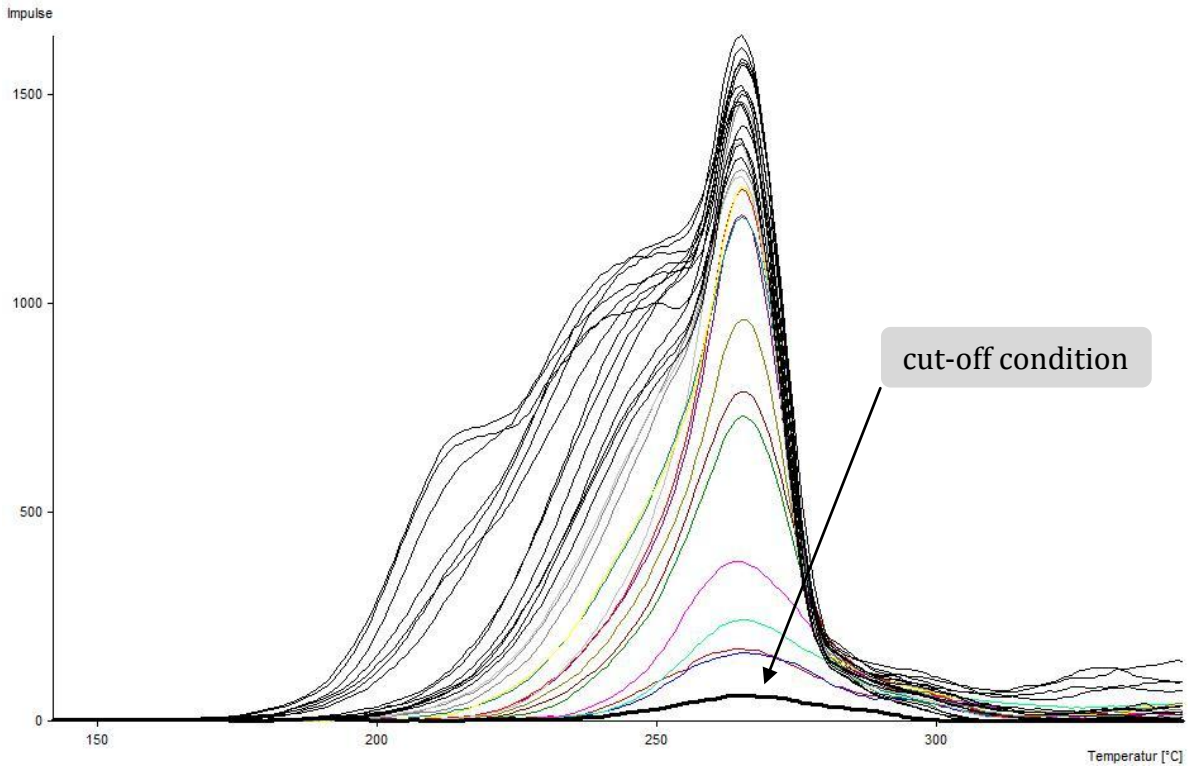

Figure IV-67: PF-TLD; T_{stop} values from 208 to 266°C

A similar situation as in figure IV-66 arose in figure IV-67. At least three peaks are suspected but only one fulfills the local maximum condition. There is also a notable high-temperature shoulder at ~290°C suggesting another peak, but the TL intensity is too low to draw a definite conclusion. The T_{stop} values for the glow curves ranged from 208 to 266°C and the glow curves were aligned at 265°C.

IV.6.3.1 Local Maximum Method T_m–T_{stop} Diagram

The local maximum method identified three peaks in the glow curves plotted before (figure IV-68).

Identified peaks for the PF-TLD using the local maximum method

Peak 1	114,7°C ± 0,47°C
Peak 2	201,1°C ± 2,99°C
Peak 3	261,2°C ± 3,8°C

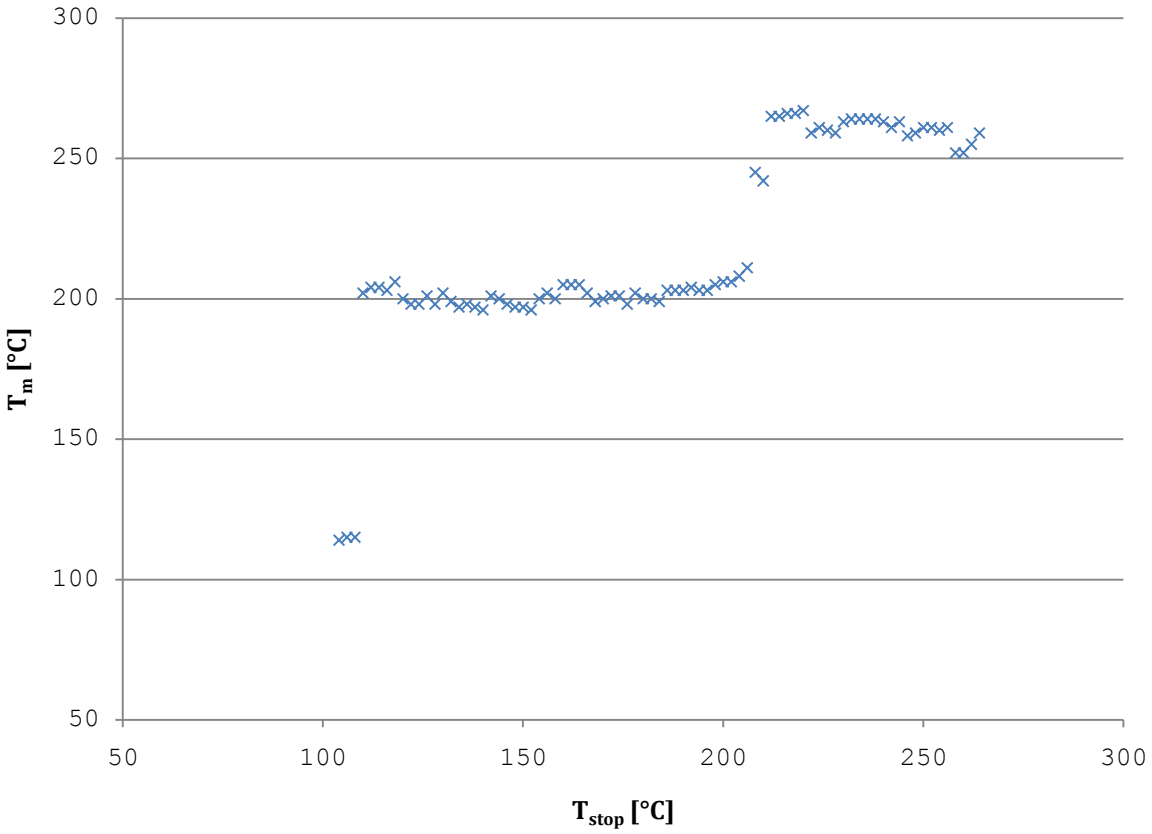

Figure IV-68: T_m-T_{stop} (100-290°C) diagram for the PF-TLD using the local maximum method

IV.6.4 Annealed Peak Method

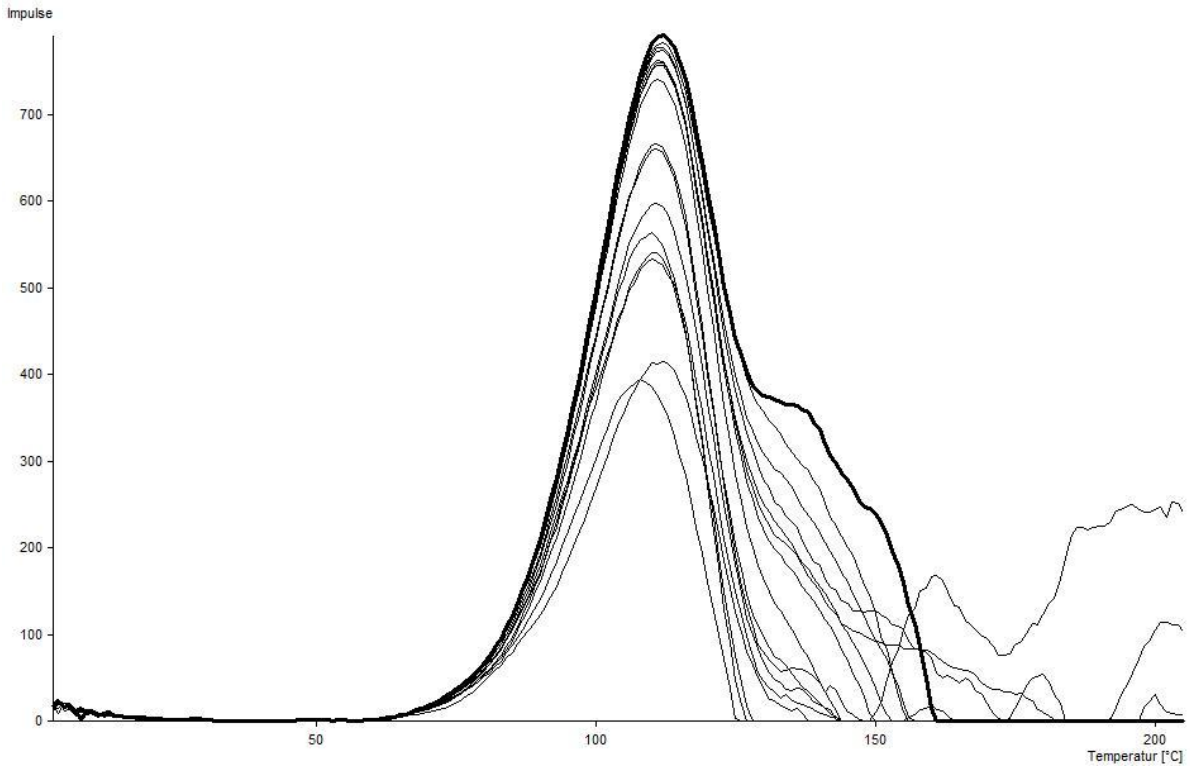

Figure IV-69: PF-TLD; annealed peak method; T_{stop} values from 100 to 134°C

Figure IV-69 shows the first peak for this method. The plotted curves cover the T_{stop} values from 100 to 134°C. Residual peaks are still at very low TL intensity which causes the significant artifacts at higher temperatures to result from the subtraction.

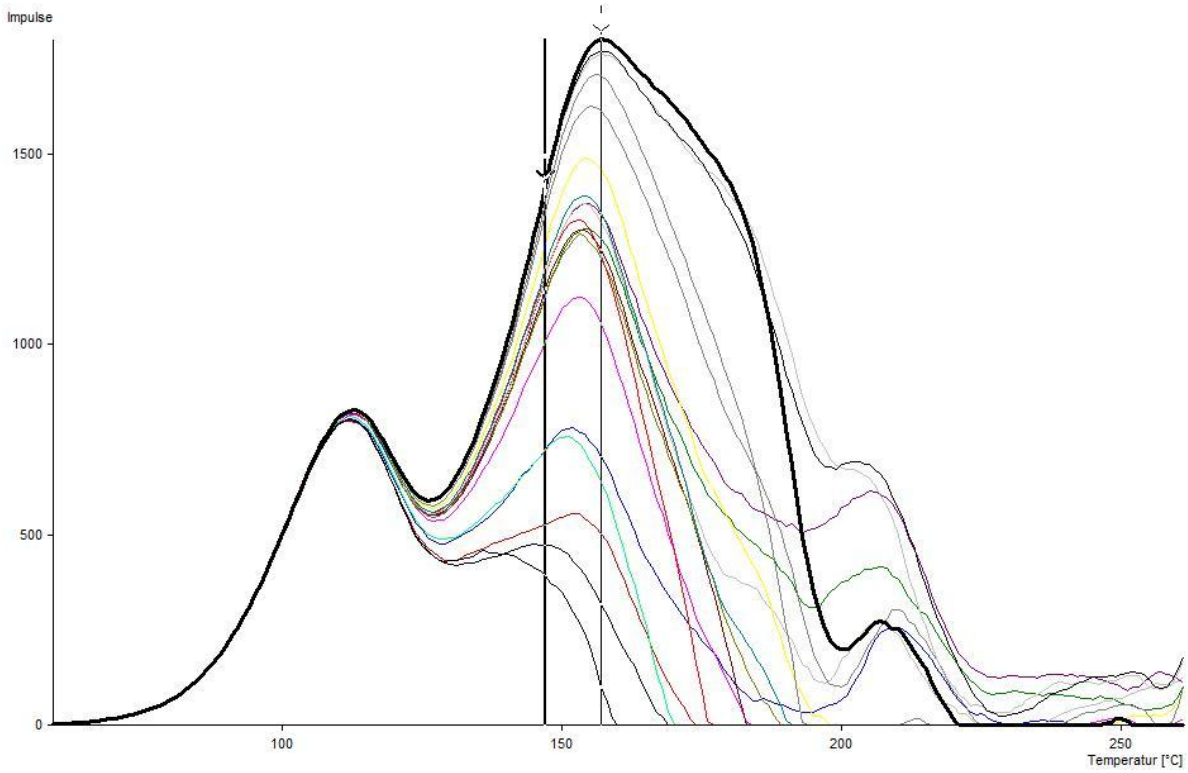

Figure IV-70: PF-TLD; annealed peak method; T_{stop} values from 136 to 174°C

Figure IV-70 shows the development of the second peak detected with this method. The two cursors mark the first and the last peak position. The reason for this drift can be seen as well, as the following peak already forms the high-temperature shoulder of the glow curves. T_{stop} values range from 136 to 174°C.

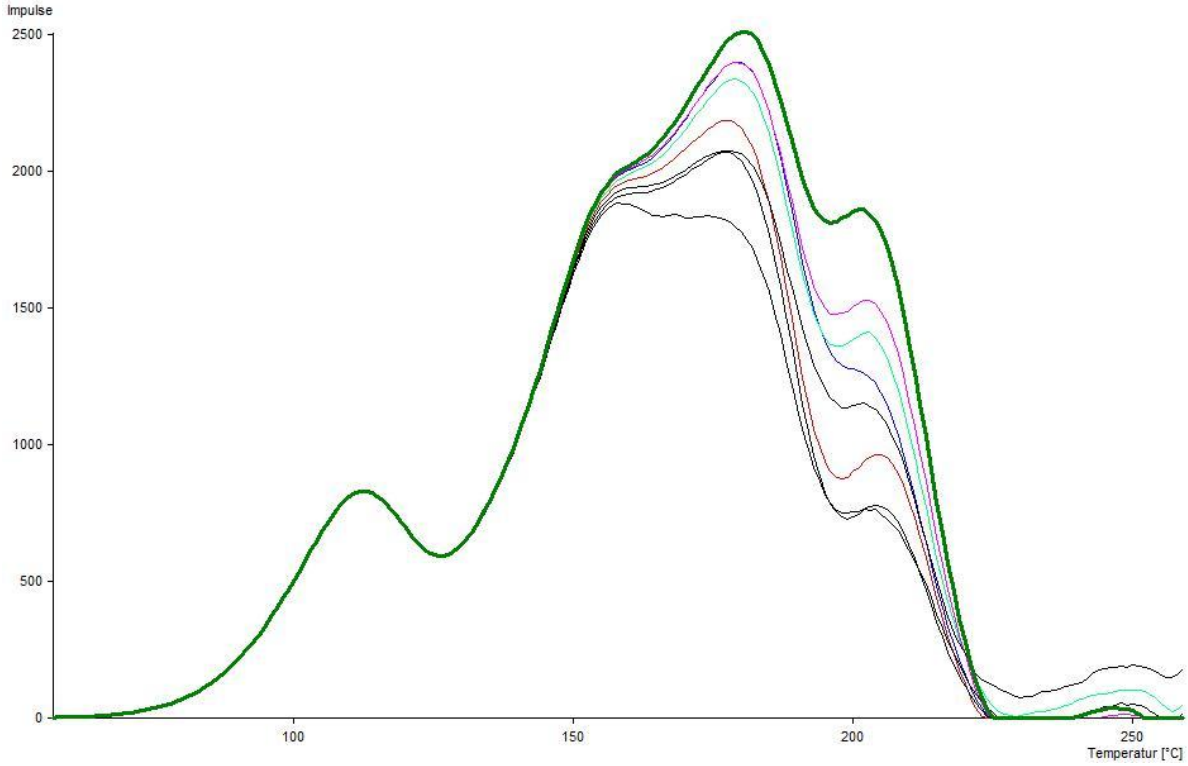

Figure IV-71: PF-TLD; annealed peak method; T_{stop} values from 176 to 188°C

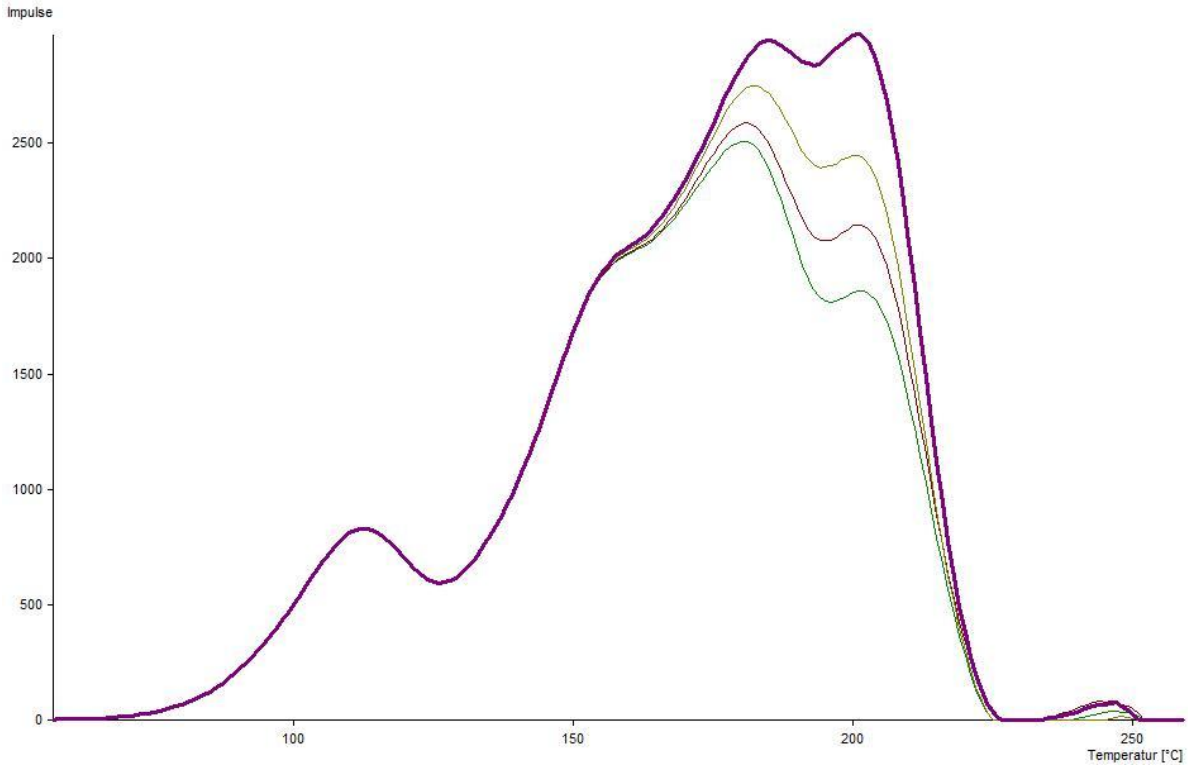

Figure IV-72: PF-TLD; annealed peak method; T_{stop} values from 188 to 196°C

Figure IV-71 and IV-72 show the development of the next two peaks using the curves for T_{stop} = 176 to 188°C (IV-71) and

T_{stop}= 188 to 196°C (IV-72). Peak 3 (in figure IV-71) exhibits a certain shift like the previous peak as its intensity increases, owing to the already significant peak at higher temperature. The reason why it is not as distinct as with peak 2 (figure IV-70) is that its intensity is much higher, compared to the following peak.

IV.6.4.1 Annealed Peak Method T_m–T_{stop} Diagram

Using the data from all the measurements shown above, four peaks could be identified with the annealed peak method (figure IV-73).

Identified peaks for the PF-TLD using the annealed peak method

Peak 1	111,1°C ± 3,48°C
Peak 2	154,1°C ± 4,58°C
Peak 3	178°C ± 2,78°C
Peak 4	201°C ± 2,29°C

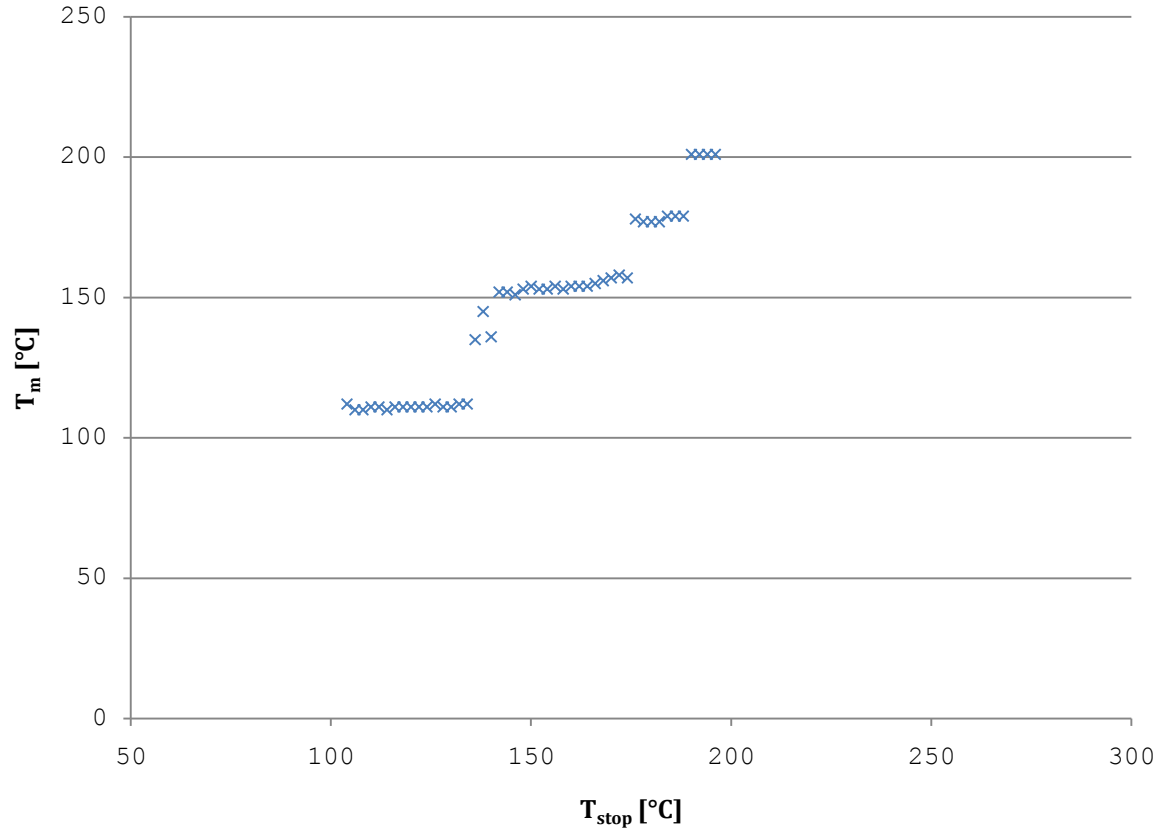

Figure IV-73: T_m-T_{stop} (100-196°C) diagram for the PF-TLD using the annealed peak method

The three points between plateau one and two (figure IV-73; T_{stop} values of 136, 138 and 140°C) mark the temperatures where peak 2 is low in intensity and, therefore, is heavily influenced by peak 1.

IV.6.5 Deconvolution Method

Using GLOW FIT six peaks have been identified from the 95 measurements. The plotted plateaus (figure IV-74) are not as flat as for other phosphors especially TLD-600 or TLD-700. This effect can also be recognized with the PG crystals. It is possibly caused by the slight variations in the contact area of the single crystals and, therefore, the resulting heating behavior.

Identified peaks for the PF-TLD using GLOW FIT

Peak 1	119,4°C ± 3,02°C
Peak 2	152°C ± 1,56°C
Peak 3	178°C ± 2,05°C
Peak 4	202,2°C ± 4,73°C
Peak 5	238,5°C ± 2,3°C
Peak 6	260,9°C ± 1,56°C

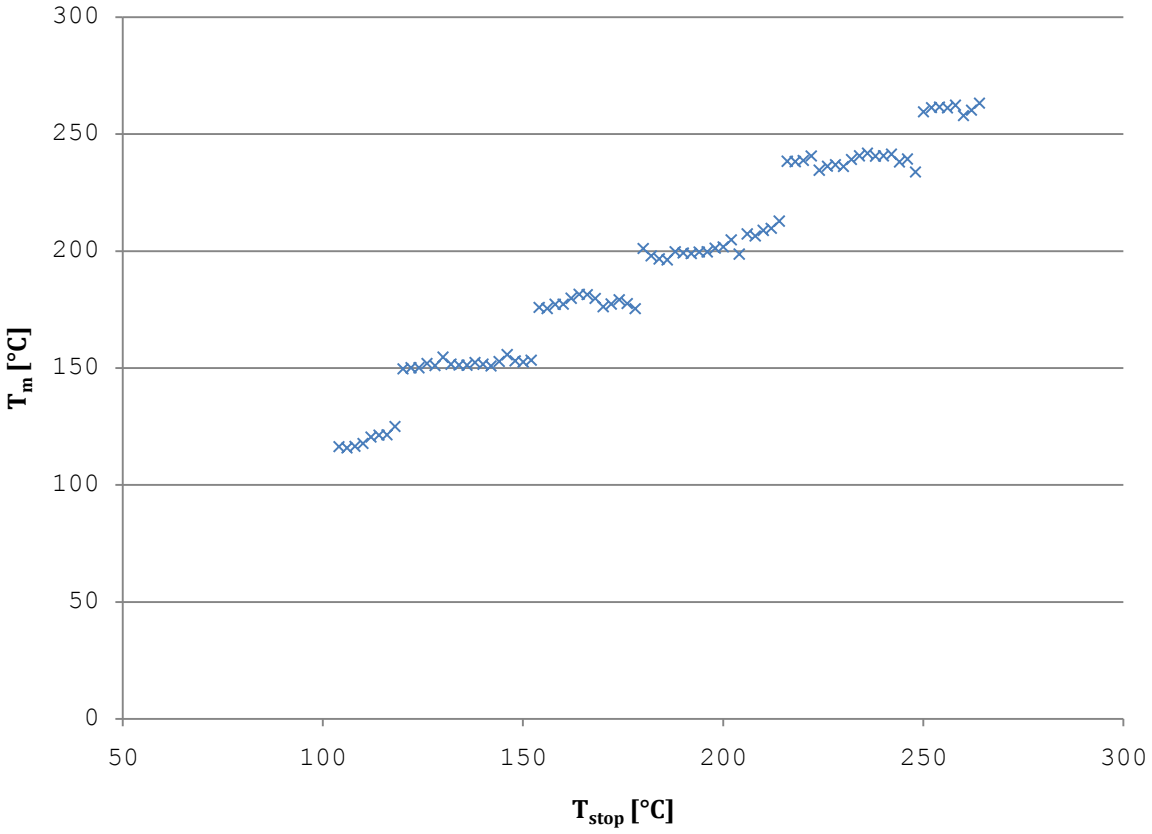

Figure IV-74: T_m-T_{stop} (100-290°C) diagram for the PF-TLD using the deconvolution software GLOW FIT

IV.6.6 PF crystal: Results

Identified peaks for the PF crystal

Local Maximum	Annealed Peak	Deconvolution
114,7°C ± 0,47°C	111,1°C ± 3,48°C	119,4°C ± 3,02°C
	154,1°C ± 4,58°C	152°C ± 1,56°C
	178°C ± 2,78°C	178°C ± 2,05°C
201,1°C ± 2,99°C	201°C ± 2,29°C	202,2°C ± 4,73°C
		238,5°C ± 2,3°C
261,2°C ± 3,8°C		260,9°C ± 1,56°C

The results of the three methods are plotted together in figure IV-75. Again, the annealed peak method identified within its temperature region the same peaks as the deconvolution software.

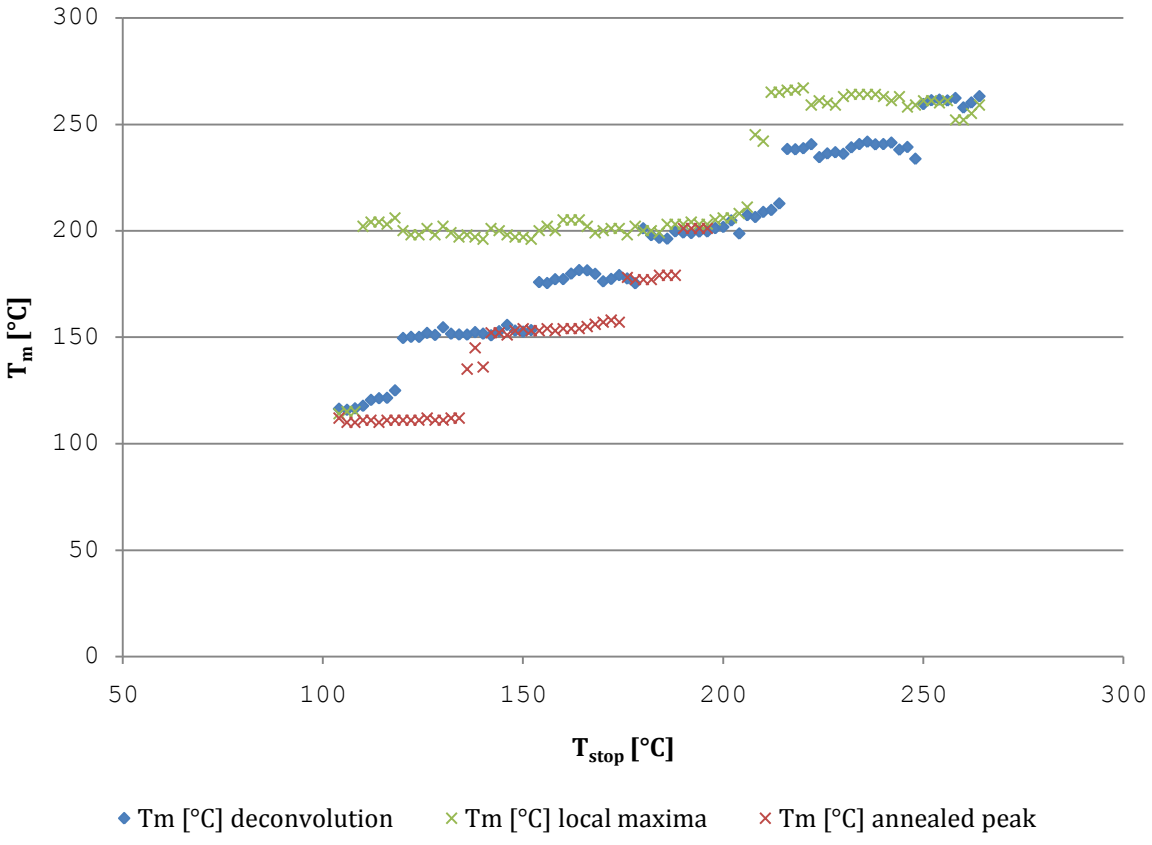

Figure IV-75: Results for the PF-TLD

IV.7 PG (LiF:Mg,Ti with ~1260 ppm Mg, ~11,5 ppm Ti, natural Li isotopic ratio; single crystals)

IV.7.1 Experimental Protocol

Irradiation Parameters:

distance from source	1,43 m
duration	16 h
source	Cs-137
absorbed dose	8,07 mGy
number of dosimeters	12

One day passed between radiation and measurement. The annealing process followed the day after the measurement, and was the same as with the TLD-300, TLD-600, TLD-700 and PG dosimeters, which took 24 hours (see chapter III.1.2.3).

Measurement Parameters:

heating rate	$1°Cs^{-1}$
heating interval	~25°C – 420°C
T_{stop} increment	2°C
T_{stop} interval	84°C – 248°C

IV.7.2 Reference Curve

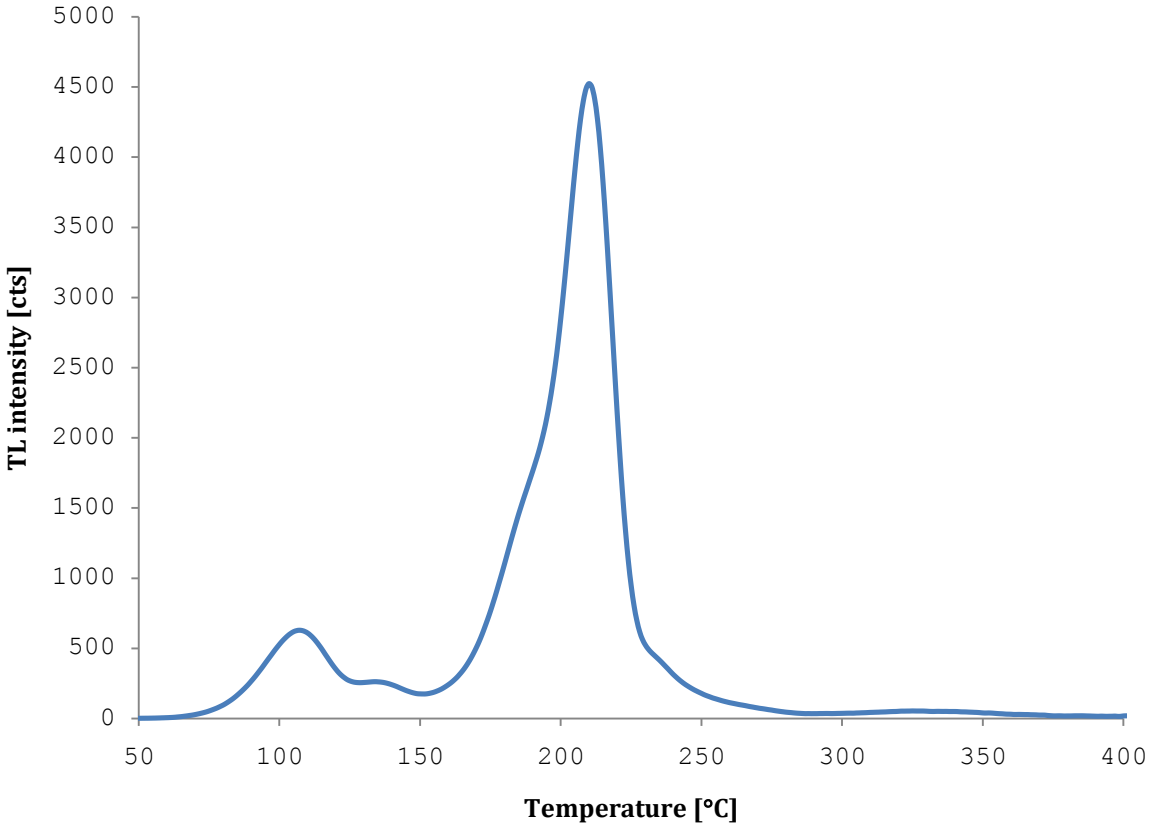

Figure IV-76: Reference curve for the PG-TLD

The reference curve (figure IV-76) was obtained from 36 measurements. Each of the twelve TLDs was measured three times, and then the arithmetic mean for the position of the highest peak intensity was calculated. All curves were then aligned at this temperature, in this case 208°C. The maximum shifts were -4°C and +3°C. The final step was obtaining the normalized mean of all the curves which is the curve shown in figure IV-76. This curve will be used in the annealed peak method and is shown here as a reference.

IV.7.3 Local Maximum Method

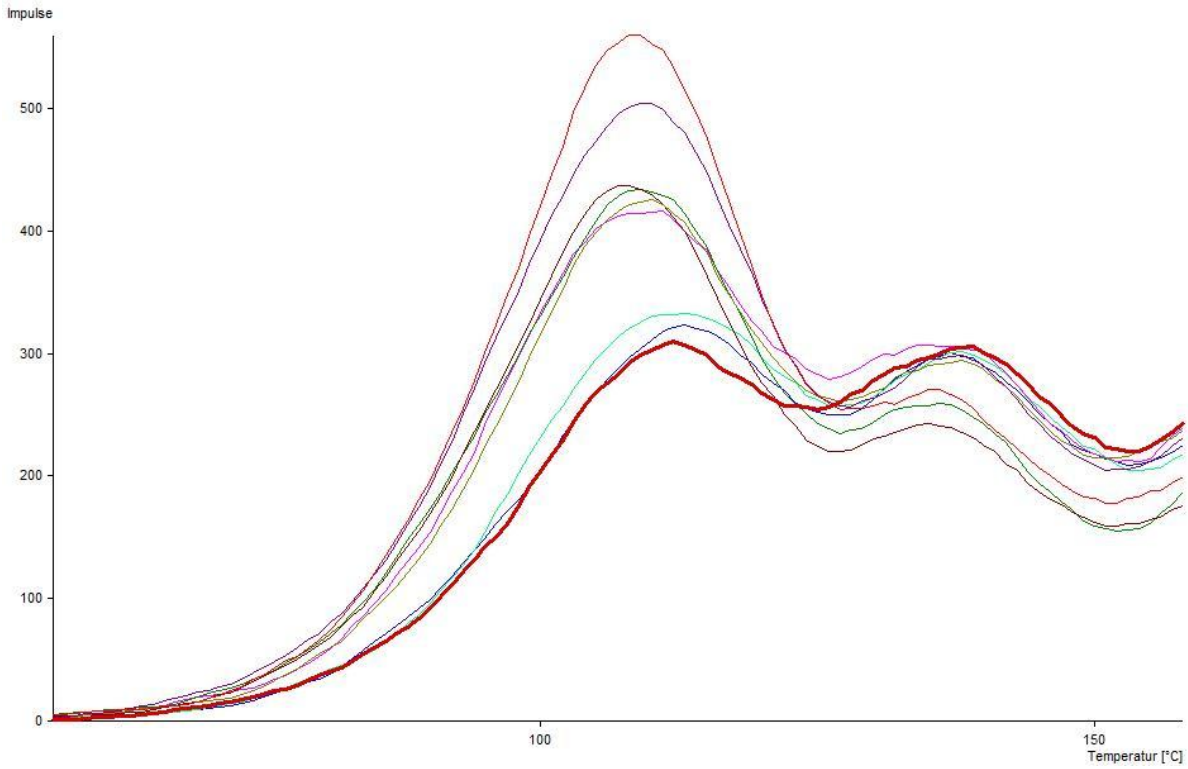

Figure IV-77: PG-TLD; T_{stop} values from 84 to 100°C

Plotted glow curves (figure IV-77) have been obtained for T_{stop} values from 84 to 100°C. They show the first local maximum for the PG crystals. They were aligned at 213°C for better visibility. The red curve represents the cut-off condition for this peak.

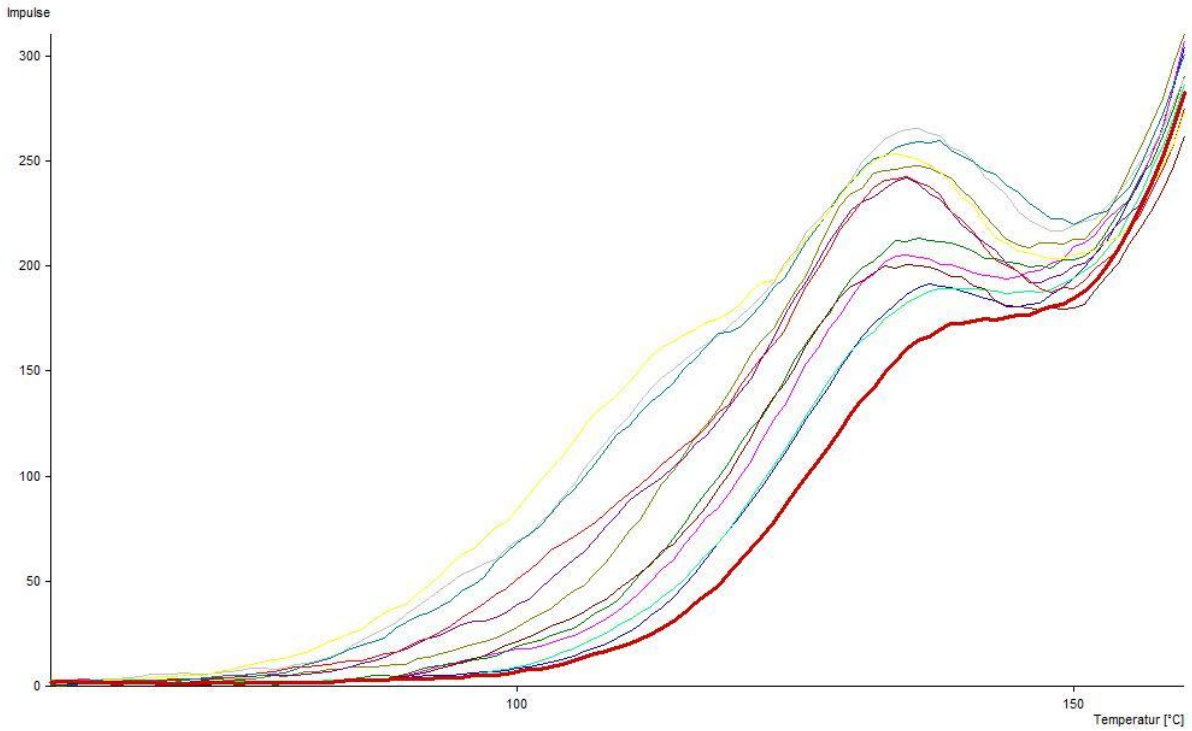

Figure IV-78: PG-TLD; T_{stop} values from 102 to 124°C

The next peak (figure IV-78) was obtained from T_{stop} values from 102 to 124°C, with the curves being aligned at 209°C. TL intensity was very low, but the visible peak was separated sufficiently from its higher-temperature neighbors to be resolved with this method.

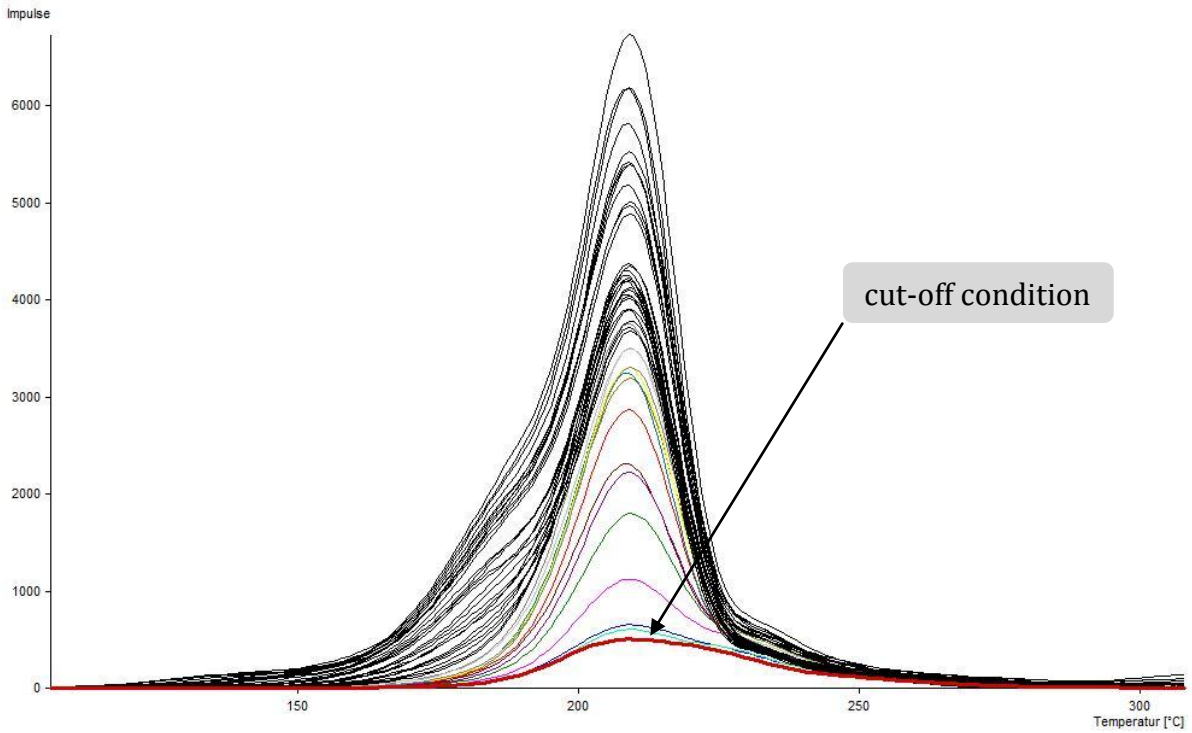

Figure IV-79: PG-TLD; T_{stop} values from 126 to 214°C

The following peaks did not develop a local maximum, so this method "jumped" to the main peak at 208°C. The plotted glow curves (figure IV-79) are for T_{stop} values ranging from 126 to 214°C, aligned at 209°C.

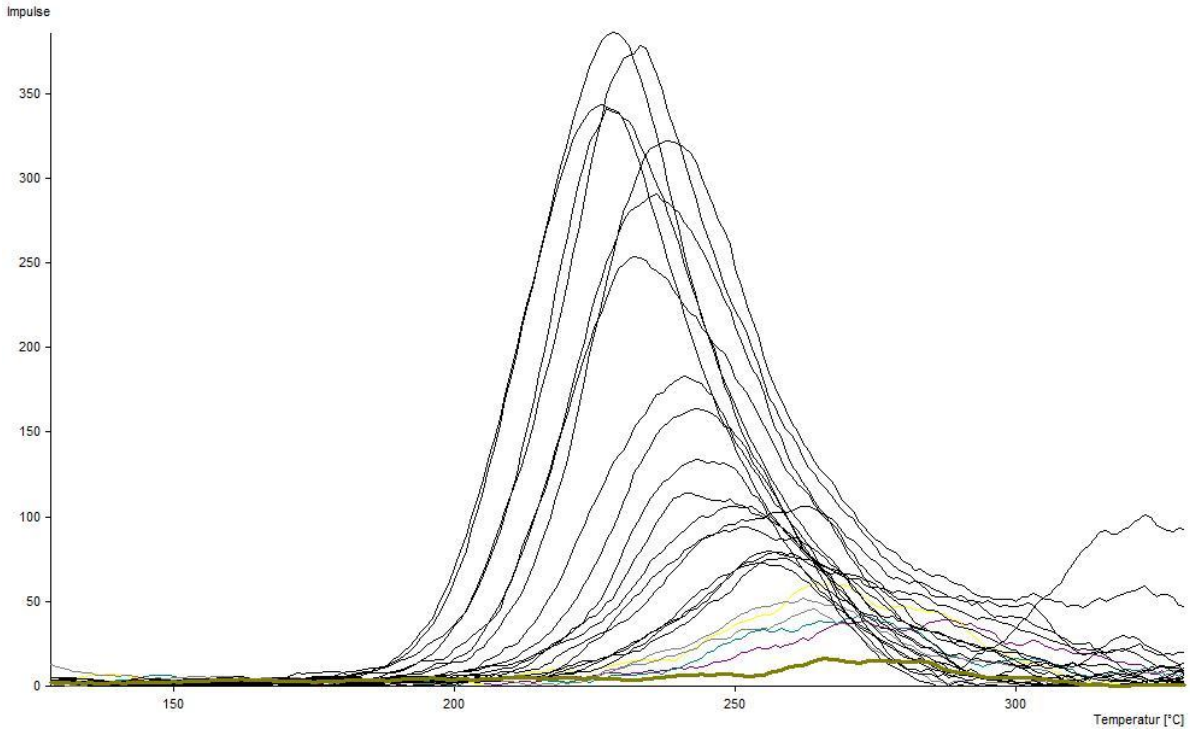

Figure IV-80: PG-TLD; T_{stop} values from 216 to 268°C

Figure IV-80 shows the last peak identified with the local maximum method. The plotted glow curves were measured at T_{stop} values from 216 to 268°C and have not been aligned. The peak seen here shows the behavior attributed to a second-order peak, whose T_m value increases with increasing T_{stop}. Since the TL intensity was very low, the glow curves for T_{stop} above 248°C were not used in the calculation for the T_m-T_{stop} diagram.

IV.7.3.1 Local Maximum Method T_m–T_{stop} Diagram

The local maximum method identified four peaks in the glow curves plotted above. However, peak 4 showed no plateau at all and can be interpreted as a second-order peak. Since no plateau is developed, the statistical uncertainty is rather large.

Identified peaks for the PG-TLD using the local maximum method

Peak 1	110,2°C ± 1,93°C
Peak 2	135,7°C ± 1,75°C
Peak 3	210°C ± 2,14°C
Peak 4	242,2°C ± 10,9°C

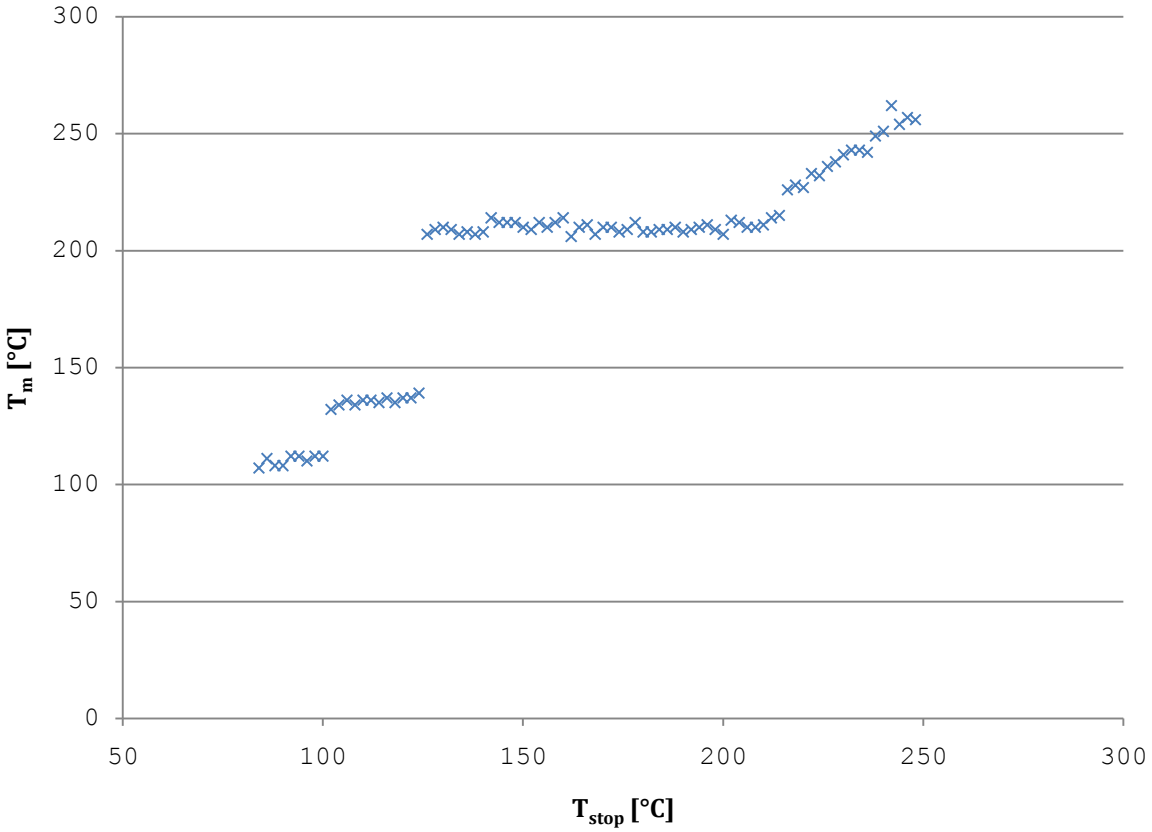

Figure IV-81: T_m-T_{stop} (100-290°C) diagram for the PG-TLD using the local maximum method

IV.7.4 Annealed Peak Method

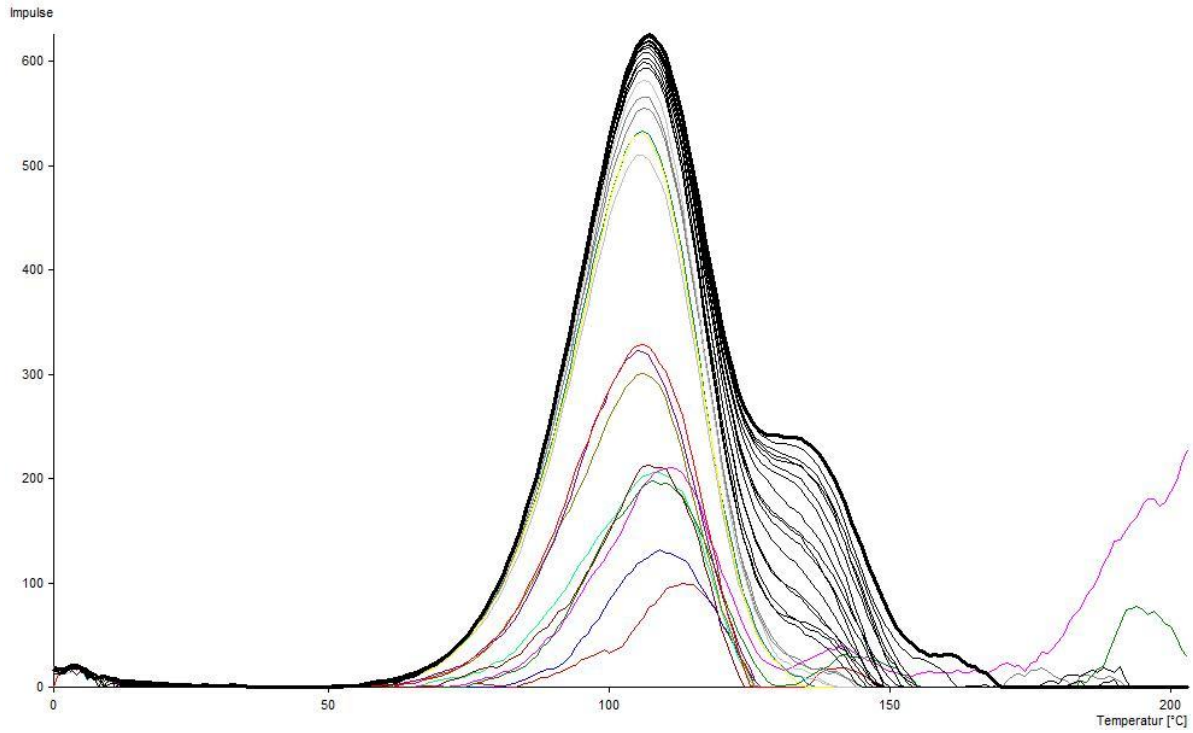

Figure IV-82: PG-TLD; annealed peak method; T_{stop} values from 84 to 146°C

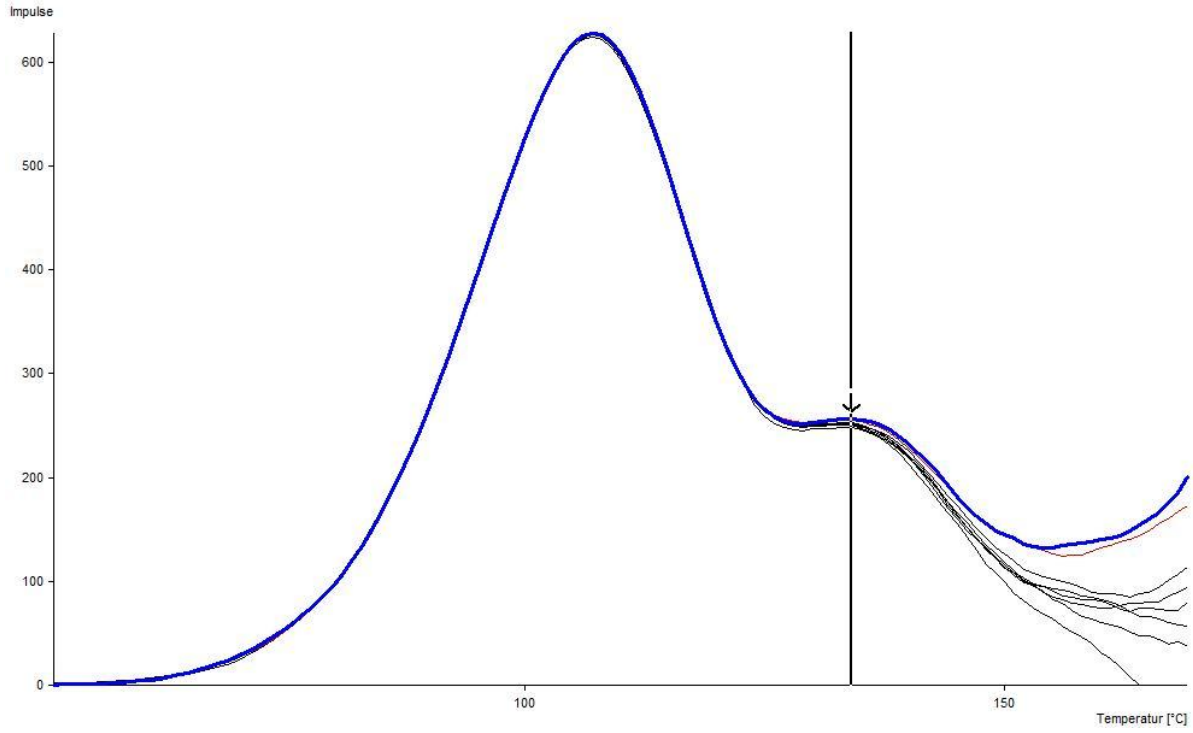

Figure IV-83: PG-TLD; annealed peak method; T_{stop} values from 148 to 162°C

Figure IV-82 (T_{stop} values from 84 to 146°C) and figure IV-83 (T_{stop} values from 148 to 162°C) show the first two peaks found with the annealed peak method.

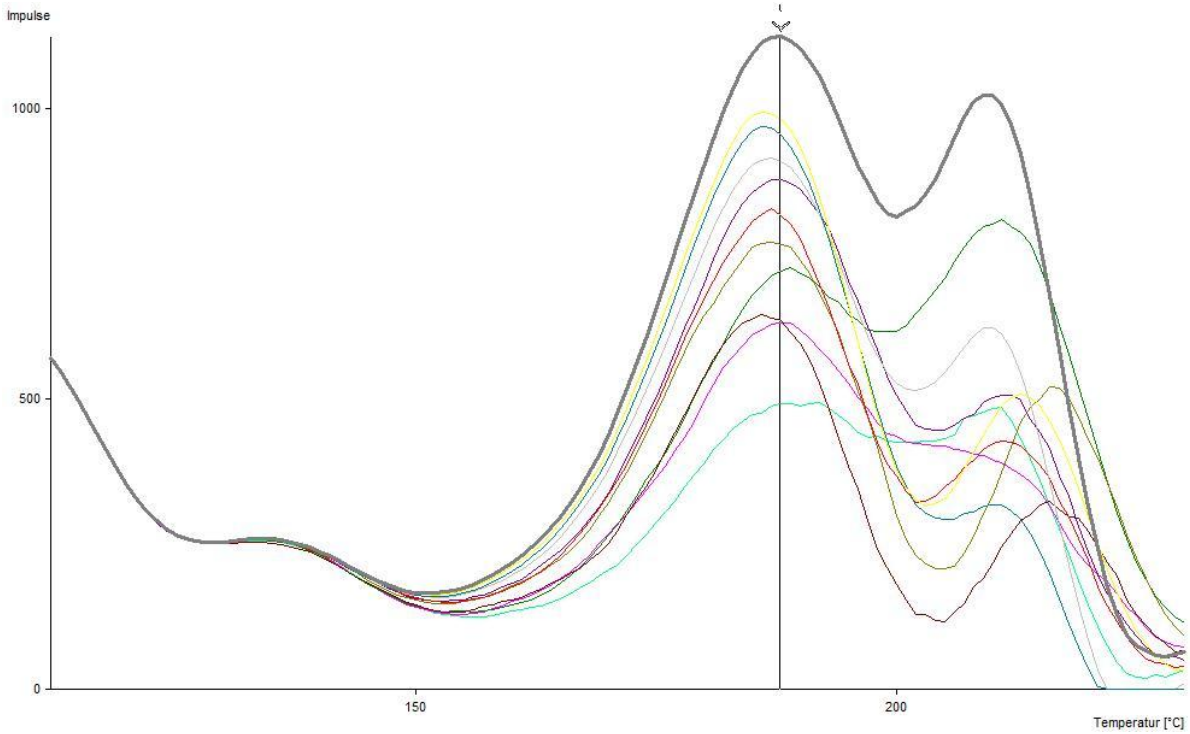

Figure IV-84: PG-TLD; annealed peak method; T_{stop} values from 164 to 184°C

Peaks 4 and 5 gain intensity almost at the same rate as seen in figure IV-84 with increasing T_{stop}. This accounts for the stable T_m values of peak 3. The shown T_{stop} values ranged from 164 to 184°C.

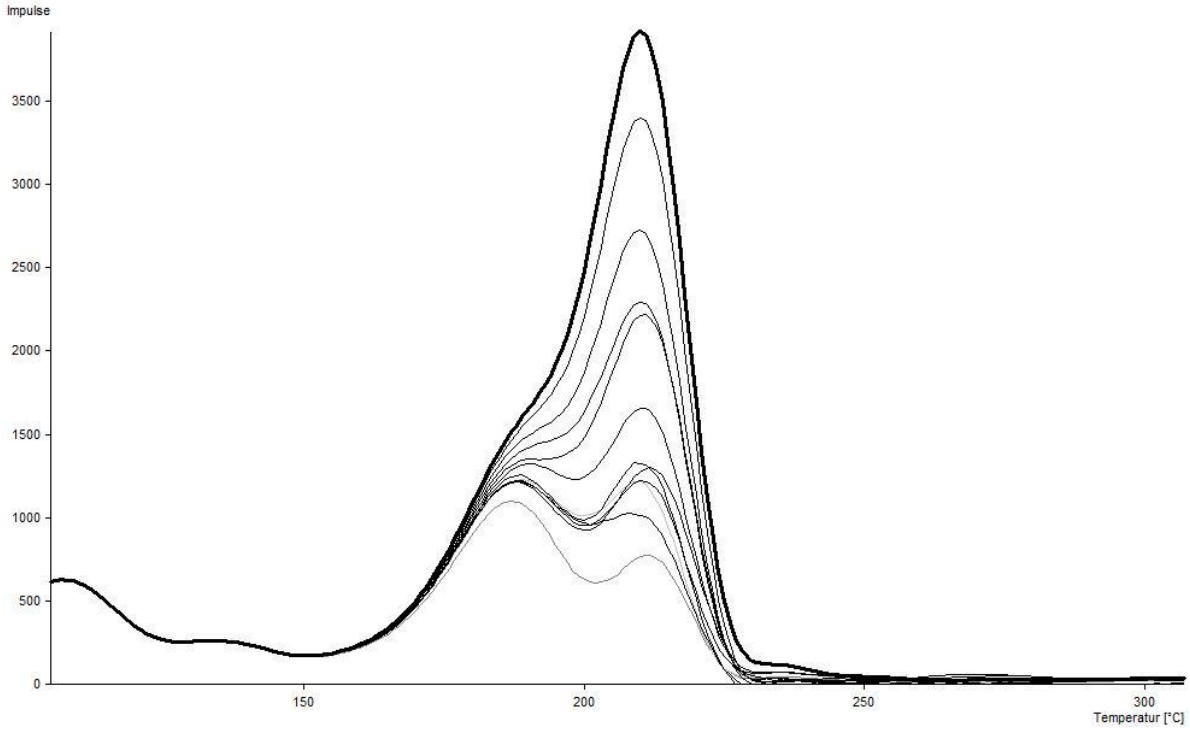

Figure IV-85: PG-TLD; annealed peak method; T_{stop} values from 186 to 210°C

The last peak identified using this method was found with T_{stop} values ranging from 186 to 210°C (figure IV-85).

IV.7.4.1 Annealed Peak Method T_m–T_{stop} Diagram

Using all the data from the annealed peak method, four peaks could be identified. Since additional subtraction is necessary to obtain these curves, the statistical uncertainty is higher than with the conventional technique, in spite of the "stable" T_m values.

Identified peaks for the PG-TLD using the annealed peak method

Peak 1	107,1°C ± 4,15°C
Peak 2	133,3°C ± 3,03°C
Peak 3	187,5°C ± 2,75°C
Peak 4	209,9°C ± 2,41°C

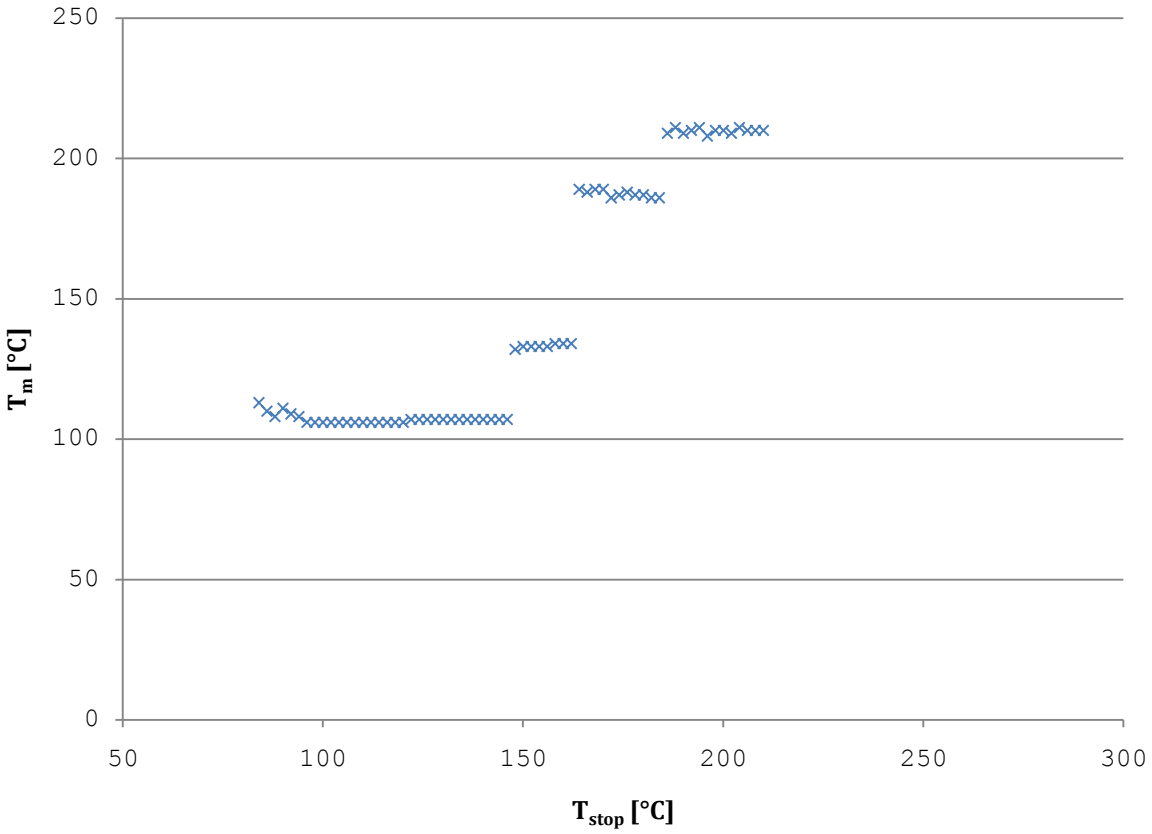

Figure IV-86: T_m-T_{stop} (84-210°C) diagram for the PG-TLD using the annealed peak method

IV.7.5 Deconvolution Method

Using GLOW FIT six peaks were identified from the 82 deconvolutions. As mentioned earlier, the last peak (~249°C) appears to be a second-order peak and, therefore, it was not possible to locate it with GLOW FIT, since the current version does only support first-order kinetics. Hence, the T_m for peak 5 shown in figure IV-87 is affected by a rather large uncertainty.

Identified peaks for the PG-TLD using GLOW FIT

Peak 1	107,9°C ± 1,65°C
Peak 2	135°C ± 3,59°C
Peak 3	183,7°C ± 2,75°C
Peak 4	208,57°C ± 2,2°C
Peak 5	230,3°C ± 5,58°C
Peak 6	249,7°C ± 6,24°C

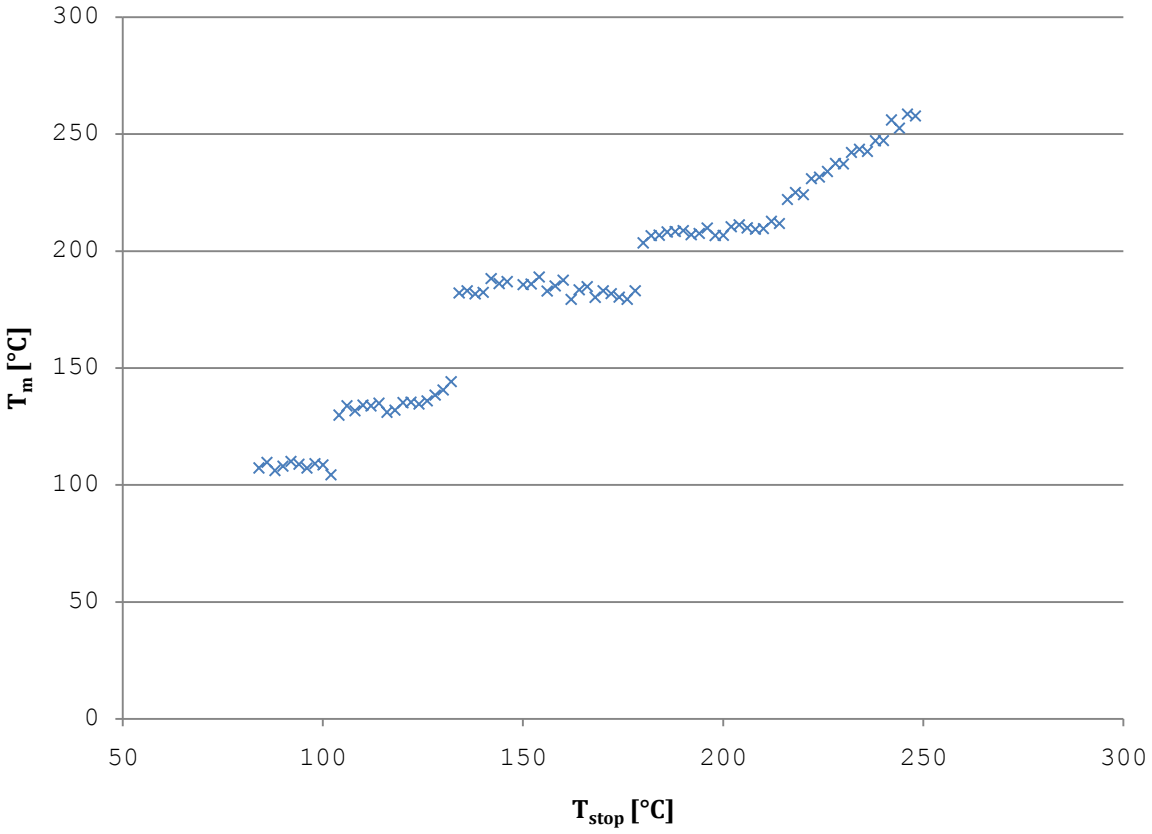

Figure IV-87: T_m-T_{stop} (84-248°C) diagram for the PG-TLD using the deconvolution software GLOW FIT

IV.7.6 PG crystal: Results

Identified peaks for the PG crystal

Local Maximum	Annealed Peak	Deconvolution
110,2°C ± 1,93°C	107,1°C ± 4,15°C	107,9°C ± 1,65°C
135,7°C ± 1,75°C	133,3°C ± 3,03°C	135°C ± 3,59°C
	187,5°C ± 2,75°C	183,7°C ± 2,75°C
210°C ± 2,14°C	209,9°C ± 2,41°C	208,57°C ± 2,2°C
		230,3°C ± 5,58°C
242,2°C ± 10,9°C		249,7°C ± 6,24°C

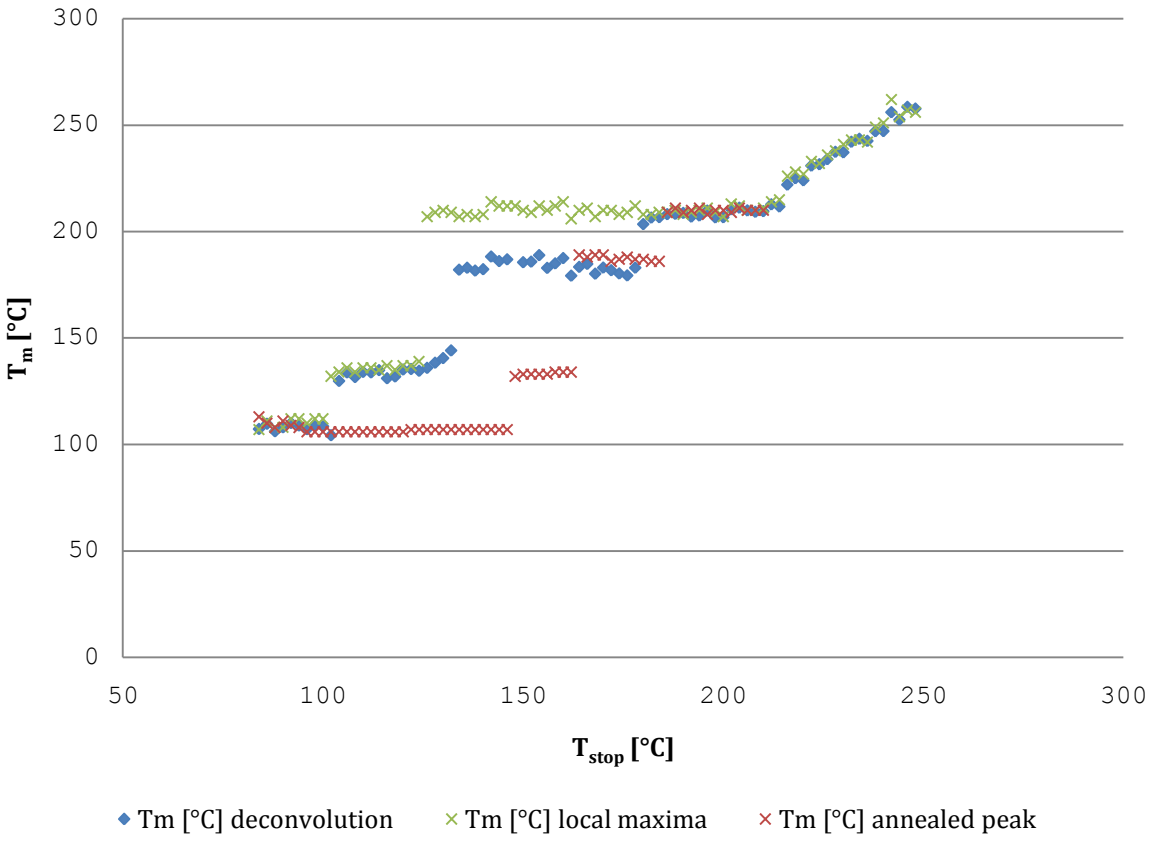

Figure IV-88: Results for the PG-TLD

The results of the three methods are plotted together in figure IV-88. Again, the annealed peak method provides results in good agreement with the deconvolution.

V. Summary

Comparing the results of the three methods, the advantages and problems of each become apparent.

The presence of a local maximum is the basic evaluation method for the T_m-T_{stop} technique. The identifiable peaks generally were few and only the dominant peaks could be resolved. The resolution was poor, although when curves of increasing T_{stop} values were plotted together it was possible to perceive but not to locate other peaks. The only exception to this has been MTT-7. Since the glow curve of this TLD type does not show a dominant but rather several, partly overlapping peaks with almost equal intensity, it was possible to resolve almost all of the peaks that could be found with the other methods.

The annealed peak method on the one hand finds (within its applicable temperature interval) the same number of peaks as the deconvolution. This is a great advantage if no a priori knowledge of the peak structure of the given TLD class is available, since this method resolves the glow curve structure without the need to define starting values for the deconvolution algorithm. On the other hand, with the current protocol the applicable temperature interval is limited. An additional problem is the need for a certain glow curve structure (i.e. a dominant peak). As seen with the MTT-7 measurements, this method does not deliver satisfactory results in absence of a dominant (main) peak.

Deconvolution is found to be the method of choice for this work. Since this method does not rely on glow curve structures, it is universally applicable and resolves all glow curves with unmatched accuracy. A potential problem with this method is the need for a priori knowledge concerning the number of peaks to be found.

Deconvolution Result Summary

MTT-7	Tempered MTT-7	TLD-700	TLD-600	PF	PG	TLD-300
LiF:Mg,Ti						CaF_2: Tm
^{7}Li			^{6}Li	natural Li isotopic ratio		
50ppm Mg; 120ppm Ti		300ppm Mg; 11ppm Ti		151ppm Mg 11,5ppm Ti	1260ppm Mg 11,5ppm Ti	
extruded chips				single crystal		
112,8±0,7°C		115,2±1,4°C	112,6±1,7°C	119,4±3,0°C	107,9±1,7°C	105,6±1,3°C
127,3±1,5°C					135±3,6°C	127,6±1,9°C
147,8±1,3°C		152,6±2,2°C	152,7±1,6°C	152±1,6°C		150,7±2,2°C
177,2±2,5°C	175,9±1,6°C	177,5±0,8°C	175,5±1,1°C	178±2,1°C	183,7±2,8°C	181,6±4,0°C
195,2±1,7°C	196,6±3,9°C	199,9±2,7°C	198,9±2,6°C			
213,6±3,2°C				202,2±4,7°C	208,6±2,2°C	
234±2,0°C	232,6±3,4°C		229,9±4,7°C	238,5±2,3°C	230,3±5,6°C	226,4±2,2°C
255±4,1°C	253,1±0,6°C				249,7±6,2°C	255,5±5,8°C
262±2,4°C	260,7±0,9°C	262±5,2°C	262,6±3,2°C	260,9±1,6°C		
		306,6±2,0°C	300,7±7,2°C			
330,1±3,1°C						

This table compiles all the deconvolution results obtained within this work. As can be seen, most of the used TLDs were LiF type of phosphors with differing Mg and Ti dopant concentration. In addition, different isotope enrichment of Li was used. The only exception was TLD-300 which is CaF_2 based. Another distinction is made regarding single-crystal or extruded-chip phosphors.

Comparing the MTT-7 with the tempered MTT-7 detectors, the two "missing" peaks (~213 and ~330°C) are of note (the first three are annealed in the tempering process). It is clear that the tempering process has an influence not only on the first three peaks but on the peaks with higher T_m values, too. This is best seen comparing the reference glow curves of figure IV-38 and

IV-55. The high temperature shoulder curvature in figure IV-38 cannot be seen in figure IV-55 anymore, which is the aforementioned peak at ~213°C. This behavior cannot be explained with the models presented in chapter II, since it would suggest a very broad lower-temperature shoulder (in the order of ~80°C), which would result in a much broader peak than the curvature in figure IV-38 suggests. The peak resolved at T_m ~330°C for the MTT-7 TLDs is also "found" with the tempered MTT-7 measurements. However, due to the low residual TL intensity at these T_{stop} values these measurements had to be discarded. All the other peaks for the MTT-7 TLDs (tempered and non-tempered) show first-order kinetic behavior.

The T_m values for the TLD-600 and 700 glow curves correlate well except for the peak at ~230°C. Since no plateau forms for this peak over several T_{stop} values, the statistical uncertainty is high. One possible explanation is that this peak is of second-order kinetics. Another possibility would be a broad peak at high temperatures (e.g. ~262°C) which necessitates the deconvolution to "place" a peak at this T_m value. Since the TLD-700 phosphor which exhibits a very similar glow curve does not show this behavior, it seems that a deconvolution artifact is more plausible. The other peaks (TLD-600 and TLD-700) show first-order kinetics behavior.

Comparing the T_m values of the PF and PG crystals, only three of the peaks resolved for the PG crystals (T_m ~183; 208; 230°C) seem to correlate with the PF values. The big difference in Mg dopant concentration (151 ppm Mg for PF; 1260 ppm Mg for PG) is the most likely reason. All of the identified peaks show first-order behavior except for the peak at T_m ~249°C. The T_m-T_{stop} diagram shows a steady ascending slope (see figure IV-87) and does not form a plateau over a large temperature interval (T_{stop} ~32°C). This indicates a second-order peak.

The TLD-300 were the only CaF_2 based phosphors studied in this work. All identified peaks show first order kinetics behavior except for the last peak at T_m ~255°C shown in figureIV-10. The increase in peak position would suggest a second-order peak, however judging from the glow curves seen in figure IV-4 it is more likely that this behavior comes from two first order peaks, which cannot be resolved separately, rather than one second order peak.

References

[1] S.W.S McKeever, Thermoluminescence of Solids. Cambridge: University Press, 1985, pp. 76-87.

[2] Puchalska, M., et al., GLOW FIT - A new Tool for Thermoluminescence Glow-Curve Deconvolution. Radiat.Meas. (2006), doi:10.1016/j.radmeas.2006.03.008

[3] S.W.S McKeever, Thermoluminescence of Solids. Cambridge University Press, 1985, pp. 1-5.

[4] Stöcker, H.et al., Taschenbuch der Physik, 5th ed. Frankfurt am Main: Harri Deutsch, 2005, pp. 967.

[5] Hajek, M., Vana, N., Biologische Strahleneffekte, 2007, pp. 11

[6] Badurek, G, Biological and Medical Applications of Nuclear Physics II, 2007, pp. 30

[7] Chen, R., McKeever, S.W.S., Theory of Thermoluminescence and Related Phenomena. Singapore: World Scientific, 1997

[8] Randall, J.T., Willkins, M.H.F., Phosphorescence and Electron Traps: I. The Study of Trap Distributions. London: Proc. R. Soc., 1945, pp. 366-389

[9] Halperin, A., Braner, A.A., Evaluation of Thermal Activation Energies from Glow Curves. Phys. Rev.117 (2), 1960, pp. 408-415

[10] Garlick, G.F.J., Gibson, A.F., The Electron Trap Mechanism of Luminescence in Sulphide and Silicate Phosphors. Proc. Phys. Soc. 60, 1948, pp. 574-589

[11] Vana, N., Erlach, R., Fugger, M., Gratzl, W., Reichhalter, I., A computerised TL read out system for dating and

phototransfer measurements. *Int. J. Radiat. Appl. Instrum. D* 14, 1988, pp. 181–184.

[12] Berger, T., Hajek, M., On the linearity of the high-temperature emission from ^{7}LiF:Mg,Ti (TLD-700). *Radiat. Meas.* (2008), doi:10.1016/j.radmeas.2008.06.004